Air Blast Effects on Structural Shapes

by

Graeme Ballantyne, Andrew S. Whittaker, Amjad J. Aref and Gary F. Dargush
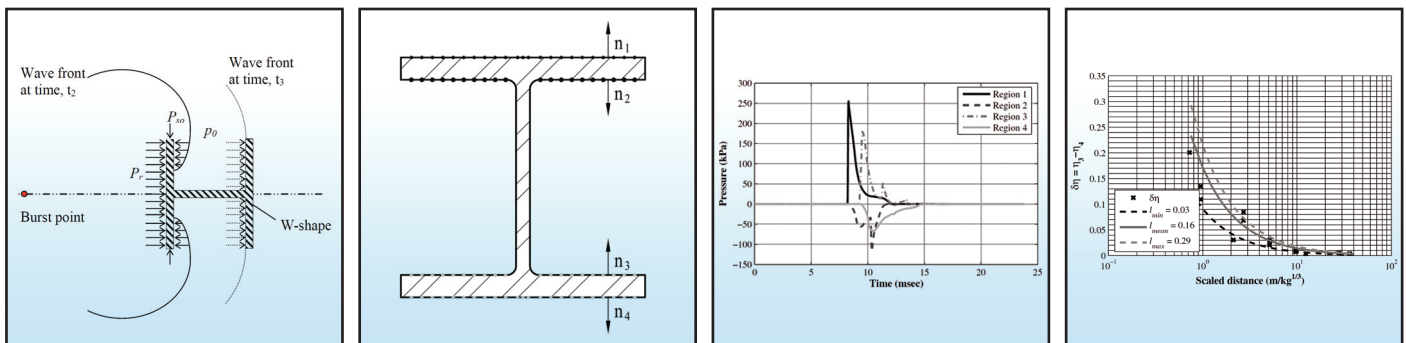
NOTICE

This report was prepared by the University at Buffalo, State University of New York as a result of research sponsored by MCEER through a grant from the Earthquake Engineering Research Centers Program of the National Science Foundation under NSF award number EEC-9701471 and other sponsors. Neither MCEER, associates of MCEER, its sponsors, the University at Buffalo, State University of New York, nor any person acting on their behalf:

a. makes any warranty, express or implied, with respect to the use of any information, apparatus, method, or process disclosed in this report or that such use may not infringe upon privately owned rights; or

b. assumes any liabilities of whatsoever kind with respect to the use of, or the damage resulting from the use of, any information, apparatus, method, or process disclosed in this report.

Any opinions, findings, and conclusions or recommendations expressed in this publication are those of the author(s) and do not necessarily reflect the views of MCEER, the National Science Foundation, or other sponsors.

Air Blast Effects on Structural Shapes

by

Graeme Ballantyne,[1] Andrew S. Whittaker,[2] Amjad J. Aref[2] and Gary F. Dargush[3]

1   Graduate Student, Department of Civil, Structural and Environmental Engineering, University at Buffalo, State University of New York
2   Professor, Department of Civil, Structural and Environmental Engineering, University at Buffalo, State University of New York
3   Professor and Chair, Department of Mechanical and Aerospace Engineering, University at Buffalo, State University of New York

Preface

The Multidisciplinary Center for Earthquake Engineering Research (MCEER) is a national center of excellence in advanced technology applications that is dedicated to the reduction of earthquake losses nationwide. Headquartered at the University at Buffalo, State University of New York, the Center was originally established by the National Science Foundation in 1986, as the National Center for Earthquake Engineering Research (NCEER).

Comprising a consortium of researchers from numerous disciplines and institutions throughout the United States, the Center's mission is to reduce earthquake losses through research and the application of advanced technologies that improve engineering, pre-earthquake planning and post-earthquake recovery strategies. Toward this end, the Center coordinates a nationwide program of multidisciplinary team research, education and outreach activities.

MCEER's research is conducted under the sponsorship of two major federal agencies: the National Science Foundation (NSF) and the Federal Highway Administration (FHWA), and the State of New York. Significant support is derived from the Federal Emergency Management Agency (FEMA), other state governments, academic institutions, foreign governments and private industry.

MCEER's NSF-sponsored research objectives are twofold: to increase resilience by developing seismic evaluation and rehabilitation strategies for the post-disaster facilities and systems (hospitals, electrical and water lifelines, and bridges and highways) that society expects to be operational following an earthquake; and to further enhance resilience by developing improved emergency management capabilities to ensure an effective response and recovery following the earthquake (see the figure below).
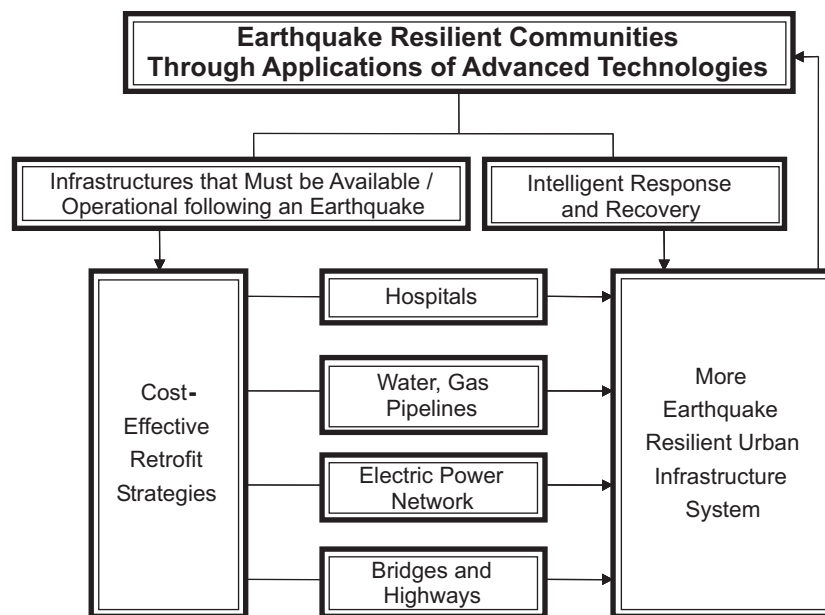
A cross-program activity focuses on the establishment of an effective experimental and analytical network to facilitate the exchange of information between researchers located in various institutions across the country. These are complemented by, and integrated with, other MCEER activities in education, outreach, technology transfer, and industry partnerships.

This report investigates the effect of short-duration blast loadings on structural shapes of finite width. A series of numerical analyses on W-shapes are performed using a computational fluid dynamics code. Results such as peak reflected overpressure and reflected impulse are compared to values computed using empirical data reported in the literature for reflecting surfaces of infinite width. Significant reductions in loading are observed. The finiteness of the width dimension allows a low pressure wave to propagate inwards on the front surface of the section, lowering the pressure more quickly than if the section had infinite width. As the blast wave engulfs the section over its width and depth, there is a component of positive pressure on the rear face of the section that opposes the positive pressure on the front surface, which can substantially reduce the net pressure loading below that computed using empirical data. The percentage reduction varies as a function of the size of charge and standoff distance, with the largest reductions observed for small charges and large standoff distances.

ABSTRACT

Following the recent increase in bombings over the last 10 years, blast loading has become a research topic of renewed interest. Many different approaches exist in the design of blast resistant structures, with many designs beginning initially from the simplified hand procedures. Hopkinson and Cranz generated experimental data for key loading parameters such as peak overpressure, arrival time, impulse, and load duration. These parameters are then used to determine a simplified loading history to design the member or structure. A possible oversight of this approach is that the experimental data from which the loading parameters are determined is based on a reflective surface of considerable size, effectively infinite, such as a bomb shelter. Individual structural members however have much smaller widths and could be considered finite surfaces in most scenarios, potentially lowering the loading.

A study was performed to investigate the effect of a W-shape section with finite dimensions on the loading parameters. Two main mechanisms were hypothesized for reducing the loading; 'clearing' and 'wrap-around'. Using the code Air3d, design of experiment procedures and linear regression techniques, a series of analyses were performed. For a given charge mass, held constant for a range of stand-off distances, R, impulse is approximately proportional to 1/R when considering an infinite surface. The impulse when clearing is considered is still proportional to 1/R, however, it is 40-60% lower than the experimental value of impulse, which represents a substantial reduction. The impulse when 'wrap-around' can occur is no longer proportional to 1/R but rather $1/R^2$. The implications of such a relationship are dramatic, as for a 10 fold increase in R the impulse is 1% of the previous value rather than 10% as the Hopkinson-Cranz data suggests.

ACKNOWLEDGMENTS

TABLE OF CONTENTS

SECTION   TITLE   **PAGE**

TABLE OF CONTENTS (CONT'D)

LIST OF TABLES

SECTION 1

INTRODUCTION

1.1   Historical Background

Blast engineering and analysis, as with many fields of research, has developed somewhat sporadically over the last sixty to seventy years based upon events throughout this period. Towards the end of World War 2, extensive work was carried out in blast resistant design by government bodies in both the United Kingdom (UK) and United States of America (USA). Particular attention was given to loading effects of nuclear explosions following the deployment of the Hiroshima and Nagasaki atomic bombs. The momentum of this work along with the escalation of the Cold War resulted in continued development in the field of blast engineering amongst government institutions throughout the world. The result of this research was that significant advances were made in structural dynamics and various procedures were developed that were applicable to many structural systems and loading conditions, some of which are documented in Norris et al. (1959) and Biggs (1964).

As well as advances in the structural aspects of blast events, understanding of combustion and explosion phenomena, explosion characteristics and many other effects was greatly improved. Baker et al. (1983) produced a comprehensive text covering many aspects of blast loading.

Despite these advances, attention gradually shifted from blast research to earthquake engineering following a series of damaging earthquakes on the west coast of the USA; including the San Fernando (1971), Loma Prieta (1989) and Northridge (1994) earthquakes, which coupled with the resolution of the Cold War reduced effort in blast engineering research between the early 1980's and mid 1990's.

1.2   Recent High Profile Blast Events

Recent or current events play a large role in both academic interest and funding opportunities. In 1992, a bomb was detonated in the financial district of London, UK, close to the Baltic Exchange building at 30 St Mary's Axe. The Exchange building itself was virtually destroyed and nearby buildings severely damaged, at an estimated cost of $700 million. In 1993, a

terrorist group detonated a 1500lb car bomb below Tower 1 of the World Trade Center (WTC) in the underground parking garage.   The blast created a 100ft hole in a number of the sublevel floors while claiming 6 lives and injuring over 1000 people.   A few years later, in 1995, a car bomb in Oklahoma City, USA, was detonated next to the Murrah Federal Building that had devastating effects on the Murrah Building and surrounding structures.   Over the following ten years, a dramatic increase in terrorist activity saw numerous attacks on influential buildings throughout the world; Canary Wharf, London, UK (1996); Khobar Towers, Khobar, Saudi Arabia (1996);   US Embassy, Dar es Salaam, Tanzania (1998); US Embassy, Nairobi, Kenya (1998); World Trade Center, New York, USA (2001); US Consulate, Bali, Indonesia (2002); Jakarta Marriot Hotel, Jakarta, Indonesia (2003); and the Australian Embassy, Jakarta, Indonesia (2004).   This heightened terrorist threat saw a substantial increase in blast related research in the USA, UK and Australia.

1.3   Current Methodologies and Standards

Despite research activities for over fifty years, there were very few civilian design standards and documentation that considered blast resistant design.   Some guidance was available through US Army Technical Manual TM5-1300 (DOA, 1990), however, after the terrorist attacks on the World Trade Center in 2001, government documentation was subsequently restricted and difficult to obtain.   Blast design guidelines were created and textbooks published including the American Institute of Steel Construction (AISC) Blast Guide (AISC, 2005) document produced in 2006 that addresses steel structures.   In this guide, individual members are designed as Single Degree of Freedom (SDOF) systems and connections are designed such that redistribution of load is possible.   Whilst offering some new direction, many guidelines such as the upcoming ASCE Blast Standard (ASCE, 2007), draw heavily on the work of Norris (1959), Biggs (1964) and Baker et al. (1983).

1.4   Surface Explosions

Many categories of explosions exist: spherical bursts, hemispherical bursts, underwater explosions, internal explosions are a few.   The type of explosion considered in this study is a spherical burst from an ideal 'point' source.

Most modern explosives can be classed as ideal 'point' sources since the chemical compounds used have very high energy densities (i.e. the volume of the domain consumed by the explosive compound is tiny, thus, as far as the surroundings are concerned, the energy comes from a point source) and the speed of reaction is very high such that all the energy is released at almost the same time. The difference between spherical and hemispherical bursts is related to the distance from a large reflective surface.

A spherical burst is an explosion that occurs removed from any reflective surface, for example a device detonated high in the atmosphere. At the time of detonation, a detonation wave front travels out radially through the explosive inducing further detonation of the material. The reaction products are gases at high temperature and pressure that then expand outwards at the shockwave velocity and a layer of compressed air forms in front of the expanding gas as the surrounding air is forced out of the volume it previously occupied. This layer of compressed air is the blast wave and it continues to propagate outwards in a radial fashion from the point source. A hemispherical burst is often the same device as a spherical burst but is located on a large reflective surface such as the ground. The design charts presented for spherical bursts that relate blast wave parameters to scaled distance can be used for hemispherical bursts provided that the mass of the device is increased by a factor of 1.8 for modern high explosives (theoretically, an infinitely rigid reflective surface would magnify the energy by 2 since there would be no energy absorbed by the surface). Baker et al. (1983) provides a thorough treatment of the nature of many explosion types and the characteristics of the corresponding blast waves that are not considered in this study.

1.5   Blast Wave Characteristics

The current method of establishing the pressure loads by hand involves experimental data that provide quantities to define the blast wave such as peak pressure, arrival time, positive duration and positive impulse. After a given arrival time of the shockwave, t_a, an instantaneous rise in pressure to the peak value, is observed. The pressure then decays in an exponential manner to ambient in a time interval denoted as the 'positive phase duration', t_d. Positive phase impulse, i^+, is the area below the positive phase portion of the pressure history. Due to overexpansion of the gas surrounding the charge, contraction induces a suction or negative phase that typically is

of much lower magnitude but greater duration than the positive phase.   For the purposes of design, idealized pressure histories are often used that typically ignore the negative phase.   Two main approaches exist; enforce equality of the positive phase impulse (essentially results in a slightly shorter t_d but actual i^+) or assume a linear decay rather than exponential (essentially results in a larger impulse but actual t_d).   Figure 1-1 shows a typical blast pressure history, generated from the Air3d (Rose, 2006) code, at a location away from the burst point and idealized histories based upon the above discussion.
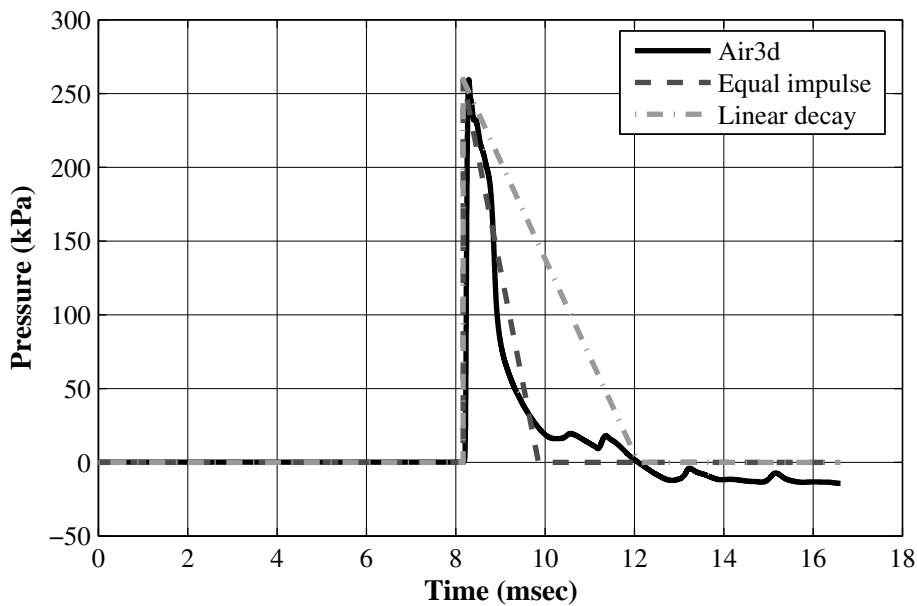
Figure 1-1: Actual and Idealized Pressure Histories ($R = 6.63m$, $m_{tnt} = 14.6kg$, $Z = 2.71 m / \sqrt[3]{kg}$)

Throughout the years, experiments have been undertaken and alternative equations proposed to describe the blast wave quantities, for example; Kingery-Bulmash (1984) (KB) and Hopkinson-Cranz (HC).   Hopkinson (1915) and Cranz (1926) demonstrated that the magnitude of the blast wave characteristics is proportional to the stored energy of the charge, E_s, and the charge stand-off distance, R.   Common practice in blast engineering is to use a scaled distance Z rather than the charge stand off, R, and is calculated according to equation (1-1) below.   In addition to scaled distance, common practice is to relate the stored energy of any charge to an equivalent

mass of TNT based upon the ratio of the energy densities of the explosives, which is the reason for the mass term in equation (1-1) rather than an energy term.

$$Z = \frac{R}{\sqrt[3]{m_{tnt}}}$$
(1-1)

In equation (1-1), m_{tnt} is the TNT-equivalent mass. Attention to the unit system is important since Z in US units is calculated using the weight in pounds of the device rather than the device mass as is the case with SI units. SI units are used throughout this study and conversion factors are provided in Table 1-1 for convenience.

Table 1-1: Unit Conversions

Quantity	SI Unit	US Unit
Length	$1\ m$	$3.281\ ft$
Mass[1]	$1\ kg$	$0.069\ \dfrac{lbf \cdot s^2}{ft}$
Force/Weight	$1\ N$	$0.225\ lbf$
Energy/Moment	$1\ J = 1\ N \cdot m$	$0.738\ lbf \cdot ft$
Pressure/Stress	$1\ MPa$ $1\ bar$ $1\ atmosphere$	$145.04\ psi$ $14.504\ psi$ $14.696\ psi$
Scaled Range[2]	$1\ \dfrac{m}{\sqrt[3]{kg}}$	$2.521\ \dfrac{ft}{\sqrt[3]{lbf}}$
Mass Density	$1\ \dfrac{kg}{m^3}$	$1.94\text{x}10^{-3}\ \dfrac{slug}{ft^3}$
Weight Density	$1\ \dfrac{N}{m^3}$	$6.37\ \text{x}10^{-3}\ \dfrac{lbf}{ft^3}$

1.   Mass units of $lbf \cdot s^2 / ft$ are referred to as 'slugs' in the US system.

2.   The conversion for scaled range is not a true conversion in the sense that the fundamental units (Length, Mass & Time) are different. $LM^{-1/3}$ for SI and $L^{2/3}M^{-1/3}T^{2/3}$ for US since weight is inside the cube-root.

Representation of the blast wave parameters t_d, t_a, i^+ and P can be found in TM5-1300 (DOA, 1990) and Baker et al. (1983) in the form of scaled curves. Figure 1-2, Figure 1-3 and Figure 1-4 show the HC curves plotted on a log-log scale.
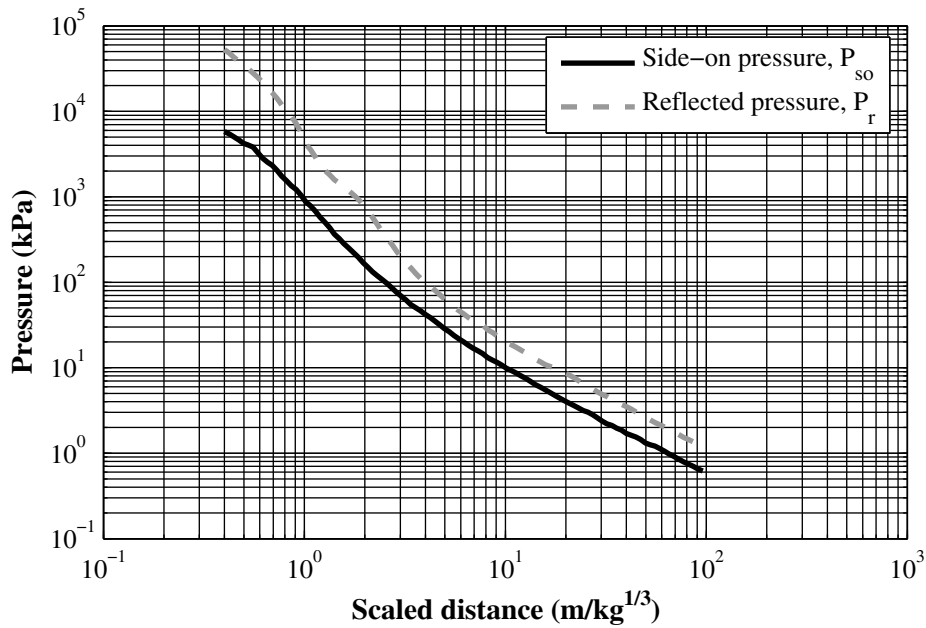
Figure 1-2: Scaled Side-on and Reflected Pressure vs. Scaled Distance for Hopkinson-Cranz
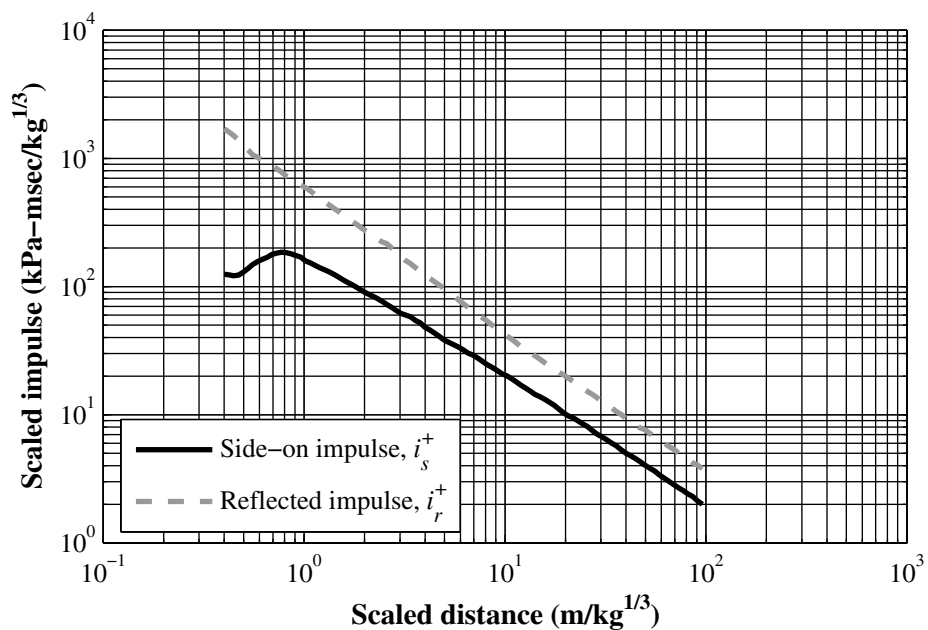
Figure 1-3: Scaled Side-on and Reflected Impulse vs. Scaled Distance for Hopkinson-Cranz
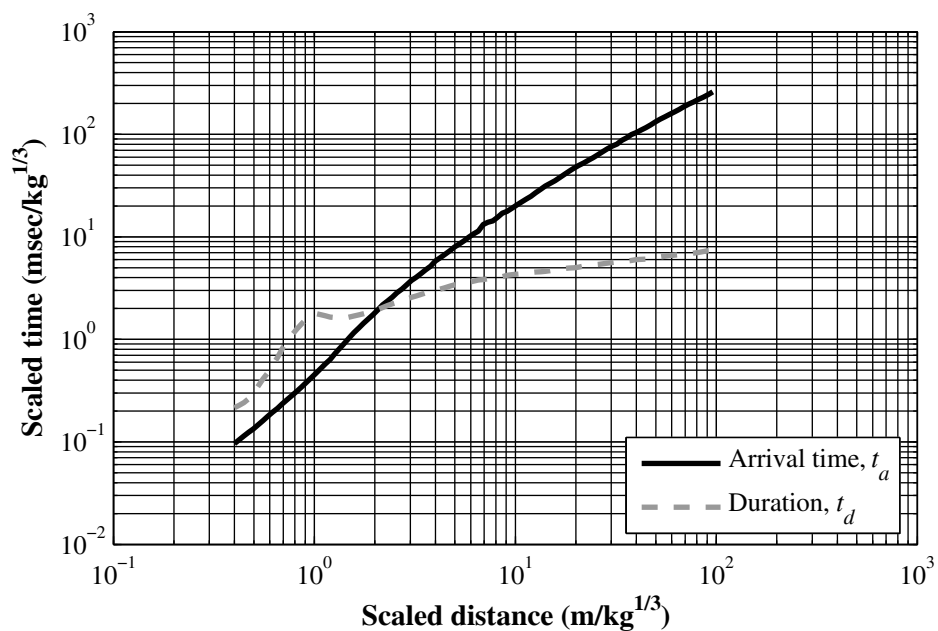
Figure 1-4: Scaled Arrival Time and Positive Phase Duration vs. Scaled Distance for Hopkinson-Cranz

Review of Figures 1-2 and 1-3 reveals that there are two traces for pressure and two traces for impulse. The difference between the two traces is related to the interaction of the blast wave with reflective surfaces. As the blast wave approaches the surface it has a side-on pressure, P_{so}, that strikes the surface and reflects back, instantaneously increasing the pressure in a process identical to the reflection of a stress wave propagating in a rod. This increased pressure is termed the reflected pressure, P_r. Since specific impulse is defined as the area below the pressure history, two impulse traces are presented for side-on and reflective impulse for the same reason. The increase due to the reflection is heavily dependent upon the angle of incidence, α, between the wave and the reflecting surface. Figure 1-5 shows the angle of incidence with respect to the reflecting surface. The ratio of the reflected pressure to side-on pressure is termed the reflection coefficient, C_R, Figure 1-6 shows the effect of α and P_{so} on the reflection coefficient. The HC curves of Figures 1-2 through 1-4 are based upon $\alpha = 0$ (reflected) and $\alpha = 90$ (side-on).
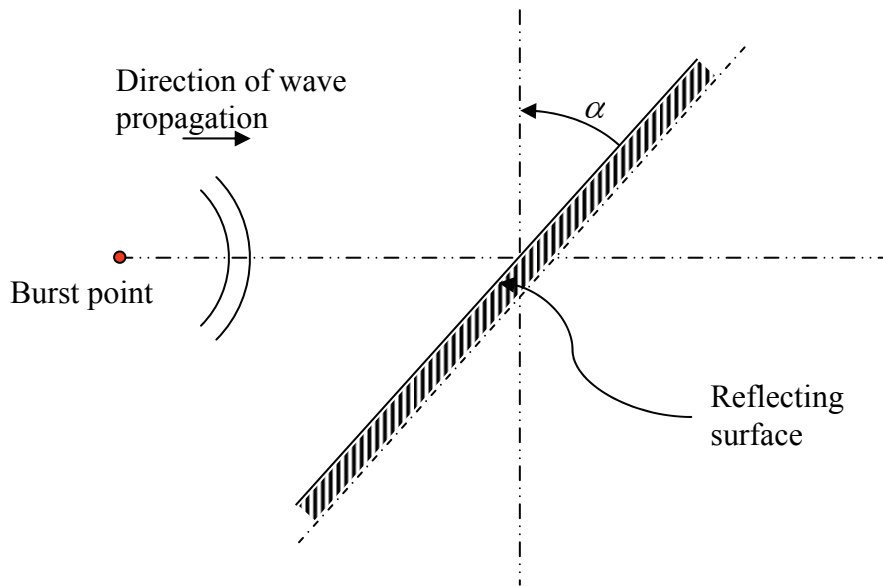
Figure 1-5: Angle of Incidence
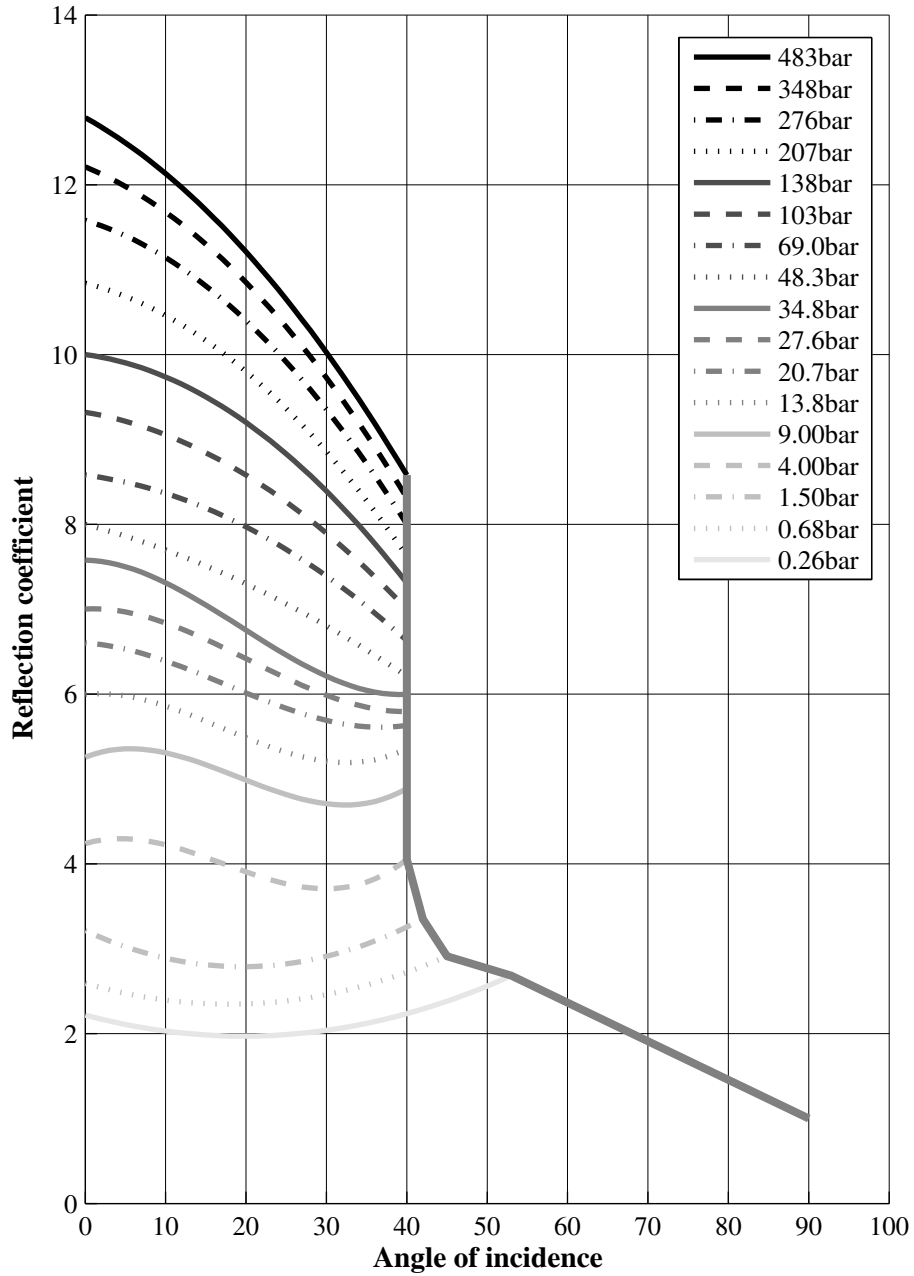
Figure 1-6: Reflection Coefficient vs. Angle of Incidence as a Function of Side-on Pressure $\left(1\,bar \approx 14.5\,psi\right)$**, Adapted from Smith and Hetherington (1994)**

Theoretical bounds were derived by Rankine and Hugoniot (1870) for normal shocks in ideal gases. Considering, $\alpha = 0$, the peak reflected pressure, P_r, is given by

$$P_r = 2P_{so} + (\gamma + 1)q_s \tag{1-2}$$

where q_s is the dynamic pressure

$$q_s = \frac{1}{2}\rho_s u_s^2 \tag{1-3}$$

where ρ_s is the density of the air and u_s is the particle velocity behind the wave front. It can be shown that

$$u_s = \frac{a_0 P_{so}}{\gamma p_0}\left[1 + \left[\frac{\gamma+1}{2\gamma}\right]\frac{P_{so}}{p_0}\right]^{-\frac{1}{2}} \tag{1-4}$$

where p_0 is the ambient pressure, a_0 is the speed of sound in air at ambient conditions and γ is the ratio of specific heat ($\gamma = 1.4$ for air). Substitution of equations (1-3) and (1-4) into equation (1-2) returns

$$P_r = 2P_{so}\left[\frac{7p_0 + 4P_{so}}{7p_0 + P_{so}}\right] \tag{1-5}$$

Examination of equation (1-5) reveals that as P_{so} tends towards zero, C_R tends towards 2 ($\alpha = 0$). As P_{so} tends towards infinity, C_R tends towards 8 (this corresponds to a side-on pressure of 48.3bar when $\alpha = 0$ in Figure 1-6). Further examination of Figure 1-6 reveals that the maximum value of C_R is 12.8 and measured values of 20 have been reported by Smith and Hetherington (1994). These high reflection coefficients occur for very high pressures (small Z) and most likely close to the fireball. Here, the air is far from ideal with extreme temperatures, combustion products and dissociation effects (Smith and Hetherington, 1994), which provides a possible explanation for the breakdown of the Rankine-Hugoniot prediction.

1.6   Structural Design for Blast Events

Once a pressure history has been established for a given event, the structural system has to be designed to resist the loading. Norris et al. (1959) and Biggs (1964) provide excellent guidance

on the structural design of systems subjected to blast loading. A short overview is discussed here for the reader's convenience.

Since blast loading is obviously a transient process, the dynamic properties of the system under design are going to influence the response. Consider an elastic single degree of freedom (SDOF) undamped oscillator as shown in Figure 1-7. From elementary dynamics, the natural period of response, T_n, for such a system is simply

$$T_n = 2\pi\sqrt{\frac{m}{k}}$$
(1-6)

where m is the mass of the system and k is the spring stiffness. Biggs (1964) demonstrated that the ratio of the loading period, t_d, to the natural period of response, T_n, was a critical quantity in determining the response of the system. If t_d is less than one-third of T_n, the loading can be treated as purely impulsive without introducing significant error. Table 1-2 shows the ratio of t_d to T_n for three common structural shapes and five loading durations.
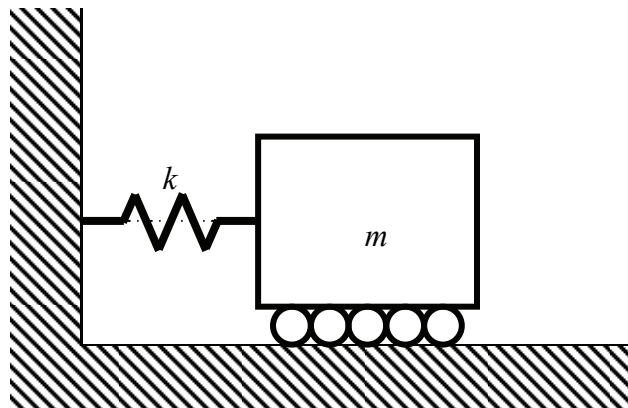
Figure 1-7: Elastic Single-Degree-of-Freedom (SDOF) Oscillator

Table 1-2: Period ratio for various structural shapes and load durations.[1,2,3]

Shape	t_d (msec)[4]	R (m)	m_{tnt} (m)	Z (m/kg$^{(1/3)}$)	t_d/T_n
W14 x 193	0.5	0.85	5	0.50	*0.03*
	1	1.10	5	0.64	*0.06*
	2	1.35	5	0.79	*0.11*
	4	4.50	5	2.63	*0.23*
	8	25.0	5	14.6	0.45
W14 x 342	0.5	0.85	5	0.50	*0.03*
	1	1.10	5	0.64	*0.06*
	2	1.35	5	0.79	*0.12*
	4	4.50	5	2.63	*0.24*
	8	25.0	5	14.6	0.49
W14 x 426	0.5	0.85	5	0.50	*0.03*
	1	1.10	5	0.64	*0.06*
	2	1.35	5	0.79	*0.13*
	4	4.50	5	2.63	*0.25*
	8	25.0	5	14.6	0.51

1.   Shaded cells indicate t_d/T_n less than 0.33, the threshold for impulse loading.

2.   Span length for shapes: 6m

3.   Span boundary conditions: clamped-pin.

4.   The values of t_d shown could be obtained using different values of R and m_{tnt}. The values shown are an example of possible combinations.

In such a loading environment, the response can be determined by imparting an initial velocity which can be calculated as

$$\dot{y}_0 = \frac{i^+}{m} \qquad\qquad (1\text{-}7)$$

where $\dot{y}_0$ is the initial velocity imparted on the system mass, m, due to the impulse, i^+. The other condition is when t_d is substantially greater than T_n. If t_d is greater than three times T_n, the loading can be classed as quasi-static since the inertial resistance of the mass is low. The pressure, P_R, then becomes the important loading characteristic in determining the response of the system.

Thus, for a given threat a scaled range can be calculated and the pressure history determined based upon the parameters in Figures 1-2, 1-3 and 1-4. Then the structural system can be designed accordingly, depending upon its own dynamic properties. Generally, the loading duration of a blast event is significantly smaller than the natural period of an element and as a result most structural design for blast events is in the impulsive regime. This implies reduction in impulse would be beneficial for the designer.

1.7 Clearing and Wrap-around

As discussed previously, the majority of the early blast research was concerned with nuclear devices and the global response of structures. As a consequence the HC curves essentially consider an infinite surface, which at a global level is acceptable – design of individual members represents a different problem as the reflecting surface of a column cannot be considered 'infinite'. Two effects that could alter the parameters obtained from the HC curves are clearing and wrap-around.

1.7.1 Clearing

Clearing is a phenomenon that occurs at the instant the reflected wave reaches the section

extremities and is discussed in Norris (1959) and Smith and Hetherington (1994). At the surface

extremities, a low pressure wave is generated at the outer corner where vortices are shed as the

blast wave passes the front surface. The low pressure shock wave (referred to as a rarefaction

wave) races inwards from the surface extremities, accelerating the decay from peak reflected

pressure to side-on pressure along the front surface. There will be no reduction in the peak

reflected pressure from clearing, however, a reduction in impulse could be observed since the

decay is accelerated by the rarefaction wave depending on how much of the surface the rarefaction wave can reach. Figure 1-8 shows a W section and illustrates the progression of the rarefaction wave along the front face. The rarefaction wave moves at the *local* speed of sound in the high pressure gas at the head of the rarefaction wave. If the particle flow velocity is high (i.e., close to the point of detonation outside the fireball) and from a region of high pressure to low pressure, the head of the rarefaction wave will propagate slowly and little clearing will be experienced (Ritzel, 2008). Further, pressure loadings within the fireball are due primarily to the ejection of detonation products and the rarefaction wave will not reduce the reflected impulse associated with the ejecta. Some current guidelines provide allowance for clearing (Norris, 1959), based upon an approximate clearing rule

$$t_c = \frac{3S}{U} \tag{1-8}$$

where S is the clearing distance, which is equal to the half width of the reflecting surface, assuming that the reflecting surface is narrow and tall, and U is the shock front velocity. Equation (1-8) is based on data collected from shock tube experiments conducted in the 1950s that had an emphasis on far-field pressure loadings from thermonuclear detonations. The utility of this equation for near-field blast loadings of short duration is questionable for near-range detonations that form most of the design threats in urban environments.

1.7.2 Wrap-around

Wrap-around is the ability of the blast wave to wrap around the section and provide a restoring force that opposes the positive impulse on the front face of the section. Consider the exposed W-shape at a stand-off from a device collinear to the axis passing through the web centerline (that is, $\alpha = 0$) shown in Figure 1-9. After a certain time, t_1, a reflected pressure is experienced on the front face of the front flange as the blast wave propagates outwards. At some time, t_2,

the wave then engulfs the front flange and the rear face of the front flange experiences a side on pressure, which opposes the reflected pressure acting upon the front face. At time, t_3, a reflected pressure is experienced by the front face of the rear flange acting in the same direction as the wave propagation. At time, t_4, a side-on pressure is experienced on the rear surface of the rear flange opposing the reflected pressure on the front face of the rear flange.
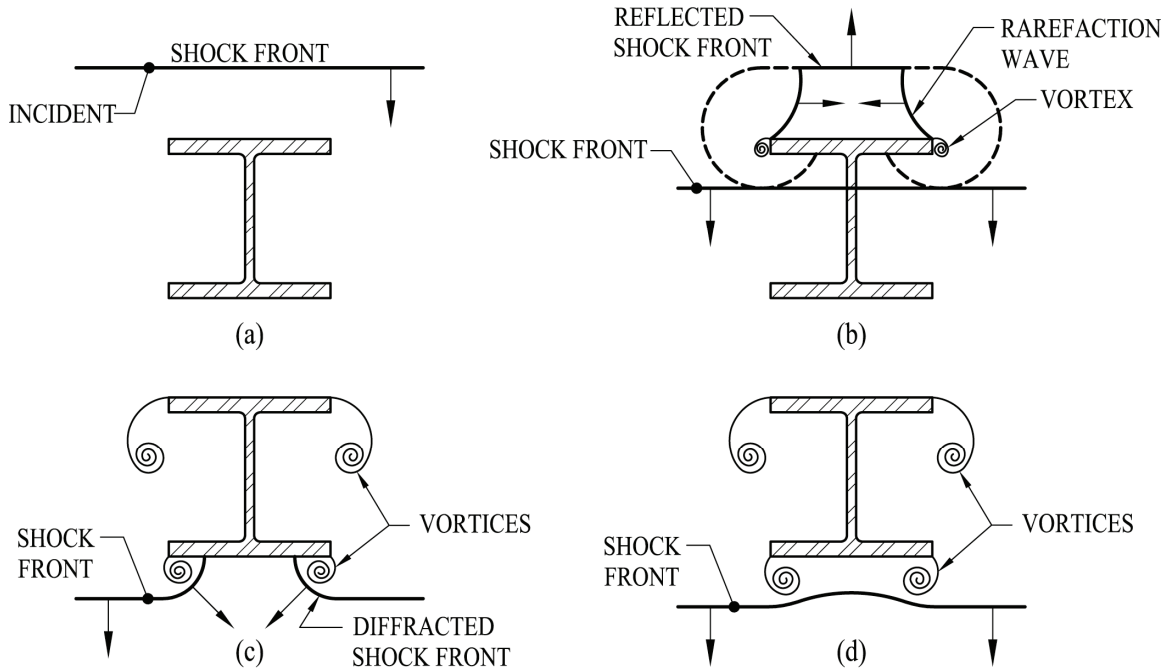
Figure 1-8: Progression of a Shock Wave Around a W-shape Section
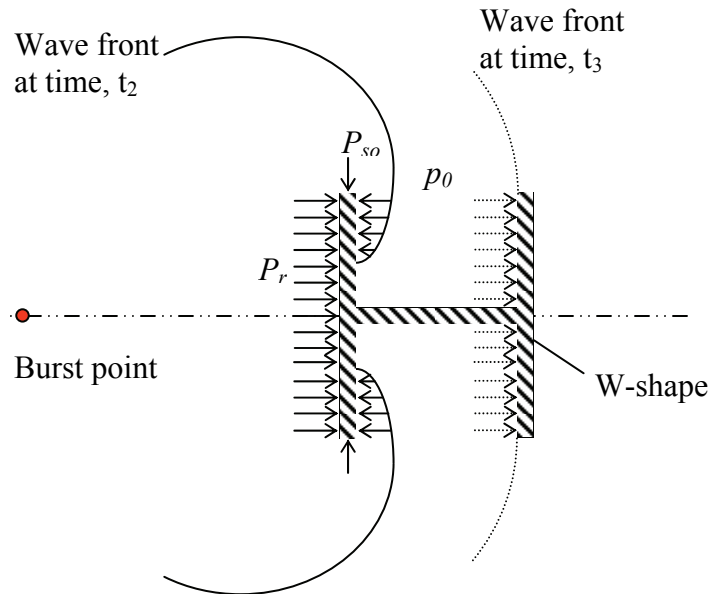
Figure 1-9: Wrap Around of a W-shape Section

1.8 Study Objective and Report Organization

1.8.1 Objectives

Two main objectives were identified when this study was undertaken: 1) examination of clearing effects on the pressure histories experienced by structural shapes, specifically the impact on impulse, and, 2) examination of wrap-around effects upon the net impulse experienced by structural shapes subjected to blast loads.

1.8.2 Organization

The following chapter discusses the various techniques and the methodology implemented in conducting the study such as Dimensional Analysis, Design of Experiments, Linear Regression and Numerical Analysis. Section 3 presents the results of the study and the subsequent discussion relating to those results. Conclusions and recommendations that have been drawn based upon the results and discussion are presented in Section 4.

SECTION 2

PROBLEM AND METHODOLOGY

2.1   Problem Definition

To quantify the effects of clearing and wrap around, a study of W-shape sections subjected to blast loading from a spherical charge was carried out with the intention of deriving a relationship between physical parameters and the effect on impulse through clearing and wrap-around. Figure 2-1 shows a schematic of the problem.

Numerical analysis was performed using the Air3d (Rose, 2006) code to generate pressure histories at various locations on the section.   Impulse can be calculated through integration of the pressure histories.   In order to establish a relationship over a range of scaled distances, several analyses were performed, thus allowing linear regression to be performed to estimate a relationship.
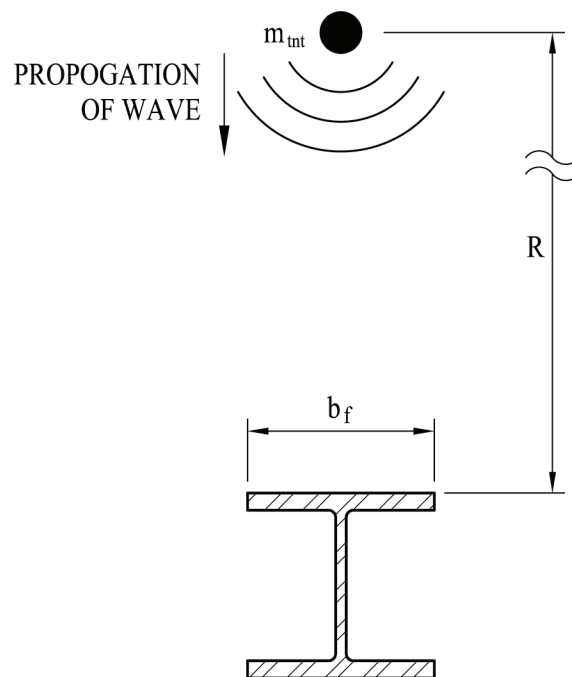
Figure 2-1: Schematic Showing Experimental Layout.

2.1.1 Assumptions and Limitations

As with any research, assumptions are required to simplify complicated events into more manageable problems. Given the complex nature of blast loading there are a number of limitations and assumptions that have been made regarding the numerical modeling, namely,

- Spherical charge (free air burst)
- Fluid-structure interaction has not been considered (i.e. material response of the section has been ignored)
- Thermal effects have not been considered.
- Only the positive phase impulse is calculated.
- Fillets/radii of fabricated/rolled sections have not been included.
- Physical bounds are placed on scaled range.

The suitability of assuming the section behaves rigidly depends upon the ratio of the loading period and natural period of the loaded element. Transient loadings with durations significantly greater than the natural period of the structure can be solved as quasi-static loading without sacrifice of accuracy. Considering a standard W18x35 cross section, with flange thickness of 0.011m, unit flange length and span (outstand) length of 0.076m; the natural period of the flange outstand is 0.65ms. With the exception of events that occur due to a very close satchel type device (small Z and small m_{tnt}) the ratio of loading duration to natural period is going to be large, such that the flange response is significantly slower than the propagation speed of the pressure wave. Clearing occurs when the pressure wave has the opportunity to clear around an object, thus clearing will still be present even if large deformations occur. Secondly, accurate modeling of non-linear fluid-structure interaction at high-strain rates is a computationally extensive procedure and the accuracy of current approaches is questionable. Thus, for the purposes of this study, rigid cross-sections were assumed.

Neglecting the thermal effects of the device is appropriate given the rapid loading duration. The time required for a constantly applied temperature of 1000 degrees on the front and back faces to

increase the flange core temperature by 100 degrees is 0.3secs (Carslaw and Jaeger, 1959), which is orders of magnitude longer than the actual loading duration. This implies that the actual temperature rise in the flange would be insufficient to alter the material properties of the steel. Another thermal effect is the rise in temperature related to internal work of the material. As the section becomes severely deformed, an increase in the material temperature would occur. Due to the rapid nature of the blast loading, in essence the internal work generation is an adiabatic process with around 90% of the work done being converted to heat (Meyers, 1994). Consideration of the temperature rise is pointless since a rigid material assumption has already been made and the increase in deformation due to temperature will likely be small. The thermal effect from internal work was neglected in this study.

Only the positive phase impulse is considered in the analysis for two main reasons. Firstly, a degree of conservatism is retained, which, given the complicated nature of the loading is deemed prudent. Secondly, the values of impulse that we obtain from the HC curves or the KB equations are positive phase impulse.

Since the section has been assumed rigid, there is no benefit in considering the radii of the W-shape section in the numerical analysis. Ignoring the radii in the analysis will have a minimal effect on the overall impulse as they will only affect the pressure histories in the immediate vicinity of the web, which represents a very small proportion of the W-shape cross section.

Finally, physical limitations exist on Z. At low Z, pressures are very high and the loading environment is severe (potentially in the fireball). The applicability of the HC curves begins to break down for a number of reasons. As Z becomes small, the shape of the charge alters the loadings dramatically. The HC data considers an ideal point source, thus, uncertainty regarding the details of the charge makes simplified hand procedures impractical at small Z. Furthermore, such close-in events will have extremely high pressures causing substantial changes in the cross section that invalidate the modeling assumptions of the analysis and the use of simplified hand procedures for structural design. A scaled range of $Z = 1\,m/\sqrt[3]{kg}$ is likely within the fireball based on data presented in Baker et al. (1983), Merrifield and Wharton (2000) and Ritzel (2008), thus the lower limit taken on Z is approximately $1\,m/\sqrt[3]{kg}$. An upper distance was chosen based

upon a realistic minimum threat at a realistic maximum stand off, that is, the maximum Z occurs when the smallest charge mass is detonated at the maximum stand off $Z_{max} = \left(R_{max} / \sqrt[3]{m_{min}} \right)$.

2.1.2 Calculation of impulse

Impulse is the integral of the pressure history. To determine the impulse on W-shape cross-sections using the code, the sections were discretized into 44 monitoring areas that had a monitoring point at the centre of each area. The impulse was broken down into 4 main regions. Region 1 represents the front face of the front flange, Region 2 represents the rear face of the front flange, Region 3 represents the front face of the rear flange and Region 4 represents the rear face of the rear flange. Breaking the section surface down into separate regions allows the positive impulse imparted on each region to be determined. Note that the pressure wave loading always opposes the surface normal and consequently the positive phase impulse on each region also acts in the opposite direction of the surface normal. Figure 2-2 shows a diagram of the discretized section identifying the regions and their respective surface normal (n_1 through n_4). Note that the problem is symmetric about the centerline of the web, thus, only half the section was modeled.

The net impulse on a region was calculated as an area-average of pressure integrated over time as follows;

$$i_R^+ = \frac{1}{A_R} \sum_{n=j}^{k} \int_0^{t^+} A_n p_n(t) dt \tag{2-1}$$

where i_R^+ is the impulse on the region under consideration, A_R is the area of the region under consideration, A_n is the tributary area of the nth monitoring location and $p_n(t)$ is the pressure history for the nth monitoring location. Note that the limits of integration imply only the positive phase is included in the calculation, which is consistent with the previous assumptions. The values for j and k that define the summation in equation (2-1) are identified below for each region, along with the corresponding definition of A_R. The values increase from left to right as drawn.

For region 1: $j = 1$, $k = 12$, $A_R = b_f / 2$

For region 2: $j = 13$, $k = 22$, $A_R = (b_f - t_w)/2$

For region 3: $j = 23$, $k = 31$, $A_R = (b_f - t_w)/2$

For region 4: $j = 32$, $k = 44$, $A_R = b_f / 2$
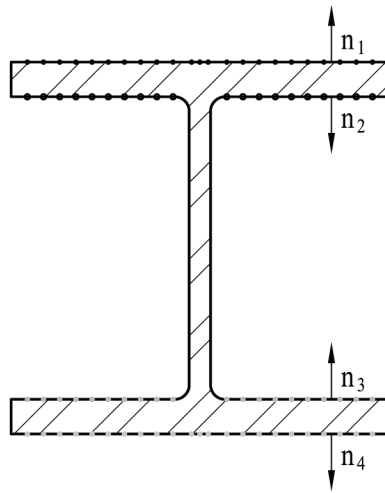
- REGION 1 MONITORING POINTS
- REGION 2 MONITORING POINTS
- REGION 3 MONITORING POINTS
- REGION 4 MONITORING POINTS

Figure 2-2: Layout of Monitoring Locations on W-shape for Experiments

2.2 Methodology

Given the volatile nature of explosives, difficulty in accurate instrumentation and the high cost of physical experiments; a numerical study was performed to determine if a reduction in impulse can be expected from clearing and wrap-around. Various techniques were utilized and are described in detail below.

2.2.1 Dimensional Analysis

One of the main problems in any study of this nature is correct identification of the parameters that influence the results. Rather than simply guessing, a more scientific approach was adopted utilizing dimensional analysis (Greenberg, 1988).

Dimensional analysis is frequently used to reduce the number of unknown parameters in a given problem by determining non-dimensional relationships that are a combination of the chosen physical parameters. Familiar quantities derived by these methods can be found in fluid mechanics, for example; Reynolds Number, Mach Number and Biot Number. Dimensional analysis can also be used to determine similitude relations for experiment design.

Review of the problem and a little thought allows an estimation of the parameters that we expect impulse to have a strong dependency on and neglect those which we expect a weak dependency. Table 2-1 shows the chosen variable, symbol and fundamental units (fundamental units being units of Mass, Length and Time).

Table 2-1: Dimensional Analysis Variables

Variable	Symbol	Fundamental Units
Speed of sound in medium	c	LT^{-1}
Ambient pressure	p_0	$ML^{-1}T^{-2}$
Source energy	E_s	ML^2T^{-2}
Volume enclosed by blast wave	V	L^3
Side-on overpressure pressure	P_s	$ML^{-1}T^{-2}$
Side-on impulse	i_s	$ML^{-1}T^{-1}$
Width of Flange	b_f	L
Depth of Flange	d	L
Aspect ratio $\left(R/b_f\right)$	θ	$M^0L^0T^0$

Once the variables have been chosen, we seek to find all possible dimensionless products of the form;

$$c^{\alpha}p_o^{\beta}E_s^{\gamma}V^{\delta}P_s^{\varepsilon}i_s^{\phi}b_f^{\zeta}d^{\eta}\theta^{\kappa} = M^0L^0T^0 \tag{2-2}$$

Substitution of the fundamental units into equation (2-2) and by equating exponents of M, L and T on both sides we must satisfy the homogenous linear system;

$$\beta + \gamma + \varepsilon + \phi = 0 \tag{2-3}$$

$$\alpha - \beta + 2\gamma + 3\delta - \varepsilon - \phi + \zeta + \eta = 0 \tag{2-4}$$

$$-\alpha - 2\beta - 2\gamma - 2\varepsilon - \phi = 0 \tag{2-5}$$

Equations (2-3), (2-4) and (2-5) represent the mass, length and time exponents respectively. Writing equation (2-3) through (2-5) in matrix form gives;

$$\mathbf{A} = \begin{bmatrix} 0 & 1 & 1 & 0 & 1 & 1 & 0 & 0 & 0 \\ 1 & -1 & 2 & 3 & -1 & -1 & 1 & 1 & 0 \\ -1 & -2 & -2 & 0 & -2 & -1 & 0 & 0 & 0 \end{bmatrix} \tag{2-6}$$

$$\mathbf{x^T} = \begin{bmatrix} \alpha & \beta & \gamma & \delta & \varepsilon & \phi & \zeta & \eta & \kappa \end{bmatrix} \tag{2-7}$$

$$\mathbf{C} = \begin{bmatrix} 0 \\ 0 \\ 0 \end{bmatrix} \tag{2-8}$$

and

$$\mathbf{Ax} = \mathbf{C} \tag{2-9}$$

Performing Guass elimination of equation (2-9) returns the following solution in terms of χ ;

$$x = \begin{bmatrix} \chi_4 \\ \chi_6 - \chi_5 - \dfrac{2}{3}\chi_4 + \dfrac{1}{3}\chi_3 + \dfrac{1}{3}\chi_2 \\ -\chi_6 - \dfrac{1}{3}\chi_4 - \dfrac{1}{3}\chi_3 - \dfrac{1}{3}\chi_2 \\ \chi_6 \\ \chi_5 \\ \chi_4 \\ \chi_3 \\ \chi_2 \\ \chi_1 \end{bmatrix} \tag{2-10}$$

By systematically setting each χ to 1 and all others to zero, the value of each exponent can be determined allowing derivation of the following dimensionless quantities;

$$p' = \frac{P_s}{p_o} \quad \text{when } \chi_1 = 1 \tag{2-11}$$

$$i'_s = \frac{c \cdot i_s}{p_o^{2/3} \cdot E_s^{1/3}} \quad \text{when } \chi_2 = 1 \tag{2-12}$$

24

$$R' = \left(\frac{p_o \cdot V}{E_s} \right)^{\frac{1}{3}} \quad \text{when } \chi_3 = 1 \tag{2-13}$$

$$AR = \theta \quad \text{when } \chi_4 = 1 \tag{2-14}$$

$$b'_f = b_f \cdot \left(\frac{p_o}{E_s} \right)^{\frac{1}{3}} \quad \text{when } \chi_5 = 1 \tag{2-15}$$

$$d' = d \cdot \left(\frac{p_o}{E_s} \right)^{\frac{1}{3}} \quad \text{when } \chi_6 = 1 \tag{2-16}$$

Examination of equations (2-11), (2-12) and (2-13) reveal very good agreement with the non-dimensional parameters proposed by Sachs (1944). Equations (2-14), (2-15) and (2-16) represent additional parameters that indicate a dependency on the stored energy, ambient pressure and the section dimensions. However, since we are only considering sea level events and assuming that there are no environmental fluctuations in pressure or air density, we need not consider p_o or c as they are constants and will not improve a regression model. Equation (2-14) implies a dependency on the ratio of flange width to stand-off. However, given that stand-off and flange width are both already included in equations (2-13) and (2-15), the aspect ratio is not used as a regression variable. In addition, the width-to-depth ratio of typical structural column shapes does not vary significantly. An average ratio was assumed for the purposes of this study, $d = 1.1 b_f$, and equation (2-16) was not considered as a regression variable. From the dimensional analysis, three variables remained; charge mass (m_{tnt}), device stand-off (R) and section width (b_f).

2.2.2 Design of Experiments

Having established the key variables, it is necessary to determine the variable values at which the experiments should be carried out. Design of Experiments (DOE) is a procedure commonly used in industrial engineering for establishing the variables that effect production rates or product quality.

25

In the case of this study, the experiments are numerical analysis of a W-shape subjected to blast loading and the values that the charge mass, device stand-off and section width take are determined using DOE methods. In addition to the values that the variables take, DOE methods also dictate the different combination of values that the variables take for each experiment (or analysis run). In DOE literature, variables are known as factors and the variable values are known as factor levels. Montgomery (1991) and Roy (1990) provide information on DOE techniques.

2.2.2.1 Factorial Designs

Methods of experimentation typically revolve around one-factor-at-a-time methods whereby the level of only one factor at a time is changed while all others are held constant. An alternative approach is to use factorial designs. In a factorial design, all possible combinations of the factor levels are considered. The effect of a factor upon the response is said to be the 'main effect' of that factor, that is, changing the level (value) of a factor (variable) induces a change in the response. As well as 'main effects', the interaction of the factors with each other can have significant consequences on the outcome. By definition, one-factor-at-a-time experiments cannot capture any interaction as all other factors are held constant while one factor is changed. A worked example adapted from Montgomery (1991) is included in Appendix A for completeness.

Factorial designs offer three main advantages over traditional one-factor-at-a-time experiments. Firstly, they are more efficient (relative improvement in efficiency increases with increasing factors). Furthermore, factorial design is necessary when interactions may be present to avoid erroneous conclusions. Lastly, factorial designs allow the effects of a factor to be estimated over several levels of other factors.

2.2.2.2 2^k, 3^k and Central Composite Factorial Design

A specific class of factorial designs and one of the simplest is the 2^k factorial design. Here an experiment with 'k' factors (variables) each taking two factor levels (0 and 1, low and high) is run where 0 and 1 represents the lower and upper bounds of a factor. For this study, there are three factors (m_{tnt}, b_f, R) and the required number of analysis to complete the study is eight (2^3).

A restriction on a 2^k design is that only linear relationships can be predicted, that is, only linear interactions between factors can be observed as the levels represent the extremes of the applicable ranges.   As the factors each take only two levels then it is not possible to predict any curvature in the response (you can only fit a straight line through two points).   The logical step is to design a 3^k experiment, 'k' factors at three levels (-1, 0 and 1), thus providing a midpoint that would allow to check for curvature.

Orthogonality is an important concept of factorial designs.   Orthogonality is the optimal design criterion as it minimizes the variance of the regression coefficients.   The attractiveness of this property is that the response is only a function of the distance from the design centre and not the direction (function of only R not θ if considering a polar co-ordinate system).   It therefore makes sense to use an experimental design that provides equal precision of estimation in all directions.   In using a 3^k design, the attractive feature of orthogonality is lost as 3^k designs are not 'orthogonal'.   Thus 3^k models exhibit a degree of bias depending upon the direction.

Clearly a design that retains the attractive property of orthogonality and has the ability to test for curvature (nonlinearity) is desirable.   One classification of design that meets these requirements is a central composite design (CCD).   Figure 2-3 shows a schematic representation of a CCD for $k = 2$.   The axes in the figures represent the factors (variables) and each point represents an experiment in the design with the location along the axes relating to the factor level (variable values).   By careful selection of the level α and the number of center points, points with co-ordinates (0,0) in Figure 2-3 , an experiment can be designed based upon the 2^k factorial design that tests for curvature and meets the orthogonality condition.   Setting $\alpha = \sqrt[4]{2^k}$ ensures an orthogonal design (Montgomery, 1991).   In a CCD design however, the extremes are no longer represented by -1 and 1 but by $-\alpha$ and $+\alpha$.
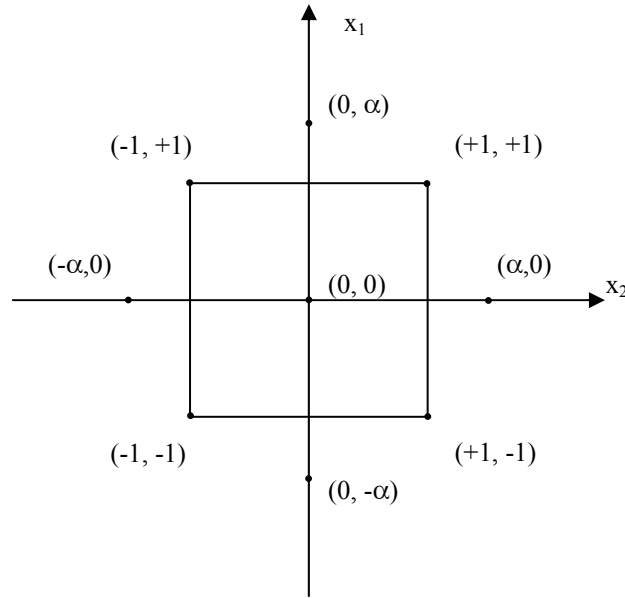
Figure 2-3: Schematic Representation of a General 2^2 Central Composite Design

2.2.2.3   Factors, Levels and Matrix of Experiments

The three factors considered here are charge mass, device stand-off and flange width.   The factorial design chosen was an 2^k orthogonal central composite design with $k = 3$ and $\alpha = 1.682$.   Table 2-2 contains the bounding values for the factors that are selected based upon realistic bounds on the physical problem.

The range of b_f was chosen based upon the minimum (0.3m) and maximum (0.5m) section widths commonly used in practice.   The range of m_{tnt} was determined based upon a 5kg satchel device being the minimum charge mass and a 1000kg vehicle device being the maximum.   The range on stand-off was decided based upon limits on scaled distance, with 3m being the minimum before scaled range became too small and 150m being a practical maximum.

The upper and lower bounds chosen for both stand-off and charge mass vary by orders of magnitude. In addition, from dimensional analysis, pressure and impulse vary with the inverse of the cube root of the mass rather than the mass.   Although the CCD design can predict curvature, to obtain best results, the range was made as linear as possible.   By taking the logarithm of the

bounds for stand-off and inverse of the cube root of mass, more linear ranges were achieved. The factor levels corresponding to $-\alpha$, -1, 0, 1, $+\alpha$ were determined based upon the modified bounds and are presented in Table 2-3.   Manipulation of these factor levels was required to obtain the physical values as input to the Air3d code.   Table 2-4 shows the matrix of experiments demonstrating the various combinations of factors and levels for the analysis. It should be noted that although DE procedures were used for experiment design, it became apparent from the results of analysis that variable interaction was minimal.

Table 2-2: Bounding Values for b_f, R & m_{tnt}

Factor	Lower Bound	Upper Bound
Flange width, b_f	0.3m	0.5m
Stand-off, R	3m	150m
Charge mass, m_{tnt}	5kg	1000kg

Table 2-3: Factor Levels

Factor Levels	$-\alpha$	-1	0	1	α
Flange width, b_f	0.300	0.341	0.400	0.459	0.500
Stand-off, $\log(R)$	0.477	0.821	1.327	1.832	2.176
Charge mass, $-0.33\log(m_{tnt})$	-0.233	-0.388	-0.616	-0.845	-1.000

Table 2-4: Matrix of Experiments

Run	Factor levels			Physical values		
	b_f	R	m_{tnt}	b_f (m)	R (m)	m_{tnt} (kg)
1	-1	-1	-1	0.341	6.63	14.6
2	-1	-1	1	0.341	6.63	341.7
3	-1	1	-1	0.341	67.87	14.6
4	-1	1	1	0.341	67.87	341.7
5	1	-1	-1	0.459	6.63	14.6
6	1	-1	1	0.459	6.63	341.7
7	1	1	-1	0.459	67.87	14.6
8	1	1	1	0.459	67.87	341.7
9	α	0	0	0.500	21.21	70.7
10	$-\alpha$	0	0	0.300	21.21	70.7
11	0	α	0	0.400	150.00	70.7
12	0	$-\alpha$	0	0.400	3.00	70.7
13	0	0	α	0.400	21.21	1000.0
14	0	0	$-\alpha$	0.400	21.21	5.0
15	0	0	0	0.400	21.21	70.7
16	0	0	0	0.400	21.21	70.7
17	0	0	0	0.400	21.21	70.7
18	0	0	0	0.400	21.21	70.7
19	0	0	0	0.400	21.21	70.7
20	0	0	0	0.400	21.21	70.7

2.2.3 Numerical Analysis

Numerical analysis was utilized to solve the matrix of experiments defined by DOE procedures. Numerical analysis presents various advantages over conventional experimentation provided that the algorithms involved are accurate, reliable and robust. Firstly, the cost associated with multiple tests is significantly less for numerical approaches than experimental methods. Secondly, more scenarios can be investigated allowing a better understanding of the problem. Finally, more information can be obtained from numerical methods as it is very difficult to instrument an experiment in a similar level of detail. Also, in the case of localized effects due to blast loading, it is highly unlikely that an experiment can be designed such that results other than qualitative can be obtained due to the small sampling rates, extreme deformations and volatile environmental conditions from the fireball.

2.2.3.1 Air3D Methodology

The numerical code used was Air3d (Rose, 2006), developed by Dr. Timothy Rose of Cranfield University specifically for examining the effects of blast waves on structures. The code solves the differential Euler equations of fluid mechanics, the tensorial representation is shown below in equation (2-17), using a finite difference method in both space and time.

$$\frac{\partial \rho}{\partial t} + \frac{\partial \rho u}{\partial x} = 0 \tag{2-17}$$

$$\frac{\partial \rho u}{\partial t} + \frac{\partial}{\partial x}\left(\rho u^2 + p\right) = 0 \tag{2-18}$$

$$\frac{\partial \rho}{\partial t}\left(e + \frac{u^2}{2}\right) + \frac{\partial}{\partial x}\left(\rho u^2 + p\right) = 0 \tag{2-19}$$

where ρ is the fluid density, u is the fluid velocity, p is the fluid pressure, e is the internal energy per unit mass for the fluid, $\partial/\partial t$ is the partial derivative with respect to time and $\partial/\partial x$ is the partial derivative with respect to space. Validation of Air3D was made using the HC curves. Results are shown in Figures 2-4 through 2-8. It is clear that Air3D provides good correlation with the HC data for the cases of side-on and reflected waves, predicting the general trends extremely well. The impulse calculated by Air3d is consistently lower than the HC values when

$Z > 2$, generally in the region of 15-20% less. Although not matching exactly, Air3d predicts the trends very well and given the uncertainty of blast loading and age of the HC data, a 20% difference is not unreasonable.
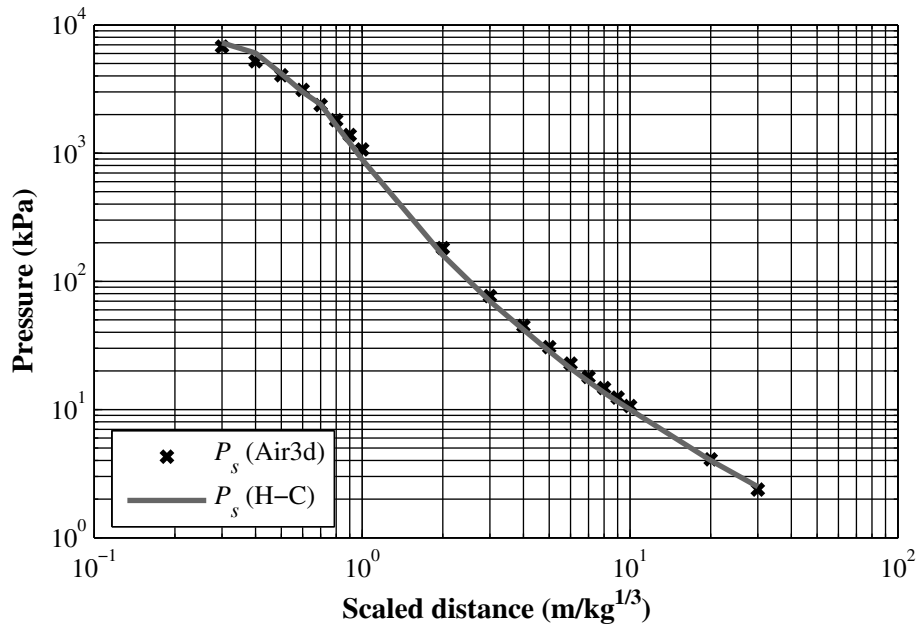
Figure 2-4: Comparison of Air3d Side-on Pressure with Hopkinson-Cranz Data
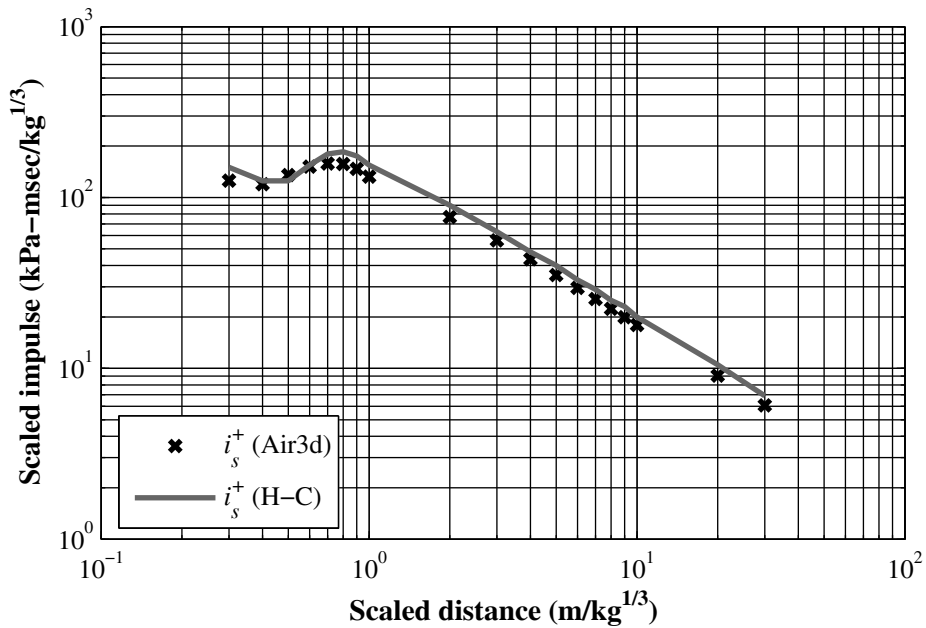
Figure 2-5: Comparison of Air3d Side-on Impulse with Hopkinson-Cranz Data
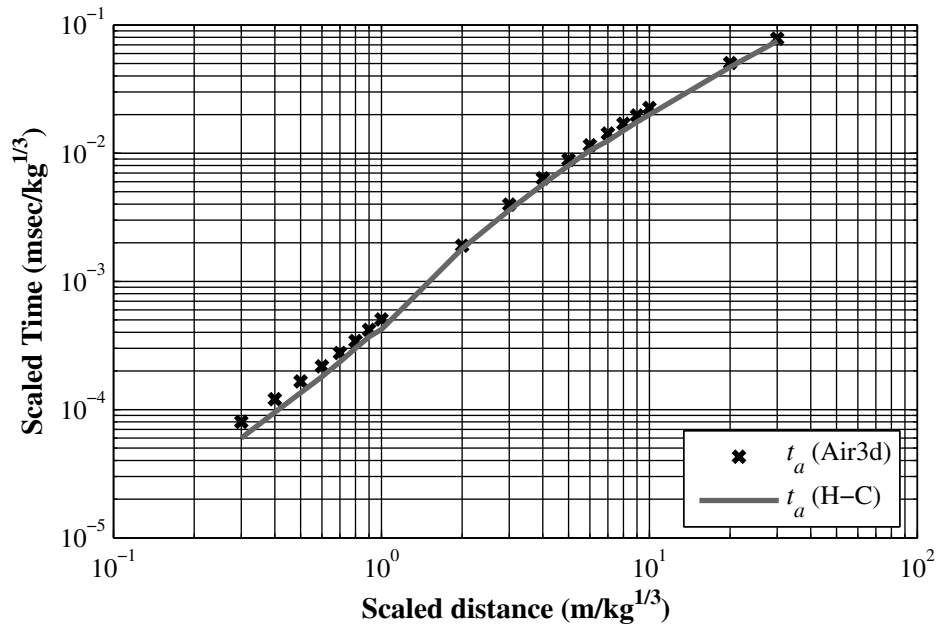
Figure 2-6: Comparison of Air3d Arrival Time with Hopkinson-Cranz Data
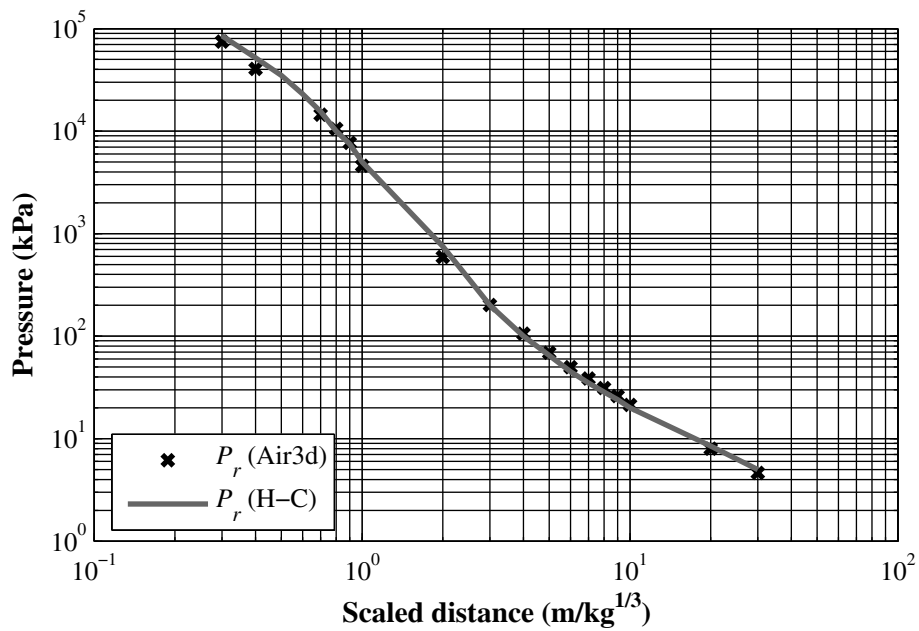
Figure 2-7: Comparison of Air3d Reflected Pressure with Hopkinson-Cranz Data
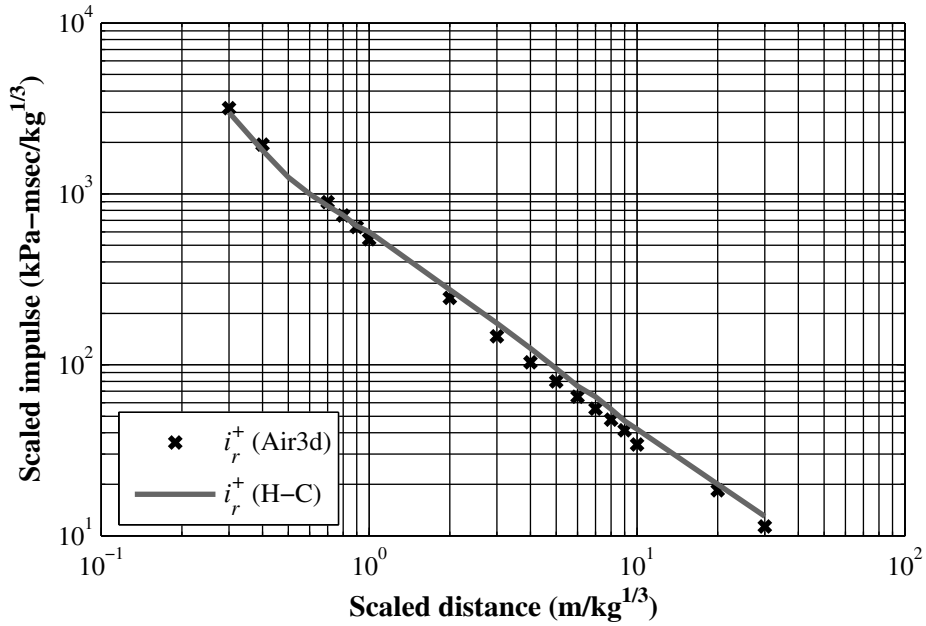
Figure 2-8: Comparison of Air3d Reflected Impulse with Hopkinson-Cranz Data

Air3d treats 3D analysis in a multi-stage process, whereby the 1D domain is solved then mapped to the 2D domain which in turn is solved before being mapped to 3D domain if required. The dimensionality of the analysis depends upon the input data provided, that is, only 1D input should be provided if a 1D analysis is required, 1D and 2D data should be provided if a 2D analysis is required and 1D, 2D and 3D data should be provided if the 3D analysis is required.

Each stage of an analysis uses a constant cell size specified by the user, although the cell size between stages can be different. The author of Air3d recommends a scaled cell size of $1\times10^{-3}\,m/\sqrt[3]{kg}$ for the 1D analysis to accurately capture the detonation process over a range of Z. No cell size is recommended for the subsequent analysis as it is largely controlled by the computational demand although the jump in cell size between 1D to 2D or 2D to 3D will affect the accuracy of the mapping procedure. =Only 2D analysis were performed in this study with the scaled cell sizes for 1D and 2D analysis of $5\times10^{-4}\,m/\sqrt[3]{kg}$ and $2.5\times10^{-3}\,m/\sqrt[3]{kg}$ respectively.

Air3d generates a domain based upon outer dimensions specified by the user, which then is discretized based upon the cell size (obtained by multiplying the scaled cell size with the cube root of the charge mass) specified for that stage of analysis.   In addition to the domain dimensions the charge mass is required to determine the initial energy of the analysis.

Reflective objects can be defined by creating geometric obstacles that void any cells whose midpoint is bounded by the obstacle edges and prevents their inclusion in the calculation, essentially behaving as a rigid surface.   The W-shape sections were created in this manner.

Data output can be defined by specification of monitoring locations in the domain; Air3d can output both temperature and pressure histories.   In order to define a monitoring location, the user specifies the co-ordinates of the desired monitoring locations in the domain for which Air3d outputs the data.   The data from a monitoring location is analogous to pressure transducers or thermocouples in the sense that no knowledge of the surface normal is included in the data, only a measure of pressure or temperature.   Thus the direction of impulse was assigned to the data manually to coincide with the surface normals.

2.2.4   Linear Regression Analysis

Linear regression analysis is a technique where observations are approximated using an assumed function and the quality of the prediction or 'goodness of fit' is assessed using statistical methods.   Linear Regression is covered in many texts, for example, Montgomery (1991) and Soong (2004) although a brief outline is presented below.   The simplest case of linear regression is when the observations are believed to be dependent upon only one variable.

2.2.4.1   Least-Squares Method of Estimation

Assuming that the random variable Y is a function of only one independent random variable x and their relationship is linear, that is

$$Y = \alpha + \beta x + \varepsilon \tag{2-18}$$

where α and β are regression coefficients and ε is the residual error. Using the least-squares method, estimation of α and β seeks to minimize the sum of the squared residuals. Consider the set $(x_1, Y_1), (x_2, Y_2), \ldots, (x_n, Y_n)$, rearranging equation (2-18) yields

$$\varepsilon_i = \hat{\alpha} + \hat{\beta} x_i - Y_i \qquad (2\text{-}19)$$

where $\hat{\alpha}$ and $\hat{\beta}$ are estimates of the regression parameters and ε_i is the residual at (x_i, Y_i). Minimization of the sum of the squared residuals allows us to estimate the regression coefficients as,

$$\hat{\alpha} = \bar{Y} - \hat{\beta}\bar{x} \qquad (2\text{-}20)$$

$$\hat{\beta} = \left[\sum_{i=1}^{n} (x_i - \bar{x})(y_i - \bar{y}) \right] \left[\sum_{i=1}^{n} (x_i - \bar{x})^2 \right]^{-1} \qquad (2\text{-}21)$$

Although the example presented considers only one variable, the process is identical for multivariable regression by simply including another regression coefficient for each random independent variable on which random variable Y depends. It is important to note that linear regression analysis provides meaningless results if the relationship between the random variable Y and the independent random variables is anything other than linear, even if a straight line appears to provide a good 'fit'.

SECTION 3

ANALYSIS, RESULTS AND DISCUSSION

3.1   Analysis

An analysis was performed using Air3d (Rose, 2006) for each of the 20 runs in the matrix of experiments presented in Table 2-4.   Pressure histories were output for the 44 monitoring locations, which were manipulated using Matlab (Mathworks, 2004) to obtain averaged pressure histories for each of the defined regions.   Region 1 comprises the front face of the front flange, region 2 the rear face of the front flange, region 3 the front face of the rear flange and region 4 the rear face of the rear flange (see Figure 2-2).   The advantage of breaking down the cross section in this fashion is that it permits examination of the influence of the average pressure history acting on each region.

3.2   Results

This results section is divided into two parts: 1) the results of the numerical analysis, and 2) the results of the linear regression analysis.   In all results, any reference to pressure is an overpressure, that is, relative to the ambient pressure.

Four different measures were used to examine different conditions.   Measure 1 considered the monitoring location in region 1 that lay closest to the web centerline.   If clearing was not present then this pressure history should return the same value of reflected impulse as the HC curves since Air3d and the HC curves for an infinite surface yield identical results (see Chapter 2). Measure 2 considered the average pressure history over region 1, thus giving a measure of the effect of clearing on reflected impulse.   Measure 3 considered the effect of wrap around on the open section (region 1 - region 2 + region 3 - region 4), to obtain the net pressure history on the open section.   The average pressure histories of all regions were summed in Matlab, based upon their surface normal to compute measure 3.   Measure 4 considered wrap-around of a closed (tubular) section with the same width and depth as the open sections.   This was achieved by considering only the average pressure histories of regions 1 and 4, again summed based upon their surface normal (region 1 - region 4).   In this measure, it was assumed that the effect of the open section does not significantly affect the pressure histories in region 4 (see Appendix B for

the validation) and therefore allows an estimation of the effect of 'encasing' open sections. Figure 3-1 compares the average pressure history for region 4 of a W-shape (neglecting the contribution of regions 2 and 3) and for a RHS of the same outer dimensions, for one of the validation cases of Appendix B. Clearly, there is minimal effect on the average pressure history.

The net reflected impulse imparted on the section for each measure was obtained by integration of the pressure histories with respect to time. The results were then compared to the HC values of reflected impulse.
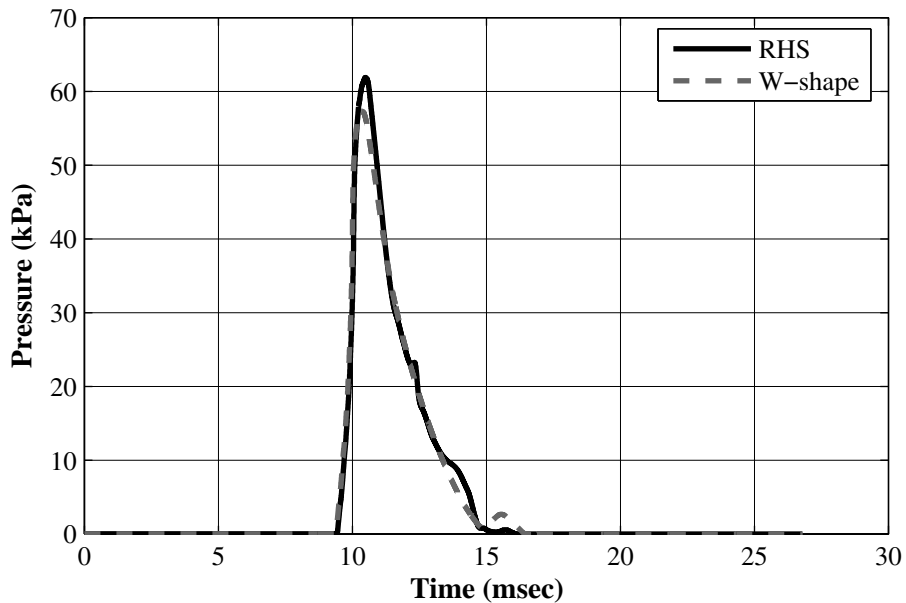
Figure 3-1: Comparison of the Average Back Face Pressure History for W-shape and RHS sections for $R = 6.63\text{m}$, $m_{tnt} = 14.6\text{kg}$ and $Z = 2.71\text{m}/\sqrt[3]{\text{kg}}$ with Section Outer Dimensions $b_f = 0.459\text{m}$, $d = 0.505\text{m}$

3.2.1 Numerical Analysis Results

Figure 3-2 and 3-3 overlay the average pressure histories per region and the pressure histories for each measure for a typical analysis, respectively. Figure 3-2 appears to have many additional peaks in the pressure histories, which is initially counter-intuitive. However, the individual histories can be explained by consideration of the interaction of the blast wave with the W-shape section. Consider the pressure histories for regions 1 and 4; both exhibit a single peak and decay to 0kPa (note that 0kPa overpressure corresponds to atmospheric pressure), which is the

expected profile for a blast wave. However, the pressure histories in regions 2 and 3 contain multiple peaks that appear to be out of phase. This is due to reflection from the flanges. As the wave engulfs the front flange, the rear face of the front flange experiences a side-on pressure (the first peak in the pressure history for region 2). The wave then propagates towards the rear flange, striking the front face of the rear flange that experiences a reflected pressure (the first peak in the pressure history for region 3). This reflected pressure wave then propagates back towards the front flange striking the rear face of the front flange as a reflected pressure causing the second peak in region 2's pressure history (which has a higher magnitude than the first peak). Meanwhile, the initial wave has engulfed the rear face of the rear flange, thus region 4 experiences a side-on pressure. Region 1 and 4 demonstrate typical profiles for a blast wave because they are not subjected to the repeated reflections that regions 2 and 3 experience from the wave reflecting back and forward between the flanges.

The region 1 peak reflected pressure, arrival time and load duration from Figure 3-2 is 255kPa, 8msec and 4.5msec respectively. For $Z = 2.17\,\mathrm{m}/\sqrt[3]{\mathrm{kg}}$ and $m_{tnt} = 14.6\,\mathrm{kg}$ the HC curves give 282kPa, 7.5msec and 5.7msec for reflected pressure, arrival time and load duration which gives percentage differences of 9.6%, 6.3% and 21.0%. Although the difference is between 5 - 20% (for the particular scaled distance and charge mass under consideration), given that there is an averaging process being performed and clearing effects are included the values are clearly of the correct order.

The side-on pressure for $Z = 2.17\,\mathrm{m}/\sqrt[3]{\mathrm{kg}}$ from the HC curves is 86.8kPa (0.87bar), which gives a reflection coefficient of 2.94 based upon a peak reflected pressure of 255kPa. The reflection coefficient from Figure 1-6 for a side-on pressure of 0.87bar and $\alpha = 0$ is approximately 2.7. These comparisons, whilst not yielding exact agreement demonstrate that the Air3d results are of the correct order. A more involved validation of the calculated measure values is contained in Appendix B.
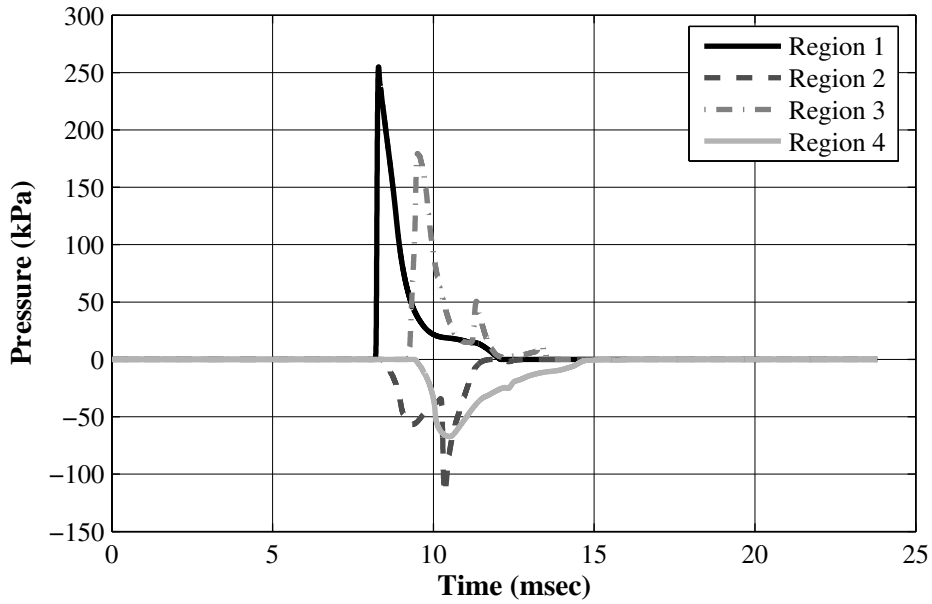
Figure 3-2: Sample Average Pressure Histories for Each Region for $R = 6.63\text{m}$ **,**
$m_{tnt} = 14.6\text{kg}$ **and** $Z = 2.71\,\text{m}/\sqrt[3]{\text{kg}}$
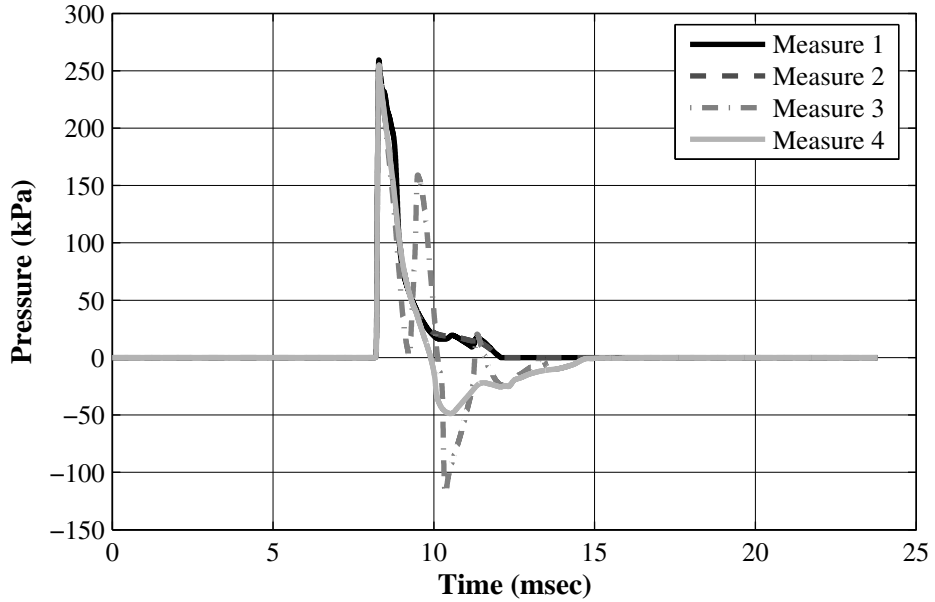
Figure 3-3: Sample Pressure Histories for each Measure for $R = 6.63m$ **,** $m_{tnt} = 14.6kg$
and $Z = 2.71m/\sqrt[3]{kg}$

Figure 3-3 presents interesting findings regarding the individual measures. The histories for measure 1 and 2 are almost identical indicating that effect of clearing is constant along the flange width (for the given charge mass, stand-off and flange width). Measure 3 and 4 both have significant regions of negative impulse opposing the positive impulse from region 1, suggesting that the net impulse for these measures will be substantially lower.

Figures 3-4 through 3-7 show the reflected impulse for each measure and the HC reflected impulse plotted against scaled distance. All 20 analyses from the matrix of experiments are plotted, although there appears to be fewer data points in Figure 3-4. This is related to the scalability of impulse; many of the analyses share identical values of Z. Thus as the scaled impulse is the same for any given Z, the data points lie exactly on top of each other (note also that runs $16 - 20$ in the matrix of experiments are identical and as such the results are identical also). As can be observed from the figures, all points are below the HC curves, therefore reduction in impulse from that predicted by the HC curves is present in all measures.

In Figure 3-4, there appears to be only 9 data points. As explained above, this is because a number of analyses share a common value of Z and the flange width does not affect measure 1 as only one monitoring location at the center of the flange is considered. Figure 3-5, however, has 15 data points indicating that the flange width does have an effect on the averaged pressure history and subsequently the impulse. Measure 1 and 2 are both approximately proportional to $1/Z$.

Figures 3-6 and 3-7 have the 15 data points, again because flange width is included in the calculation of impulse. The effect of flange width is small compared to the negative impulse portions for these measures, which was highlighted in the discussion of Figure 3-3. Measures 3 and 4 appear to be approximately proportional to $1/Z^2$ rather than $1/Z$ as is the case for measures 1 and 2.
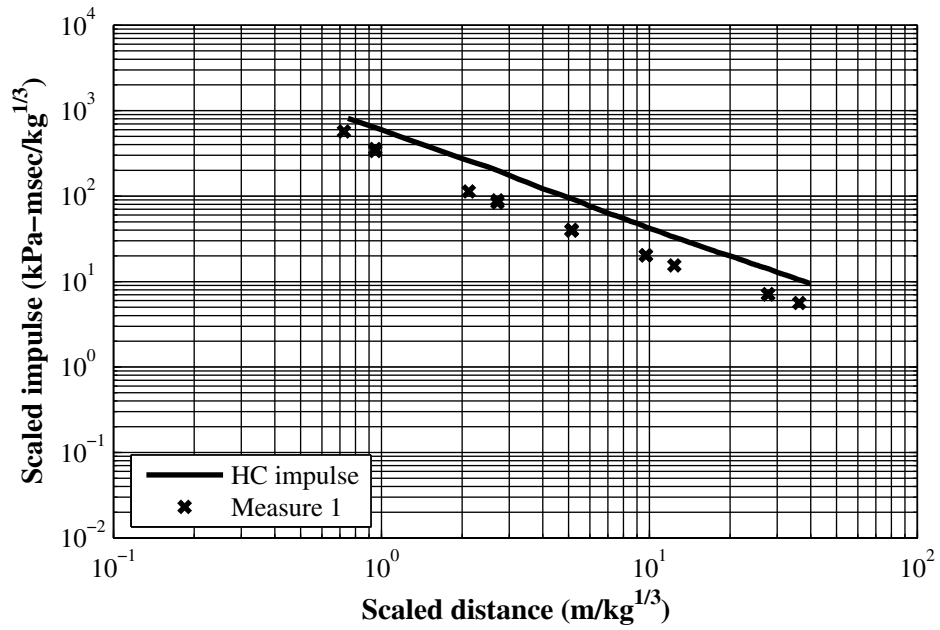
Figure 3-4: Comparison of Measure 1 to HC Reflected Impulse vs. Scaled Distance
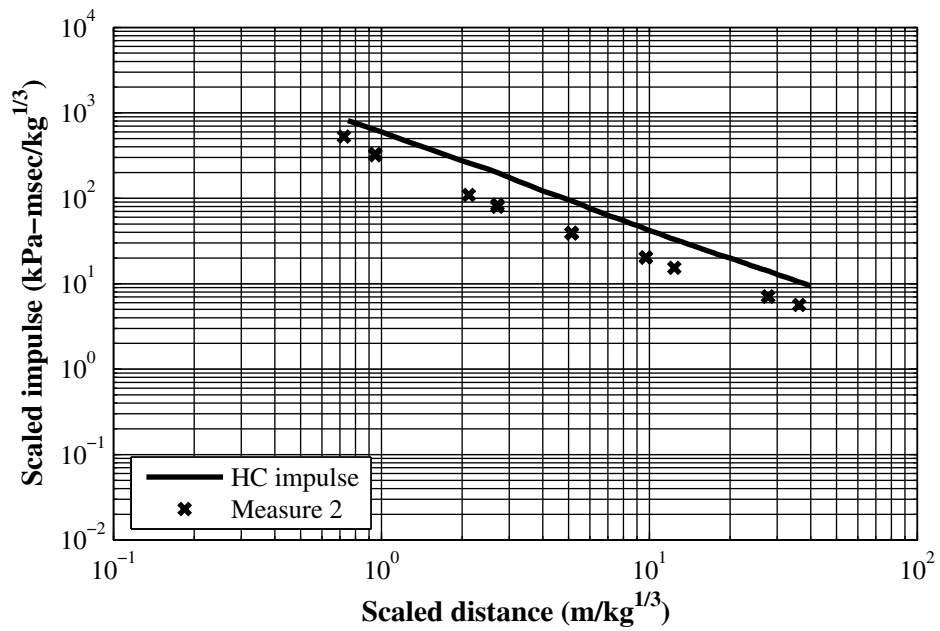
Figure 3-5: Comparison of Measure 2 to HC Reflected Impulse vs. Scaled Distance
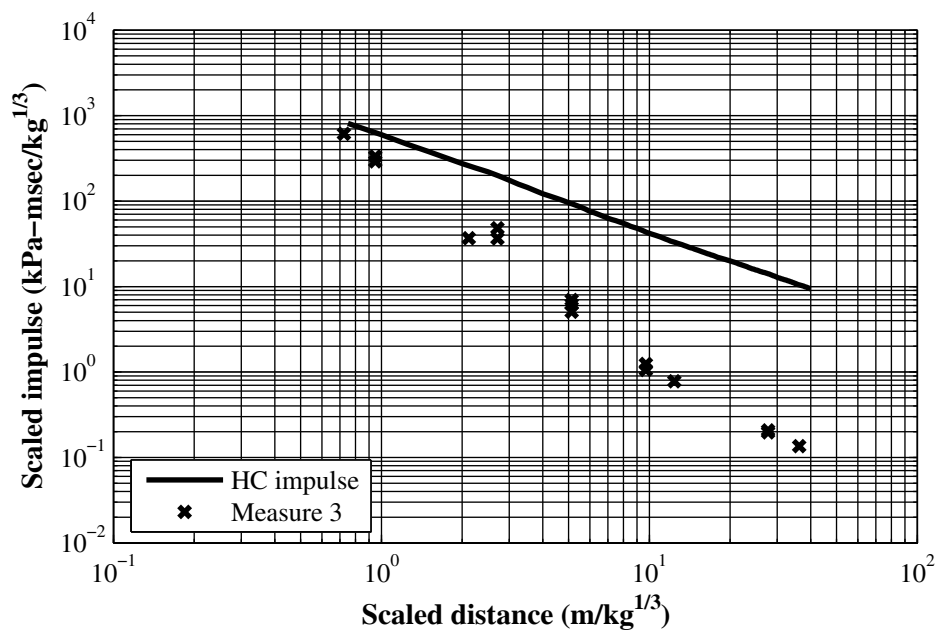
Figure 3-6: Comparison of Measure 3 to HC Reflected Impulse vs. Scaled Distance
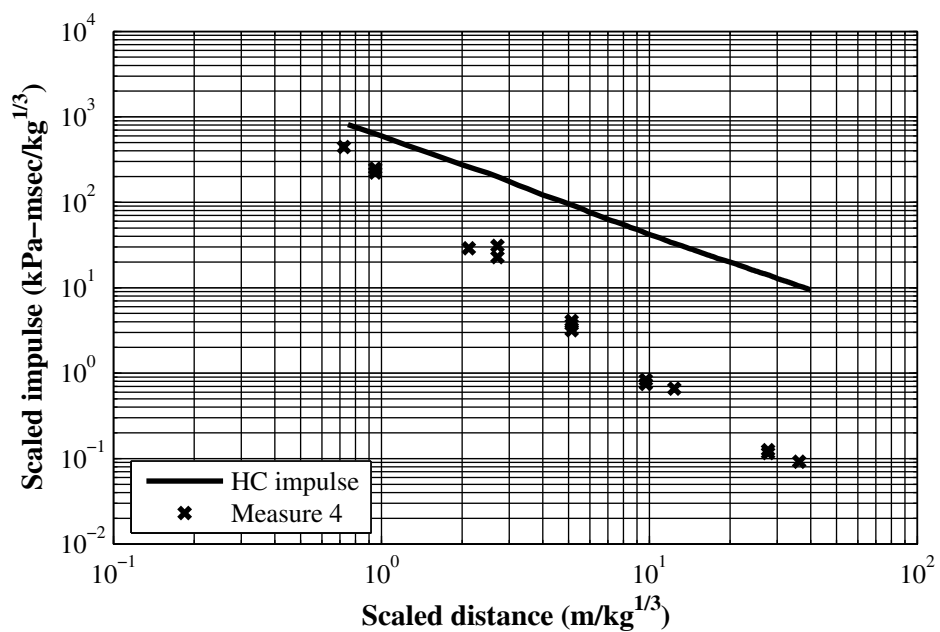
Figure 3-7: Comparison of Measure 4 to HC Reflected Impulse vs. Scaled Distance

The reflected impulse reduction factor, relative to the HC curves, is shown in Figures 3-8 through 3-11, and is defined as

$$\eta_n = \frac{i_n^+}{i_{HC}^+} \tag{3-1}$$

where η_n is the reduction factor for the nth measure, i_n^+ is the net reflected impulse for the nth measure and i_{HC}^+ is the positive impulse from the HC curves (that do not consider clearing effects).

Figures 3-8 and 3-9 indicate that for measures 1 and 2 the reduction factor is constant over a wide range of scaled distance, where η_1 and η_2 average around 50%. Figures 3-10 and 3-11, however, indicate significant reductions in reflected impulse with respect to HC with increasing scaled distance. For Z larger than $11\,\mathrm{m}/\sqrt[3]{\mathrm{kg}}$ the reduction factor is approximately 0.02 that suggests for measure 3 and 4 the impulse will be 2% of the HC reflected impulse that does not account for either clearing or wrap-around.

As described previously, measure 3 considers a W-shape section subject to wrap around and measure 4 considers a rectangular hollow section with the same outer dimensions as the W-shape. Figures 3-12 and 3-13 plot the ratio of η_1 to η_2 and η_3 to η_4, respectively. Figure 3-12 reveals that η_2 is always smaller than η_1 and that the ratio approaches unity as Z increases. This would be expected as η_2 includes the effect of clearing at the flange extremities, whereas, η_1 considers the pressure history at the web centerline that will experience smaller clearing effects.

Figure 3-13 shows that η_3 is always larger than η_4 and in general, η_3/η_4, increases with increasing Z. This would be expected as measure 3 has a two reflective faces compared to measure 4's single reflective surface. Figure 3-14 shows a plot of the difference between the

reduction factors for measures 3 and 4, defined in equation (3-2) below, which can help the reader identify the impact of open versus closed sections.

$$\delta\eta = \frac{i_3^+ - i_4^+}{i_{HC}^+} = \eta_3 - \eta_4 \tag{3-2}$$

Figure 3-14 reveals that as Z increases the benefit of closing or encasing a column section becomes smaller, as the difference between the measure 3 and 4 impulses becomes small relative to the HC impulse. Thus, despite Figure 3-13 showing that η_3 is approximately a factor of 1.6 greater than η_4 when $Z = 20\,\mathrm{m}/\sqrt[3]{\mathrm{kg}}$, Figure 3-14 shows that for $Z > 10\,\mathrm{m}/\sqrt[3]{\mathrm{kg}}$ the benefit is only an additional 1% of the HC impulse. Given that η_3 is around 3% of the HC value for $Z > 10\,\mathrm{m}/\sqrt[3]{\mathrm{kg}}$, the benefit of encasing W-shape sections is likely small.
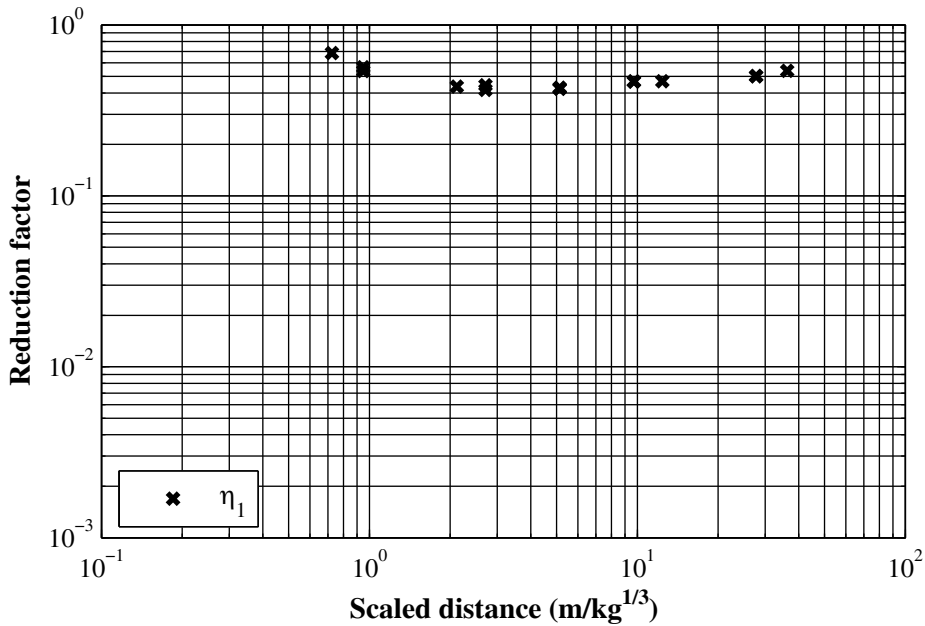
Figure 3-8: Measure 1 Reduction Factor, η_1, vs. Scaled Distance
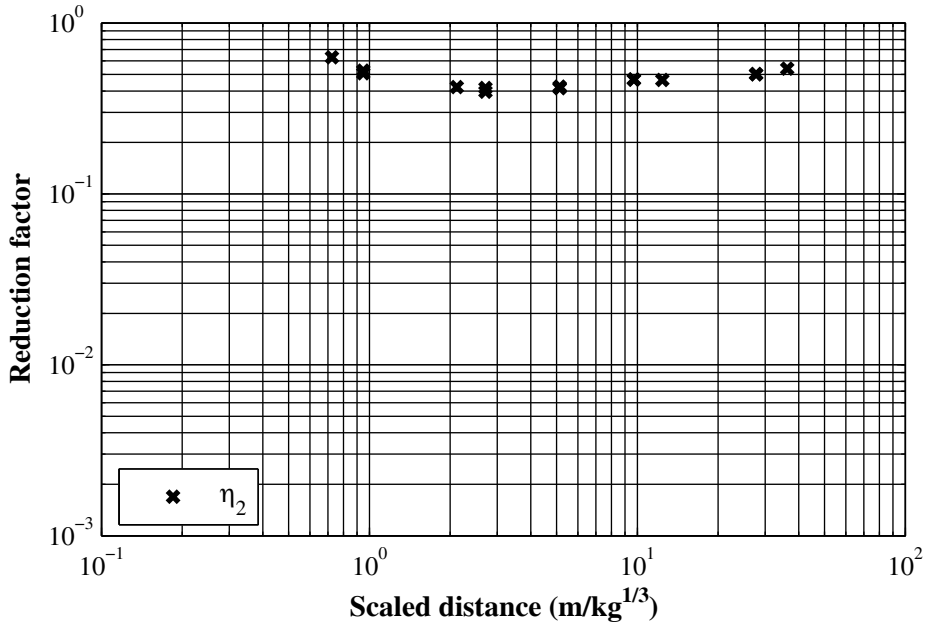
Figure 3-9: Measure 2 Reduction Factor, η_2, vs. Scaled Distance
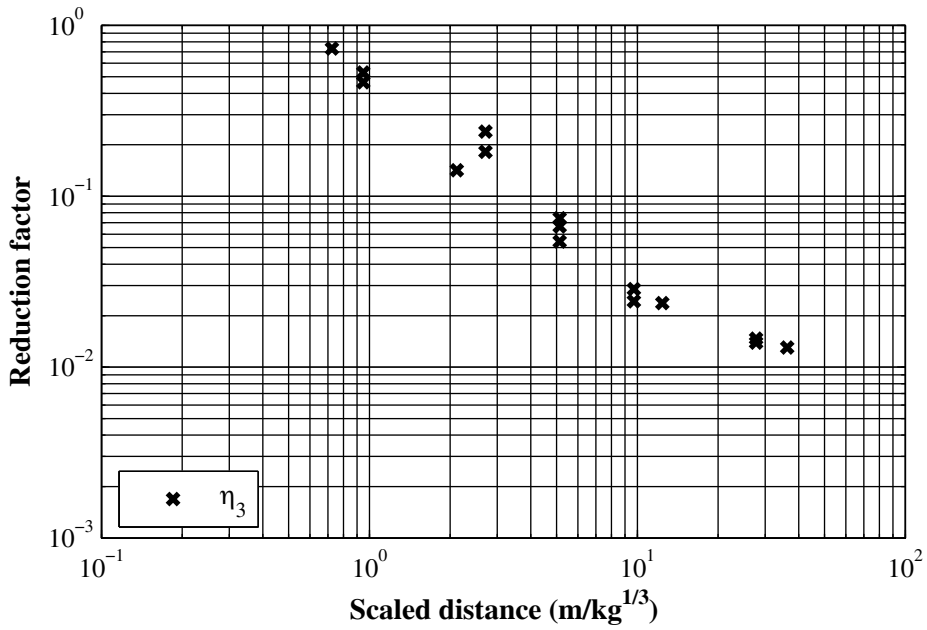
Figure 3-10: Measure 3 Reduction Factor, η_3, vs. Scaled Distance
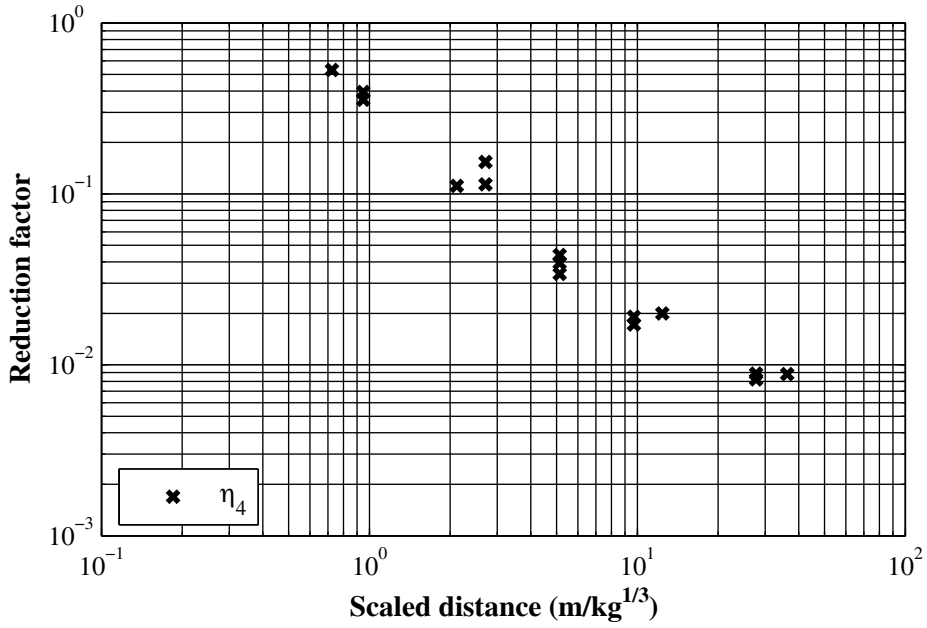
Figure 3-11: Measure 4 Reduction Factor, η_4, vs. Scaled Distance
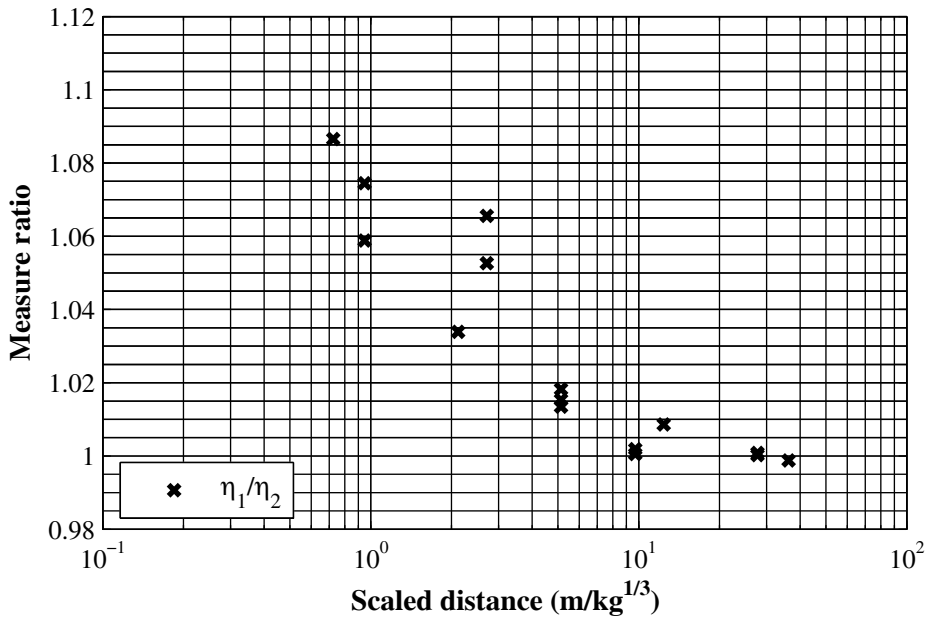
Figure 3-12: η_1/η_2 vs. Scaled Distance
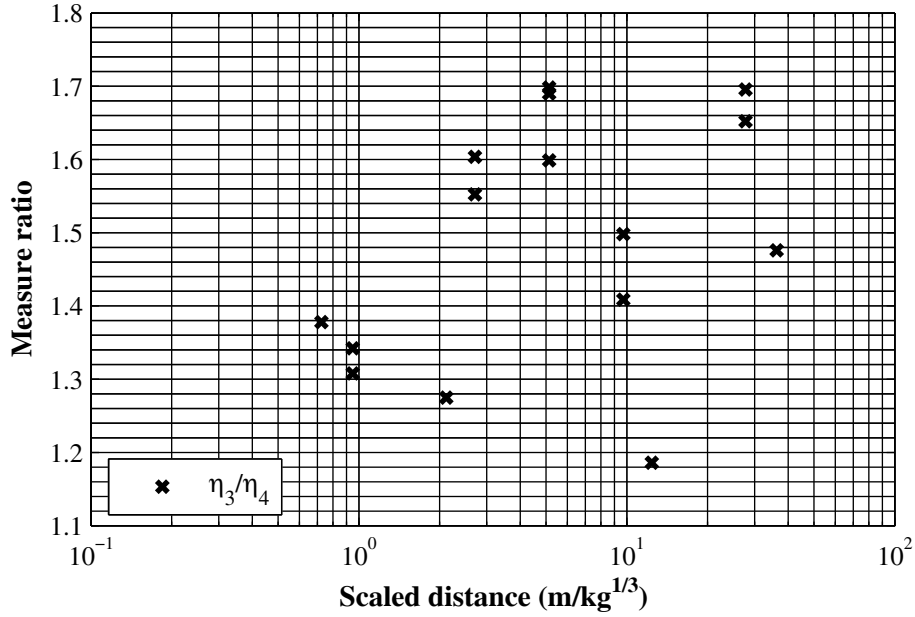
Figure 3-13: η_3/η_4 **vs. scaled distance**
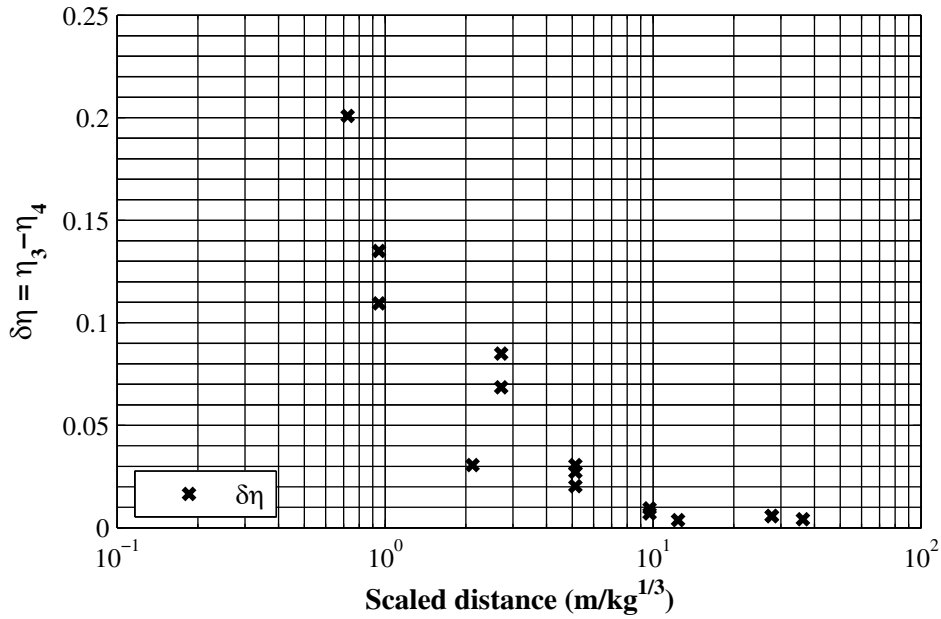
Figure 3-14: $\delta\eta = \eta_3 - \eta_4$ **vs. Scaled Distance**

3.2.2 Linear Regression Results

Linear regression analysis was performed on the data to determine relationships between reflected impulse (i^+), scaled distance (Z) and scaled flange width $\left(l = b_f / \sqrt[3]{m_{tnt}}\right)$. The

selection of scaled distance and scaled flange width as regression variables came from the dimensional analysis performed in Chapter 2, the general form of the regression equation utilized is shown below in equation (3-3).

$$\hat{y} = 10^{\hat{\beta}_0} x_1^{\hat{\beta}_1} x_2^{\hat{\beta}_2}$$
(3-3)

Taking the logarithm of equation (3-2) yields the following relationship;

$$\log_{10}(\hat{y}) = \hat{\beta}_0 + \hat{\beta}_1 \log_{10}(x_1) + \hat{\beta}_2 \log_{10}(x_2)$$
(3-4)

Equation (3-3) demonstrates that when plotted on a log-log scale, the regression parameters β_1 and β_2 represent the slope of the line $\hat{y}$ with respect to x_1 and x_2. Equations (3-5) through (3-15) below show the regression equations for the measures previously defined.

$$i_1^+ = 10^{2.483} l^{0.017} Z^{-1.162}$$
(3-5)

$$i_2^+ = 10^{2.438} l^{0.001} Z^{-1.138}$$
(3-6)

$$i_3^+ = 10^{2.790} l^{0.338} Z^{-2.271}$$
(3-7)

$$i_4^+ = 10^{2.574} l^{0.290} Z^{-2.297}$$
(3-8)

$$\eta_1 = 10^{-0.312} l^{-0.001} Z^{-0.027}$$
(3-9)

$$\eta_2 = 10^{-0.356} l^{-0.017} Z^{-0.003}$$
(3-10)

$$\eta_3 = 10^{-0.005} l^{0.320} Z^{-1.137}$$
(3-11)

$$\eta_4 = 10^{-0.220} l^{0.272} Z^{-1.163}$$
(3-12)

$$\eta_1/\eta_2 = 10^{0.044} l^{0.016} Z^{-0.024}$$
(3-13)

$$\eta_3/\eta_4 = 10^{0.216} l^{0.048} Z^{0.026}$$
(3-14)

$$\delta\eta = \eta_3 - \eta_4 = 10^{-0.464} l^{0.379} Z^{-1.080}$$
(3-15)

As previously mentioned, the exponents in equations (3-4) through (3-15) represent the slope of the each equation in the log-log space (can also be thought of as the proportionality), thus given

the small contribution of scaled flange width, DE procedures were not used to investigate variable interaction.. Consider the value of the exponent on Z for equations (3-5) through (3-8). The values confirm the observation made earlier that the reflected impulse for measures 1 and 2 is approximately proportional to $1/Z$ whereas for measures 3 and 4, the reflected impulse is proportional to $1/Z^2$.

Figures 3-15 through 3-25 show the linear regression trendlines fitted through the numerical analysis data presented above in Figures 3-4 through 3-14. Three trendlines are plotted in each figure. The light gray dashed line represents the maximum scaled flange width which was calculated as the largest flange width (0.5m) divided by cube root of the minimum charge mass (5kg), hence, $l_{max} = 0.5/\sqrt[3]{5} = 0.29 \, \text{m}/\sqrt[3]{\text{kg}}$. The dark gray dashed line represents the minimum scaled flange width which was calculated as the smallest flange width (0.3m) divided by cube root of the maximum charge mass (1000kg), hence, $l_{min} = 0.3/\sqrt[3]{1000} = 0.03 \, \text{m}/\sqrt[3]{\text{kg}}$. The light gray solid line represents an average scaled flange width, which was calculated as the average of the maximum and minimum scaled flange widths, hence, $l_{mean} = (0.29 + 0.03)/2 = 0.16 \, \text{m}/\sqrt[3]{\text{kg}}$. The solid black line shown in Figures 3-15 through 3-18 represents the HC impulse, which is included for comparison. It should be noted that linear regression should not be used for extrapolation, thus l_{max} and l_{min} represent the upper and lower bounds on the scaled flange width. Equations (3-4) through (3-15) are only valid for scaled distance $1 \, \text{m}/\sqrt[3]{\text{kg}} \leq Z \leq 30 \, \text{m}/\sqrt[3]{\text{kg}}$.
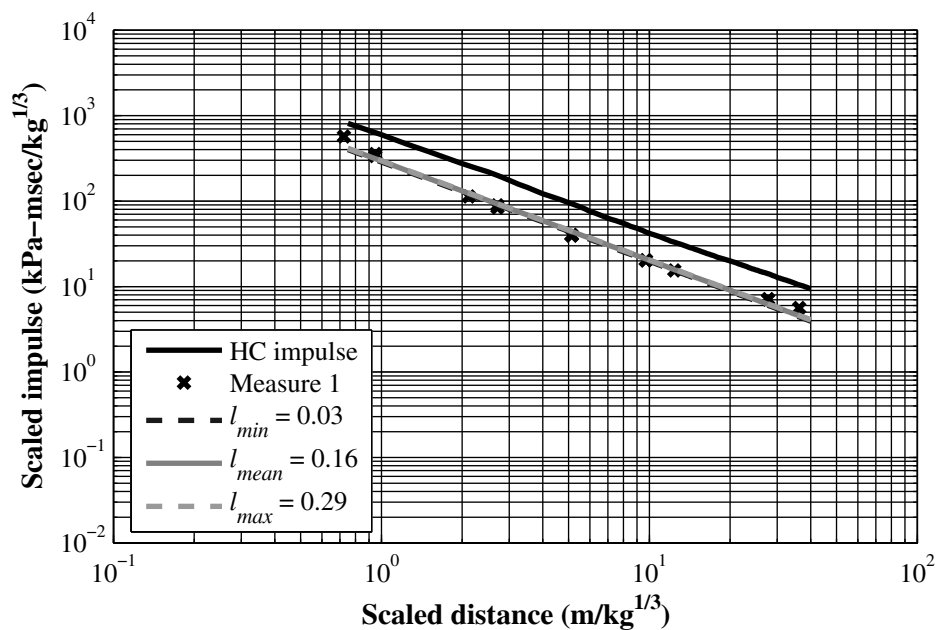
Figure 3-15: Comparison of Measure 1 Trendlines to HC Reflected Impulse
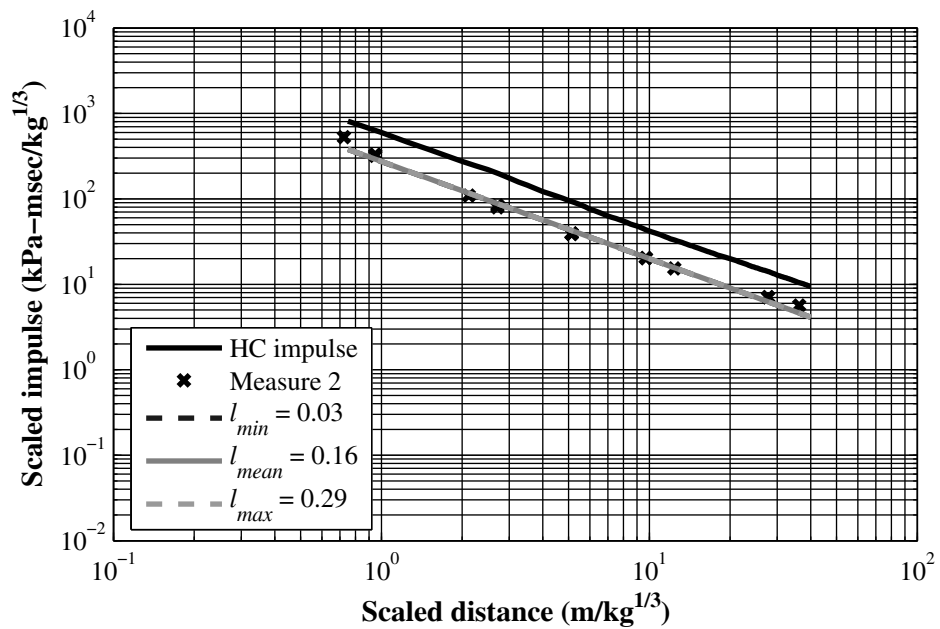
Figure 3-16: Comparison of Measure 2 Trendlines to HC Reflected Impulse
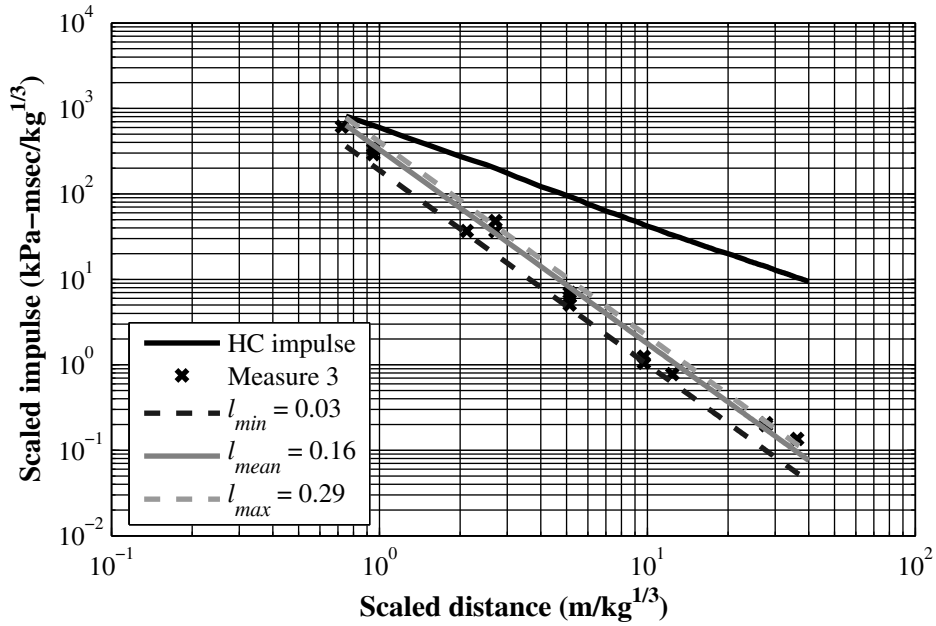
Figure 3-17: Comparison of Measure 3 Trendlines to HC Reflected Impulse
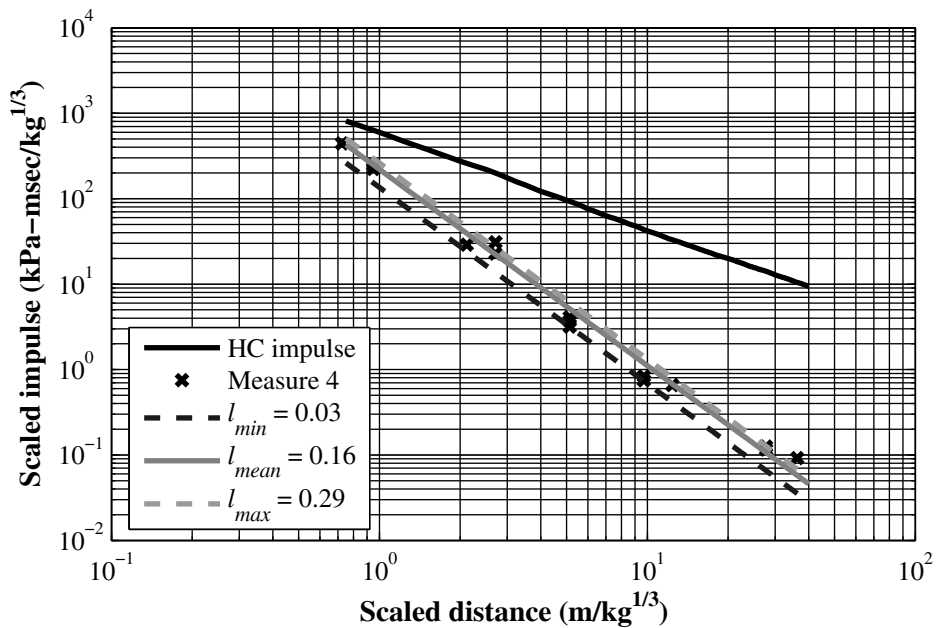
Figure 3-18: Comparison of Measure 4 Trendlines to HC Reflected Impulse

In most figures, all data points are bounded by the maximum and minimum values of scaled flange width. The reduction factor trendline is essentially constant for measures 1 and 2 for both scaled distance and flange width, which is confirmed in Figures 3-19 and 3-20 (the percentage difference between the measure and HC reflected impulse is constant). Figures 3-21 and 3-22

show that the reduction factors for measure 3 and 4 have the same slope as that of the HC reflected impulse. This is related to the relative magnitude of the Z exponents for the measures and the HC reflected impulse. This can easily be demonstrated by considering equations (3-6) and (3-7), from which;

$$i_{HC} \propto Z^{-1.15} \tag{3-14}$$

$$i_{3,4}^{+} \propto Z^{-2.30} \tag{3-15}$$

The reduction factor, η, which has been defined earlier as the ratio of the Air3d reflected impulse to the HC reflected impulse, see equation (3-1), is therefore proportional to;

$$\eta_{3,4} \propto \frac{Z^{-2.30}}{Z^{-1.15}} \propto Z^{-2.30-(-1.15)} \propto Z^{-1.15} \tag{3-16}$$
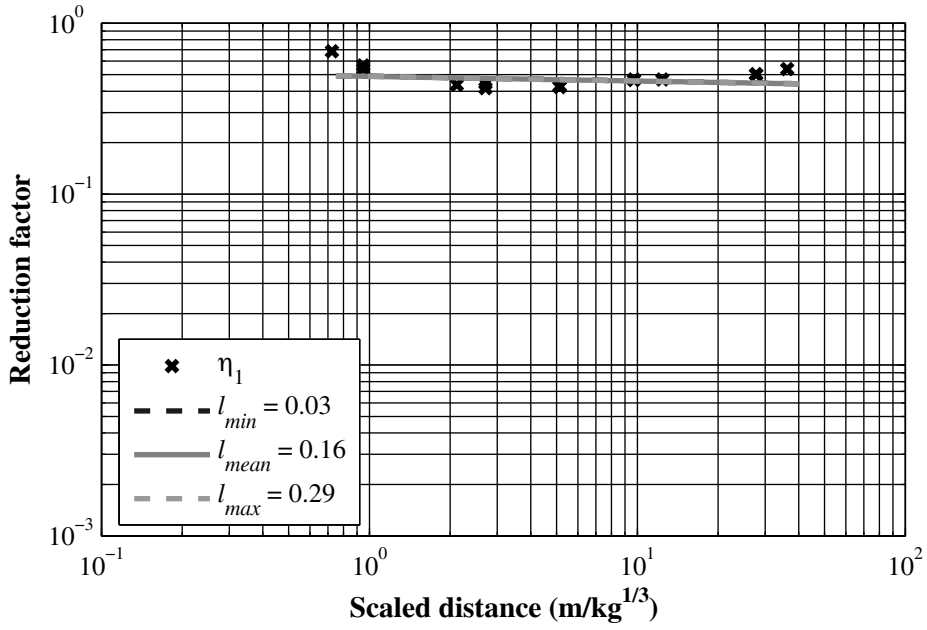
Figure 3-19: Reduction Factor, η_1, Trendlines
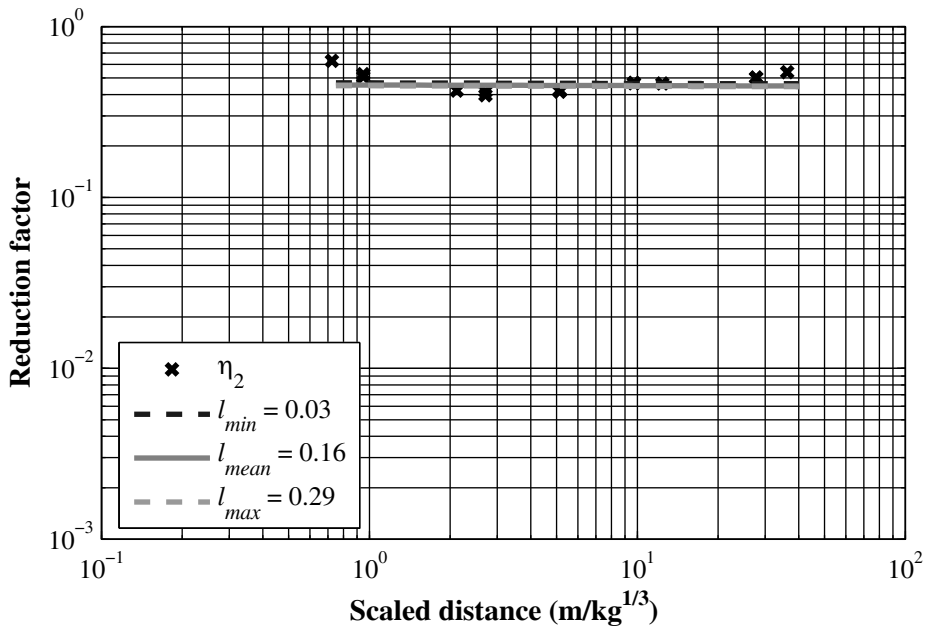
Figure 3-20: Reduction Factor η_2 Trendlines
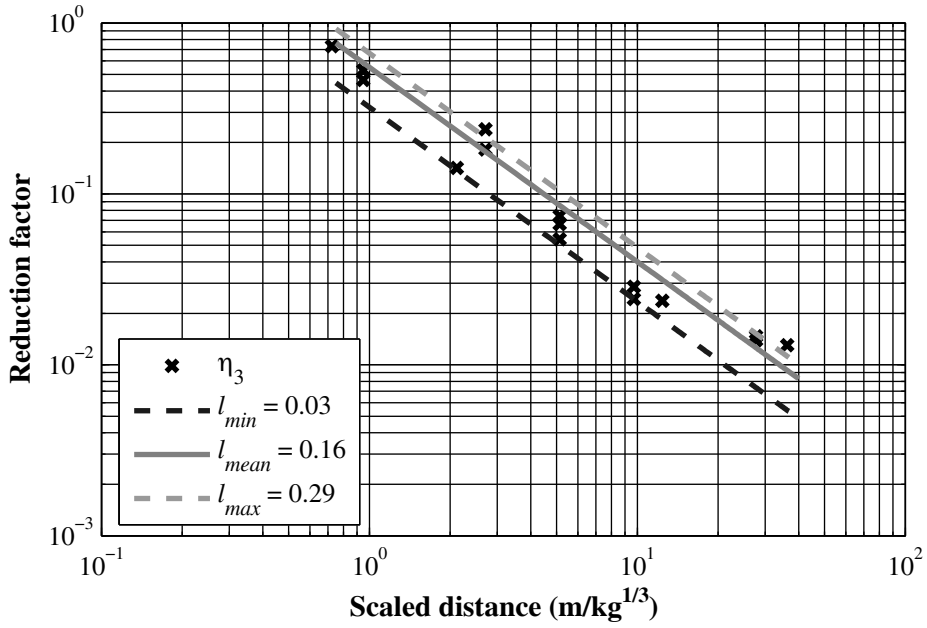
Figure 3-21: Reduction Factor η_3 Trendlines
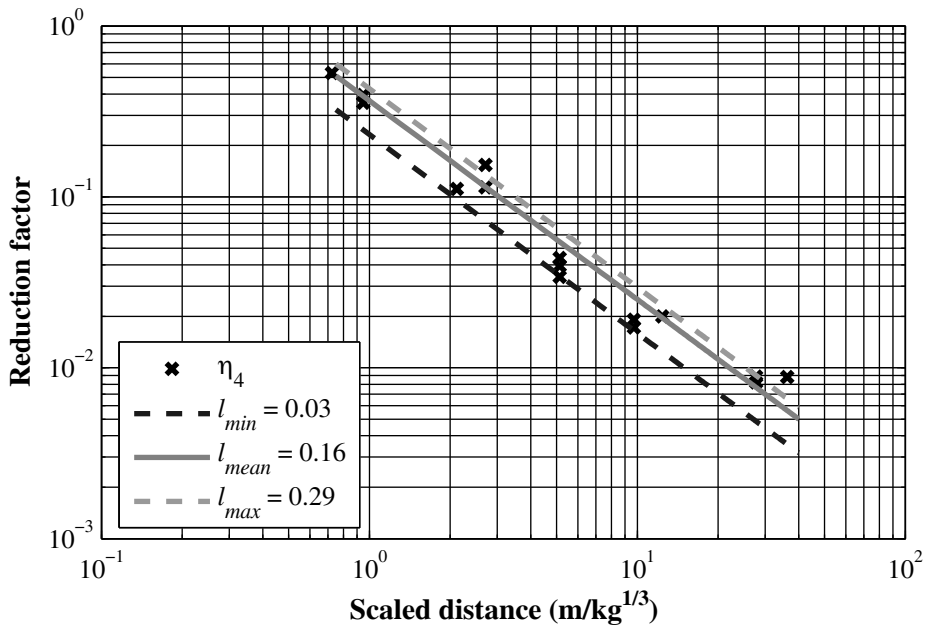
Figure 3-22: Reduction Factor η_4 Trendlines
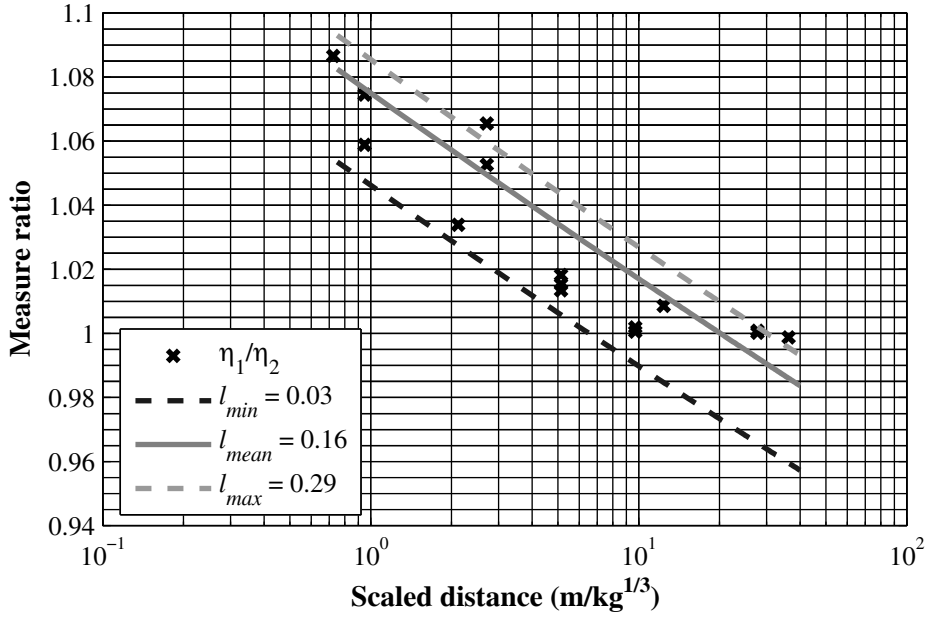
Figure 3-23: η_1/η_2 **Trendlines**
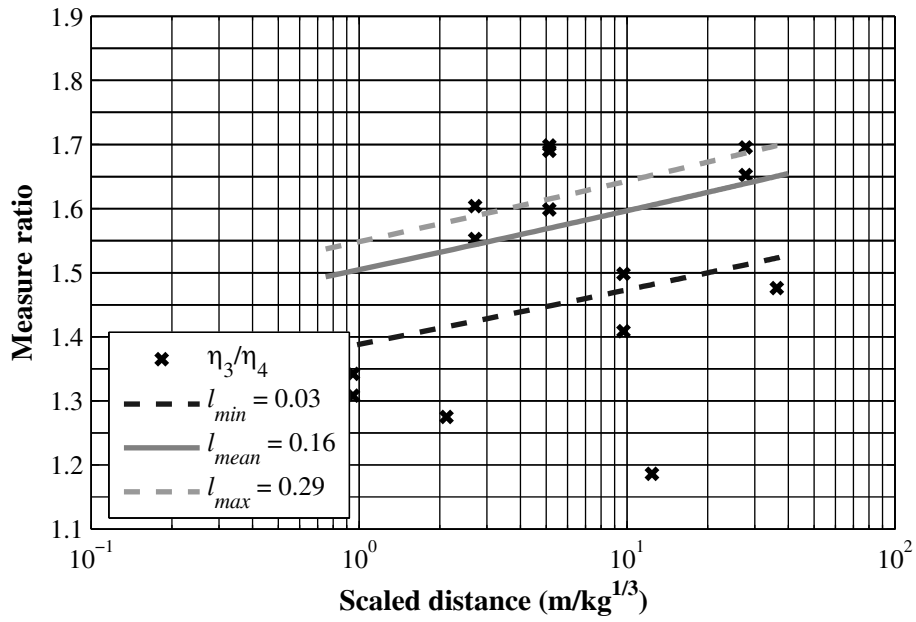
Figure 3-24: η_3/η_4 **Trendlines**
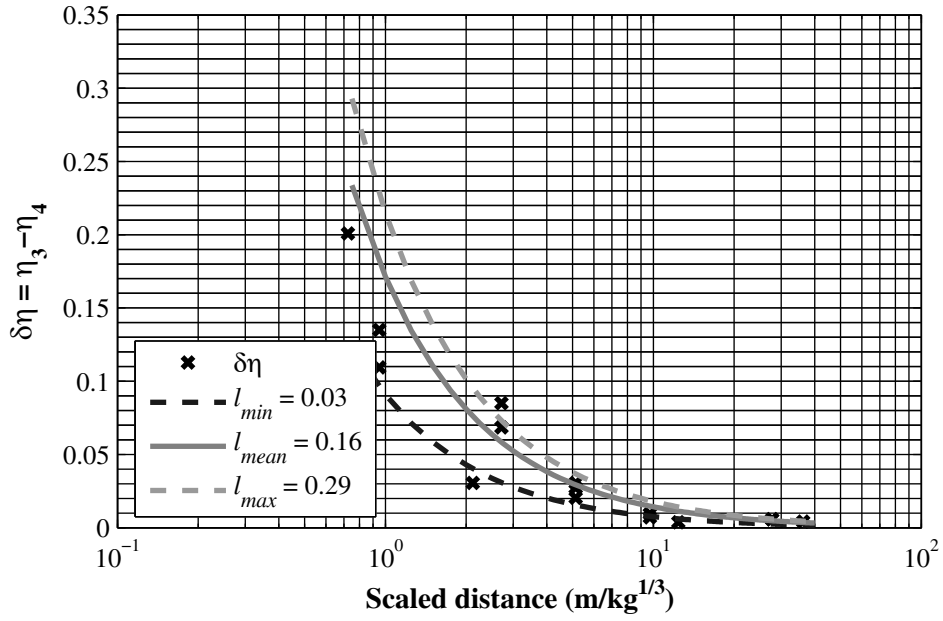
Figure 3-25: $\delta\eta$ **Trendlines**
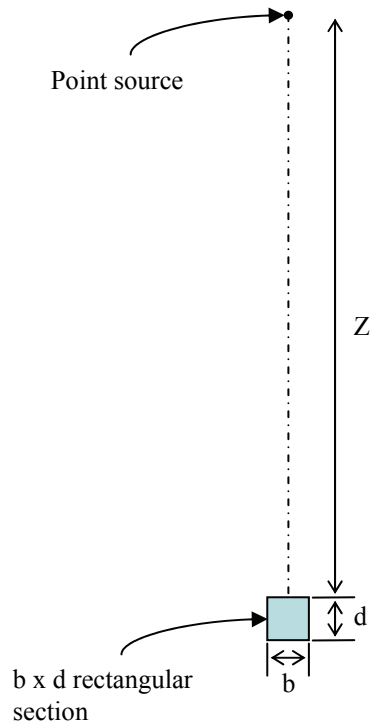
Figure 3-26: Schematic for Z^{-2} **Proof**

3.3 Discussion

It is clear that the values of impulse are much lower for a finite surface than for an infinite surface. Examination of the presented figures, along with equations (3-5) through (3-15) enables the following observations.

Firstly, examination of Figures 3-15 through 3-18 suggests that the effect of scaled flange width is modest in comparison to the effect of scaled distance, merely increasing the scatter in the results. The trendlines for measures 1 through 4 shown in Figures 3-8 through 3-11 support this observation by demonstrating that, in general, the scatter of the observed values of impulse are bounded by the maximum and minimum scaled flange width for all measures.

Secondly, the rate of decay of impulse with scaled distance, when accounting for wrap-around effects (measures 3 and 4) is much higher than that of the HC curve and measures 1 and 2. This can be observed by considering the slope of the trendlines in Figures 3-15 through 3-18 and from equations (3-5) through (3-18). As mentioned in section 3.1.2, the regression parameters represent the slope of the line when plotted on a log scale. Consider equations (3-5) through (3-18). The equations suggest that when wrap-around is considered the impulse is approximately proportional to Z^{-2}, that is, impulse is proportional to the inverse of the scaled distance squared. For infinite surfaces, the impulse is proportional to Z^{-1}, thus, on a log-log scale the impulse decays twice as rapidly when the section dimensions are finite.

This observation implies that, for sections which can be considered finite, as scaled distance increases the value of impulse decays rapidly and is substantially lower than the impulse for an infinite section at the same scaled distance. A physical interpretation of this observation is related to the relationship of reflection coefficient and scaled distance. As scaled distance becomes large, the reflection coefficient tends toward 2 in the absence of clearing according to Figure 1.6 with $\alpha = 0$. It was demonstrated in Appendix B that the time taken for the front face to clear from a reflected pressure to a side-on pressure is a fraction of the loading duration for typical W-shape sections, resulting in the front-face pressures having similar orders of magnitude as the rear-face pressures. If the pressures experienced by the rear face of the W-shape section

are considered 'canceling' pressures, at large scaled distances the canceling pressures are approximately equal to the reflected pressures, resulting in a very large percentage reduction in the impulse. A mathematical proof is presented below.

Consider Figure 3-12, a rectangular object of scaled dimensions $b \times d$ with front surface located at a scaled distance Z from a point source. From equation (3-5), the side-on impulse on the front face is approximately;

$$I_1 \propto \frac{1}{Z} \qquad\qquad (3\text{-}18)$$

and on the back face is

$$I_2 \propto \frac{1}{Z+d} \qquad\qquad (3\text{-}19)$$

The net impulse on the section is approximately;

$$I_1 - I_2 \propto \frac{1}{Z} - \frac{1}{Z+d} \qquad\qquad (3\text{-}20\text{a})$$

$$I_1 - I_2 \propto \frac{1}{Z}\left(1 - \frac{Z}{Z+d}\right) \qquad\qquad (3\text{-}20\text{b})$$

By performing a Taylor series expansion of the fraction within brackets in equation (3-20b) and truncating after the second term, it is possible to write the net impulse as;

$$I_1 - I_2 \propto \frac{1}{Z}\left(1 - \left(1 + \frac{-d}{Z}\right)\right) \qquad\qquad (3\text{-}20\text{c})$$

$$I_1 - I_2 \propto \frac{d}{Z^2} \qquad\qquad (3\text{-}20\text{d})$$

For the proof to be valid $b \ll Z$ and $d \ll Z$ must be satisfied, which for most member sections and threats will be the case.

The final observation is that the main benefit of encasing a W-shape section or filling the voids between the flanges of a W-shape section is at scaled distances lower than $10\,\mathrm{m}/\sqrt[3]{\mathrm{kg}}$ as although the ratio of η_3 to η_4 increases with increasing Z, at $Z > 10\,\mathrm{m}/\sqrt[3]{\mathrm{kg}}$, η_4 is already less than 0.05. Surprisingly, the shape or scaled width of the section has a minimal effect on impulse if compared to the effect of scaled distance, provided that the section is finite.

SECTION 4

CONCLUSION

4.1   Introduction

In general, current design procedures for blast loading involve application of simplified SDOF procedures to member design.   Two distinct approaches exist depending upon the dynamic properties of the system. For members (or structural systems) whose natural period of response is of similar magnitude or smaller than the loading duration, a quasi-static approach is utilized whereby the wave reflected pressures are the critical loading parameter.   Alternatively, for members (structural systems) whose natural period is much greater than the loading duration, initial conditions can be derived based upon the impulse imparted on the system by the blast wave.   Blast wave pressure histories can be defined using four key parameters: arrival time, load duration, peak pressure and reflected impulse.   Empirical relationships (HC curves) defining these parameters were derived from experimental data but are generally applicable to reflective surfaces that are infinite in size.   This is primarily a result of the research at that time being focused on the effects of atomic and nuclear weapons.   However, for the situation where conventional and improvised explosives are being used and individual members of structural systems are being analyzed and designed, the reflective surfaces are far from infinite.

The goal of this work was to investigate whether reductions in impulse could be observed due to the finite dimensions of a structural section.   Prior to the study, two main mechanisms were proposed that could potentially lower the impulse imparted on the member: clearing and wrap-around.   The conclusions of the study are presented below.

4.2   Conclusions

The main conclusions of the analytical studies described above are;

- When a section can be considered finite, the impulse is approximately proportional to Z^{-2} rather than Z^{-1} that applies for an infinite surface.   This effect is primarily due to the wrapping of the blast wave around the cross section although there is a contribution from clearing.   The consequence of this result is that as Z increases, the impulse

decreases rapidly, allowing a structural member to be designed for a much smaller impulse.

- The reduction in scaled impulse due to clearing is approximately constant at 50% for the range of scaled distance and scaled flange width considered in the study.

- The effect of section width is small when compared to the effect of scaled distance, provided the section width is small enough for the section to be considered 'finite'. In this study, a typical depth-to-breadth ratio of 1.1 was assumed thus the effect of section depth could not be examined in a detailed manner. However, provided that depth is small enough to be considered 'finite' the effect is most likely minimal.

- The effect of the chosen structural shape appears small when compared to the effect of scaled distance and the plan dimensions of the section can be considered to be finite. Being open or closed does not alter the scaled impulse on a section significantly if compared to the effect of the section being regarded as finite. However, at scaled distances below $10\,\text{m}/\sqrt[3]{\text{kg}}$, the influence of the structural shape becomes more important than at scaled distances greater than $10\,\text{m}/\sqrt[3]{\text{kg}}$.

4.3 Recommendations

As with most developments, further work is required to substantiate and refine the conclusions. This study identified that reflected impulse is heavily influenced by the cross-section size (finite or infinite) but additional studies are required. A discussion of further work and recommendations is contained below.

Firstly, the effect of section orientation has not been investigated as all cases in this study involved sections whose front surface was tangent to the shock front. A section which is loaded at an oblique angle may be more sensitive to the structural shape.

Furthermore, the conclusions of the report whilst being generally applicable will most likely breakdown in certain regimes. For example, at what scaled width and depth can a section be considered 'finite' or the range of scaled distance at which the structural shape has more influence on the results? Identification of such regimes is an important next step.

Further work to confirm the 3S/U calculation of clearing time (developed for atomic weapons effects) for conventional high explosives would enable use of the derivations and calculations, presented in manuals, in the open literature.

In addition, the rigid material assumption should be investigated further if only to gain additional confidence in the assumption. This, however, is not a simple task and would require highly complicated numerical analysis that can robustly deal with material non-linearity and fluid-structure interaction.   The main restriction on this type of work is material modeling of structural grade steel in these types of applications (this restriction in itself represents a significant academic challenge).

We used Air3d extensively for this study. Although Air3d is specifically intended for air-blast calculations, some additional features would be most useful.   During the solution process, the software only provides pressure and temperature data.   Access to the velocity components for the entire domain would greatly help in visualizing and interpreting results.   In Air3d, the whole domain from burst point to section (and more) has to be solved for every analysis. Significant computational effort is spent solving for cells that do not yield information of ongoing use.   An alternative approach would be to use computational fluid dynamics (CFD), which could offer a number of benefits.   CFD calculates the coupled velocity and pressure fields involved in fluid dynamics and can therefore provide additional information about the scenario.   In solving the coupled velocity and pressure fields more computational effort per timestep is required. However, this increase can be offset by CFD's ability to only model the local domain around the structural shape, dramatically reducing the number of cells in the model.   Another benefit of CFD is that most of the current commercial codes provide a framework for some level of fluid-structure interaction, an area which has already been identified as needing further work.   The final benefit of a CFD approach is that the post processing features would allow much more detailed visualization of the solved variables resulting in better understanding of the flow around the section.

Finally, and most importantly, the analytical results from this study from Air3d have no physical data to be compared to although it has been benchmarked against some forms of blast data.

CFD has even less validation in the field of blast wave propagation and supporting physical experiments are crucial before claims on the predicted reductions are made by the engineering community.

SECTION 5

REFERENCES

American Institute of Steel Construction (AISC), *AISC Blast Guide*. Chicago, IL 2006

American Society of Civil Engineers (ASCE), *ASCE Blast Standard*. Ballot version, Reston, VA 2007

Baker W.E., Cox P.A., Westine P.S., Kulesz J.J. and Strehlow R.A. *Explosion Hazards and Evaluation*. Elsevier, 1983.

Biggs J.M. *Introduction to Structural Dynamics*. McGraw-Hill, 1964.

Carslaw H.S. and Jaeger J.C. *Conduction of Heat in Solids*. Oxford University Press, 2nd Edition, 1959.

Cranz C. *Lehrbuch der Ballistik*. Springer-Verlag, Berlin, 1926.

Department of the Army (DOA). *Design of structures to resist the effects of accidental explosions*. U.S Department of the Army Technical Manual TM5-1300. Washington DC, 1990.

Greenberg M.D. *Advanced Engineering Mathematics*. Prentice Hall, 2nd Edition, 1988.

Hopkinson B. *British Ordnance Board minutes*. 13565, 1915.

Kingery C.N. and Bulmash G. *Airblast parameters from TNT spherical air burst and hemispherical surface burst*. Technical Report ARBRL-TR-02555. US Armament Research and Development Center, Ballistic Research Laboratory, Aberdeen Proving Ground, MD, April 1984.

Mathworks. MATLAB – The Language of Technical Computing, Version R14. The Mathworks, Inc. , 2004

Merrifield, R. and Wharton, R. *Measurement of the size, duration and thermal output of fireballs produced by a range of propellants*. Propellants, Explosives, Pyrotechnics, 25, pp. 179-185, 2000.

Meyers, M. A. Dynamic Behavior of Materials. John Wiley & Sons, 1994

Montgomery D.C. *Design and Analysis of Experiments*. John Wiley & Sons, 1991.

Norris C.H. *Structural Design for Dynamic Loads*. McGraw-Hill, 1959.

Rankine W.J.H *Phil. Trans. Roy. Soc.*, 1870, 160, 277-288.

Ritzel, D. Personal communication. 2008.

Rose T.A. *Air3d Version 9.0 – Computational Tool for Airblast Calculations*. Engineering Systems Department, Cranfield University, UK 2006

Roy R.K. *A Primer of the Taguchi Method*. Van Nostrand Reinhold,1990.

Sachs R.G. *The Dependence of Blast on Ambient Pressure and Temperature*. BRL Report 466, Aberdeen Proving Ground, MD, 1944.

Smith P.D. and Hetherington J.G. *Blast and Ballistic Loading of Structures*. Butterworth-Heinemann, 1994.

Soong T.T. *Fundamentals of Probability and Statistics for Engineers*. John Wiley & Sons, 2004.

APPENDIX A

FACTORIAL DESIGN

A.1 Introduction

The concept of factorial design was introduced in Chapter 2, however, lengthy discussions and cumbersome examples were avoided to improve the readability of the report. This appendix provides more detail of factorial designs through discussion of the advantages and a worked example.

A.2 Advantage of Factorials

There are three main advantages in factorial design, namely 1) they are more efficient than one-factor-at-a-time (OFAT) experiments, 2) factorial designs allow estimation of the interaction of factors, and 3) after interaction effects have been captured, then the influence of a factor at several levels of the other factors can be estimated, improving the robustness of the conclusions. Each of these advantages is explained in more detail below.

A.3 Efficiency

Typically in experimentation, OFAT experiments are used where only one variable or factor is varied and the others held constant. Factorial designs only ever have two or three levels, therefore only require 2^k or 3^k experiments (where 2 or 3 is the number of levels and k is the number of factors). The improvement in efficiency comes from the fact that in general, fewer factor levels are required to obtain the same level of information.

A.4 Interaction Effects

The second advantage of factorial designs is that the interaction between factors can be captured. For example, if we say y is a function of the factors (variables) A, B and C such that $y = f(A,B,C)$ and that factors take on two levels $(A_1, A_2; B_1, B_2; C_1, C_2)$.

When interaction effects are not present, then the change in y by changing from A_1 to A_2 is unaffected by the relative value of the factors (the change in response by changing a factor is called the 'main effect' of that factor). When interaction is present, the change in y is dependant upon the level of factors B and C. That is, when factor B is at level B_1, changing from A_1 to A_2

may cause an increase in y, however, when level B is at B_2 the same change from A_1 to A_2 may cause a reduction in y (this change in response is called the 'interaction effect' of those factors). It is this type of interaction that factorial designs can capture and OFAT experiments cannot. The significance of this is that wrong conclusions may be drawn based upon an OFAT experiment in which interaction is present, particularly when the interaction effect causes a change in the response that is of a similar order as the main effect.

A.5 Improved Robustness

Often in experimentation, linear regression is performed upon the data to be able to interpolate for factor levels (variable values) that were not examined in the actual experiments.   The danger of not capturing interaction effects is that the linear regression model is not being fitted to the appropriate data and cannot predict any existing interaction, leading to regression results that are unreliable at best and useless at worst.   By using factorial designs, it is possible to capture interaction of factors and therefore generate a more reliable and robust regression model that can be confidently used to interpolate between the factor levels.

A.6 Worked Example

A worked example taken from Montgomery (1991) to illustrate the effect of interaction is shown below. Let the main effect be the difference between the average responses at the different levels, thus there can be a main effect for each factor.

Consider the two data sets in Table A-1 for an experiment without interaction and with interaction, where A and B are factors in the response of Y.   For data set I, the main effect of A is

$$A_I = \frac{40+52}{2} - \frac{20+30}{2} = 21 \tag{A-1}$$

where the first term is the average response of Y with A at level 2 and the second term is the average response of Y with A at level 1.   Increasing factor A from level 1 to level 2 increases the average response by 21 units.   Similarly for factor B, the main effect is

$$B_I = \frac{30+52}{2} - \frac{20+40}{2} = 11 \tag{A-2}$$

When the difference in response is not the same at all levels, interaction is said to exist. Consider data set II, at the first level of B, the A effect is

$$A_{B_1} = 50 - 20 = 30 \tag{A-3}$$

and at the second level of factor B, the A effect is

$$A_{B_2} = 12 - 40 = -28 \tag{A-4}$$

Clearly from equations (A-3) and (A-4) the effect of A is not the same at the two levels of B. This suggests interaction between A and B. The main effect of A in this example is

$$A_{II} = \frac{50+12}{2} - \frac{20+40}{2} = 1 \tag{A-5}$$

Since the main effect of A is small, it suggests that there is minimal effect on the average response due to A, however, in the presence of significant interaction 'main effects' can be dwarfed by 'interaction effects'. Figure A-1 and A-2 show plots of response against factor for both data sets I and II. In Figure A-1 shows that the lines for factor B at levels I and II run parallel, demonstrating little or no interaction, while Figure A-2 shows the lines are not parallel. Clearly the ability to capture interaction effects is important.

Table A-1: Sample Data Sets

Data set I – no interaction	Data set II – with interaction

	B₁	B₂
A₁	20	30
A₂	40	52

	B₁	B₂
A₁	20	40
A₂	50	12
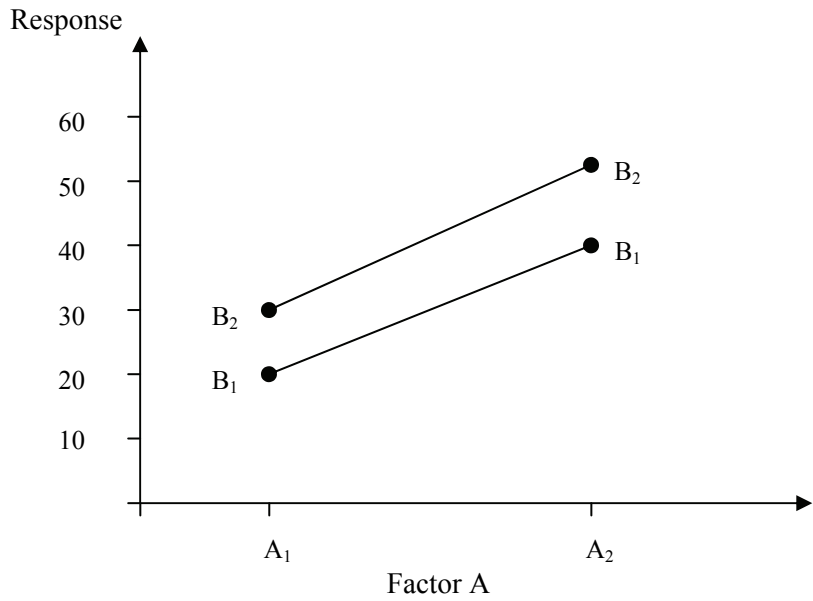
Figure A-1: Response Plot for Data Set I
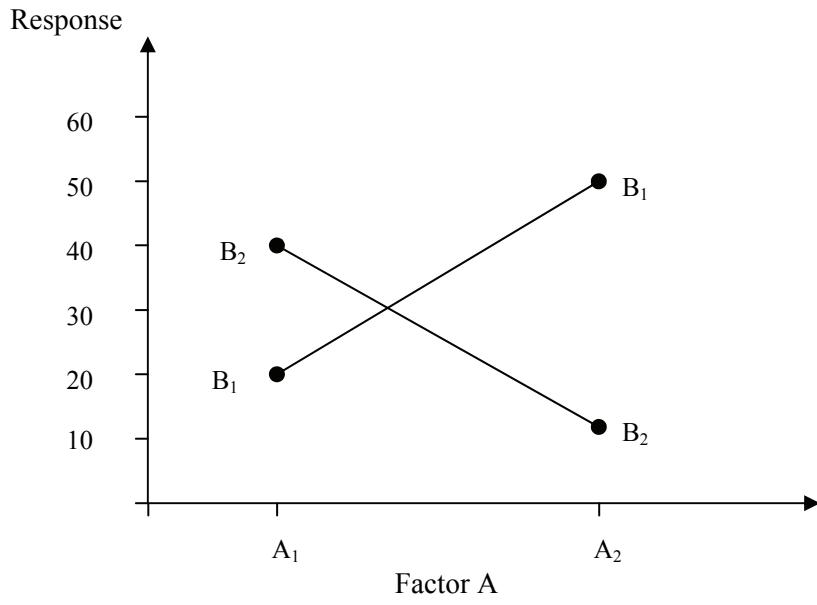
Figure A-2: Response plot for data set II

APPENDIX B

AIR3D VALIDATION

B.1 Introduction

Although Air3d was validated against the HC curves for side-on and reflected pressure and impulses in Chapter 2, further validation is required to have confidence in the results of the study.

Each of the four measures, defined in Chapter 3, is interrogated in detail for a selected combination of $R = 6.63\text{m}$, $m_{tnt} = 14.6\text{kg}$ and $b_f = 0.459\text{m}$. The measures are treated in sequential order, beginning with Measure 1.

B.2 Measure 1

Measure 1 is defined as the impulse at the 1st monitoring point (located on the front face of the front flange, closest to the web centerline). In the absence of clearing, the impulse returned for measure 1 should match exactly with CONWEP and the HC curves. Table B-1 below shows data for measure 1 from Run 5 where $R = 6.63\text{m}$, $m_{tnt} = 14.6\text{kg}$, $Z = 2.71\text{m}/\sqrt[3]{\text{kg}}$ and $b_f = 0.459\text{m}$.

Firstly, consider the values of P_r in Table B-1; HC, CONWEP and Air3d all predict a very similar value for reflected pressure. This is an expected result because peak reflected pressure is not affected by clearing. Similarly, the three values of t_a are most similar. For reflected impulse, i_r^+, HC and CONWEP are within 20% of each other, but the Air3d result is approximately 50% of the HC and CONWEP values. Norris (1959) proposed that the time taken for the reflected pressure to clear a surface can be approximated as;

$$t_c = \frac{3S}{U} \tag{B-1}$$

where t_c is the clearing time, S is the distance from the nearest free edge to the point of interest and U is the shockwave velocity. For Run 5 (see Table 2-4), $S = b_f/2 = 0.23\text{m}$ and $U \cong 463\,\text{m/s}$. From equation (B-1) the time to clear the entire front face of the flange is;

$$t_c = \frac{3 \times 0.23}{463} = 1.49 \times 10^{-3}\,s \tag{B-2}$$

The ratio of the clearing time to the CONWEP load duration, $t_c/t_d = 0.24$. This suggests that the reflected pressure has decayed to the cleared pressure in 24% of the positive phase duration (the cleared pressure is the sum of the side-on pressure and the dynamic drag pressure, for this example the peak dynamic pressure is approximately one-third of the peak side-on pressure). Here, the effect of clearing is felt across the entire front face of the flange.

The example was re-analyzed to confirm that clearing causes the shown reduction in reflected impulse. By extending the width of the W-shape to the entire domain width and holding all other analysis input at the Run 5 values, the effect of clearing was isolated. The last column in Table B-1 presents the results of this analysis. The reflected pressure and arrival time are identical for the Air3d results, as would be expected. The reflected impulse agrees very well with CONWEP and to a lesser degree the HC value, confirming that the reduction in measure 1 is solely due to clearing. Although the Air3d reflected impulse for the infinite surface is 20% lower than the HC value, this is consistent with the discussion of Air3d's validation against the HC data in Chapter 2 which showed that for $Z > 2$, Air3d predicted a value of impulse approximately 20% lower than HC curves.

Table B-1: Measure 1 Validation
($R = 6.63$m , $m_{tnt} = 14.6$kg , and $b_f = 0.459$m)

Variable	HC	CONWEP	Air3d	Air3d (Ext. flanges)
P_r (kPa)	281.50	278.9	259.5	259.5
i_r^+ (kPa-msec)	491.9	403.0	218.0	401.9
t_a (msec)	7.58	8.20	8.19	8.19
t_d (msec)	5.87	6.16	3.90	4.91

B.3 Measure 2

Measure 2 represents the area-averaged impulse across the front face of the front flange. The ability of Air3d to predict clearing was confirmed while validating measure 1. Examination of Figures 3-8 and 3-9 suggests that measure 1 and 2 give the exact same reduction in impulse. Since the effect of clearing would be greater at the extremities of the flange, one would expect measure 2 to be less than measure 1. Table B-2 shows the values of impulse and the distance from the web centerline for the 12 monitoring locations in Region 1, for Run 5. As one would expect, the impulse at the outermost monitoring location (point 12) is the minimum (increased standoff and clearing) and the impulse at the innermost monitoring location is the maximum (point 1). Figure B-1 plots the actual impulse distribution along region 1 with respect to distance from the web centerline and the numeric average impulse. The distribution is plausible with the average impulse on region 1 being 95% of the maximum (206/218 = 0.95). Measure 2 is very close to measure 1 and the difference is difficult to identify when results are plotted on a log scale. This outcome is supported by Figure 3-12, which plots the ratio of measure 1 to measure 2. At a scaled distance of $Z = 2.71 \text{m}/\sqrt[3]{\text{kg}}$ the ratio is 1.07, which is approximately equal to the inverse of 0.95. This example validates the reported results for measure 2.

Table B-2: Impulse and Distance from Centerline for Monitoring Locations [1]

($R = 6.63$m , $m_{tnt} = 14.6$kg , and $b_f = 0.459$m)

Mon. loc.	1	2	3	4	5	6	7	8	9	10	11	12
x (mm)	9.00	18.3	39.5	60.6	81.7	102	124	145	166	187	209	230
i_r^+ (kPa-msec)	218	218	218	217	215	213	211	207	203	198	187	170

1.   For monitoring locations, see Figure 2-2 and Section 2.1
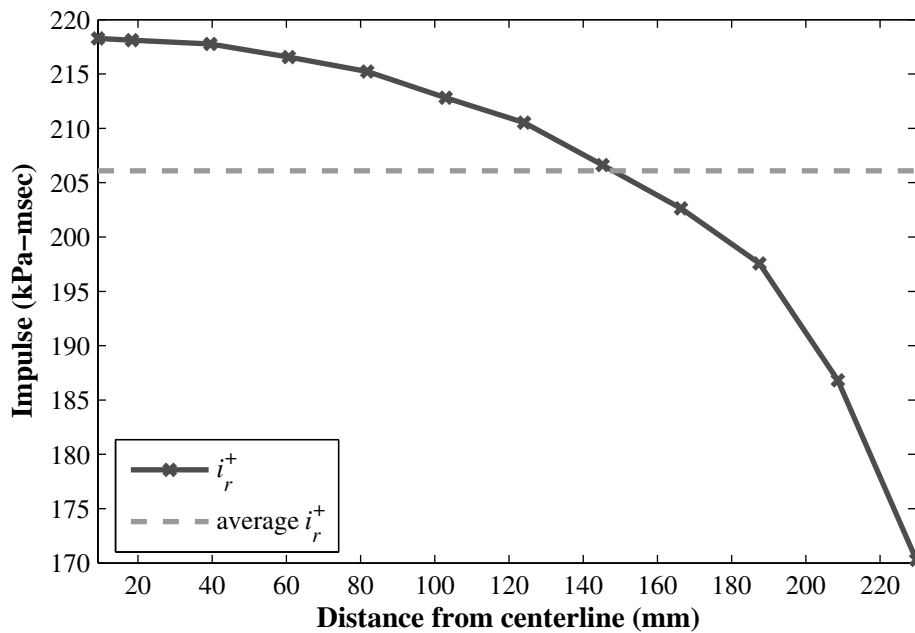
Figure B-1: Region 1 Impulse Distribution ($R = 6.63$m , $m_{tnt} = 14.6$kg **, and**

$b_f = 0.459$m **)**

B.4   Measure 3 and 4

Measures 3 and 4 are intended to capture the effect of wrap-around by combining the impulses for regions 1 through 4 based upon their surface normals. The impulse on each region is determined by integrating the area-averaged pressure history for that region. An area-average was used because 2 monitoring locations lie on the flange surface over the web and 10 monitoring locations lie on the remainder of the flange, resulting in points 1, 2, 43 and 44 having

a different tributary area than the other monitoring locations.   However, examination of Table B-3 reveals that the variation in impulse between points 1 and 2 is negligible and similarly for points 33 and 34.   Therefore, the error introduced by approximating the individual region impulse as the numeric average of the monitoring location impulse within the regions is small. Measures 3 and 4 are examined on this basis.

Table B-3: Impulse at each Monitoring Location [1]
($R = 6.63$m, $m_{tnt} = 14.6$kg, and $b_f = 0.459$m)

Mon. loc.	1	2	3	4	5	6	7	8	9	10	11	12
i_r^+ (kPa-msec)	218	218	218	217	215	213	211	207	203	198	187	170
Mon. loc.	-	-	13	14	15	16	17	18	19	20	21	22
i_r^+ (kPa-msec)	-	-	157	155	153	150	148	143	136	124	98	85
Mon. loc.	-	-	23	24	25	26	27	28	29	30	31	32
i_r^+ (kPa-msec)	-	-	187	183	179	186	183	179	176	173	166	157
Mon. loc.	33	34	35	36	37	38	39	40	41	42	43	44
i_r^+ (kPa-msec)	149	149	76	90	117	130	137	141	143	145	146	148

1.   For monitoring locations, see Figure 2-2 and Section 2.1

From the data in Table B-3, the reflected impulses on regions 1, 2, 3 and 4 are 206kPa-msec, 135kPa-msec, 177kPa-msec and 131kPa-msec, respectively.   Review of these values reveals a logical pattern;   Region 1 has the largest value since it is the closest to the charge and is a reflective surface.   Region 2 values are smaller since it experiences a side-on pressure.   Region 3 experiences a reflected wave and thus has a larger impulse than region 2 but smaller impulse than region 1 as it is further from the charge.   Region 4 has the smallest value as it experiences a side-on pressure and is furthest from the charge.   Comparison of region 1 and 3 suggests that region 4 is too close to the region 3 value of impulse.   Examination of the points 33 – 44 in Table B-3 reveal that points 33 and 34 take an unexpected jump to a value of almost twice point 35.   This can be explained by considering the behavior of a wave as it propagates around a W-shape.   As the wave strikes the section, the flow splits equally around the section (since the section is symmetric), the waves engulf the front flange and then the rear flange before the waves re-engage at the web centerline.   The passage of the waves past one another on the rear face of

the rear flange increases the side-on pressure and impulse above that associated with one wave only.

Measure 3 has been defined as the summation of regions 1 through 4, with regions 1 and 3 being additive and regions 2 and 4 being subtractive. This implies that the measure 3 value of scaled impulse is;

$$\frac{206-135+177-131}{\sqrt[3]{14.6}} = 47.8\frac{\text{kPa}\cdot\text{msec}}{\sqrt[3]{\text{kg}}} \tag{B-3}$$

Figure 3-10 for $Z = 2.71\,\text{m}/\sqrt[3]{\text{kg}}$ suggests that the measure 3 scaled impulse is approximately $50\,\text{kPa}\cdot\text{msec}/\sqrt[3]{\text{kg}}$, which indicates that the simplified numerical approach agrees very well with the area-average method. Measure 4 was intended to represent a tubular section (rectangular hollow section, RHS) with the same outer dimensions as the W-shape of measure 3 and was defined as region 1 – region 4, the value of impulse based on Table B-3 is;

$$\frac{206-131}{\sqrt[3]{14.6}} = 30.6\frac{\text{kPa}\cdot\text{msec}}{\sqrt[3]{\text{kg}}} \tag{B-4}$$

The measure 4 scaled impulse from Figure 3-11 for $Z = 2.71\,\text{m}/\sqrt[3]{\text{kg}}$ is $30\,\text{kPa}\cdot\text{msec}/\sqrt[3]{\text{kg}}$, again agreeing very well with the area-average method. The HC value of scaled impulse is $200\,\text{kPa}\cdot\text{msec}/\sqrt[3]{\text{kg}}$. Thus even at relatively small scaled distances ($Z = 2.71\,\text{m}/\sqrt[3]{\text{kg}}$), a 4 and 7 fold reduction in scaled impulse is realized from measure 3 and 4 respectively.

In addition to the above validation of measure 4, it is necessary to demonstrate that the impulse for region 4 of a W-shape is very similar to that of a RHS with the same outer dimensions, which would validate the assumption that (region 1 – region 4) returns the net impulse on a RHS shape. Six additional analyses (B1 through B6) were performed in order to validate this assumption, using three W-shapes and three tubular sections. The analysis details were $R = 2.44$, 6.63 and 12.22m, $m_{tnt} = 14.6\text{kg}$, and $b_f = 0.459\text{m}$ which corresponds to $Z = 1$, 2.71 and $5\,\text{m}/\sqrt[3]{\text{kg}}$.

Table B-4 shows the values of impulse at each of the monitoring locations for analyses B1 through B6.   The average impulse for region 4 for B1 through B6 is 607, 589, 131, 129, 41 and 42kPa-msec respectively.   The percentage difference is calculated below;

$$\left(1-\frac{i_{B1}^+}{i_{B2}^+}\right)\times100=\left(1-\frac{607}{589}\right)\times100=-3\% \tag{B-5}$$

$$\left(1-\frac{i_{B3}^+}{i_{B4}^+}\right)\times100=\left(1-\frac{131}{129}\right)\times100=-2\% \tag{B-6}$$

$$\left(1-\frac{i_{B5}^+}{i_{B6}^+}\right)\times100=\left(1-\frac{41}{42}\right)\times100=2\% \tag{B-7}$$

It is clear from equations (B-5) through (B-7) that the region 4 impulse of a W-shape is essentially unaffected by regions 2 and 3, therefore ignoring regions 2 and 3 allows a most reasonable estimate of the net impulse on a RHS with the same outer dimensions.

B.5   Summary

Given the complicated nature of blast loading, exact solutions are rare which makes validation of numerical results difficult, however, the requirement of validation still exists.   Using HC curves and CONWEP, the values generated by Air3d were validated.   The trends predicted in Chapter 3 have been interrogated, justified and approximated using simplified, transparent procedures that agreed well with the data in Chapter 3.

Table B-4: Impulse at each Monitoring Location in Region 4 [1]

Run B1: W-shape ($R = 2.44$m, $m_{tnt} = 14.6$kg, and $b_f = 0.459$m)											
Mon. loc.	**33**	**34**	**35**	**36**	**37**	**38**	**39**	**40**	**41**	**42**	**43**	**44**
i_r^+ (kPa-msec)	825	850	8	432	482	529	578	637	676	720	752	798
Run B2: RHS ($R = 2.44$m, $m_{tnt} = 14.6$kg, and $b_f = 0.459$m)											
Mon. loc.	**33**	**34**	**35**	**36**	**37**	**38**	**39**	**40**	**41**	**42**	**43**	**44**
i_r^+ (kPa-msec)	799	820	7	441	471	510	555	615	654	699	730	773
Run B3: W-shape ($R = 6.63$m, $m_{tnt} = 14.6$kg, and $b_f = 0.459$m)											
Mon. loc.	**33**	**34**	**35**	**36**	**37**	**38**	**39**	**40**	**41**	**42**	**43**	**44**
i_r^+ (kPa-msec)	149	149	76	91	117	130	137	141	143	145	146	148
Run B4: RHS ($R = 6.63$m, $m_{tnt} = 14.6$kg, and $b_f = 0.459$m)											
Mon. loc.	**33**	**34**	**35**	**36**	**37**	**38**	**39**	**40**	**41**	**42**	**43**	**44**
i_r^+ (kPa-msec)	145	145	92	89	109	123	132	139	142	145	146	144
Run B5: W-shape ($R = 12.2$m, $m_{tnt} = 14.6$kg, and $b_f = 0.459$m)											
Mon. loc.	**33**	**34**	**35**	**36**	**37**	**38**	**39**	**40**	**41**	**42**	**43**	**44**
i_r^+ (kPa-msec)	43	43	33	37	40	41	42	42	42	43	43	43
Run B6: RHS ($R = 12.2$m, $m_{tnt} = 14.6$kg, and $b_f = 0.459$m)											
Mon. loc.	**33**	**34**	**35**	**36**	**37**	**38**	**39**	**40**	**41**	**42**	**43**	**44**
i_r^+ (kPa-msec)	44	44	35	38	40	41	42	42	43	43	43	44

1.   For monitoring locations, see Figure 2-2 and Section 2.1

MCEER Technical Reports

MCEER publishes technical reports on a variety of subjects written by authors funded through MCEER. These reports are available from both MCEER Publications and the National Technical Information Service (NTIS). Requests for reports should be directed to MCEER Publications, MCEER, University at Buffalo, State University of New York, Red Jacket Quadrangle, Buffalo, New York 14261. Reports can also be requested through NTIS, 5285 Port Royal Road, Springfield, Virginia 22161. NTIS accession numbers are shown in parenthesis, if available.

NCEER-87-0001 "First-Year Program in Research, Education and Technology Transfer," 3/5/87, (PB88-134275, A04, MF-A01).

NCEER-87-0002 "Experimental Evaluation of Instantaneous Optimal Algorithms for Structural Control," by R.C. Lin, T.T. Soong and A.M. Reinhorn, 4/20/87, (PB88-134341, A04, MF-A01).

NCEER-87-0003 "Experimentation Using the Earthquake Simulation Facilities at University at Buffalo," by A.M. Reinhorn and R.L. Ketter, to be published.

NCEER-87-0004 "The System Characteristics and Performance of a Shaking Table," by J.S. Hwang, K.C. Chang and G.C. Lee, 6/1/87, (PB88-134259, A03, MF-A01). This report is available only through NTIS (see address given above).

NCEER-87-0005 "A Finite Element Formulation for Nonlinear Viscoplastic Material Using a Q Model," by O. Gyebi and G. Dasgupta, 11/2/87, (PB88-213764, A08, MF-A01).

NCEER-87-0006 "Symbolic Manipulation Program (SMP) - Algebraic Codes for Two and Three Dimensional Finite Element Formulations," by X. Lee and G. Dasgupta, 11/9/87, (PB88-218522, A05, MF-A01).

NCEER-87-0007 "Instantaneous Optimal Control Laws for Tall Buildings Under Seismic Excitations," by J.N. Yang, A. Akbarpour and P. Ghaemmaghami, 6/10/87, (PB88-134333, A06, MF-A01). This report is only available through NTIS (see address given above).

NCEER-87-0008 "IDARC: Inelastic Damage Analysis of Reinforced Concrete Frame - Shear-Wall Structures," by Y.J. Park, A.M. Reinhorn and S.K. Kunnath, 7/20/87, (PB88-134325, A09, MF-A01). This report is only available through NTIS (see address given above).

NCEER-87-0009 "Liquefaction Potential for New York State: A Preliminary Report on Sites in Manhattan and Buffalo," by M. Budhu, V. Vijayakumar, R.F. Giese and L. Baumgras, 8/31/87, (PB88-163704, A03, MF-A01). This report is available only through NTIS (see address given above).

NCEER-87-0010 "Vertical and Torsional Vibration of Foundations in Inhomogeneous Media," by A.S. Veletsos and K.W. Dotson, 6/1/87, (PB88-134291, A03, MF-A01). This report is only available through NTIS (see address given above).

NCEER-87-0011 "Seismic Probabilistic Risk Assessment and Seismic Margins Studies for Nuclear Power Plants," by Howard H.M. Hwang, 6/15/87, (PB88-134267, A03, MF-A01). This report is only available through NTIS (see address given above).

NCEER-87-0012 "Parametric Studies of Frequency Response of Secondary Systems Under Ground-Acceleration Excitations," by Y. Yong and Y.K. Lin, 6/10/87, (PB88-134309, A03, MF-A01). This report is only available through NTIS (see address given above).

NCEER-87-0013 "Frequency Response of Secondary Systems Under Seismic Excitation," by J.A. HoLung, J. Cai and Y.K. Lin, 7/31/87, (PB88-134317, A05, MF-A01). This report is only available through NTIS (see address given above).

NCEER-87-0014 "Modelling Earthquake Ground Motions in Seismically Active Regions Using Parametric Time Series Methods," by G.W. Ellis and A.S. Cakmak, 8/25/87, (PB88-134283, A08, MF-A01). This report is only available through NTIS (see address given above).

NCEER-87-0015 "Detection and Assessment of Seismic Structural Damage," by E. DiPasquale and A.S. Cakmak, 8/25/87, (PB88-163712, A05, MF-A01). This report is only available through NTIS (see address given above).

NCEER-87-0016   "Pipeline Experiment at Parkfield, California," by J. Isenberg and E. Richardson, 9/15/87, (PB88-163720, A03, MF-A01). This report is available only through NTIS (see address given above).

NCEER-87-0017   "Digital Simulation of Seismic Ground Motion," by M. Shinozuka, G. Deodatis and T. Harada, 8/31/87, (PB88-155197, A04, MF-A01). This report is available only through NTIS (see address given above).

NCEER-87-0018   "Practical Considerations for Structural Control: System Uncertainty, System Time Delay and Truncation of Small Control Forces," J.N. Yang and A. Akbarpour, 8/10/87, (PB88-163738, A08, MF-A01). This report is only available through NTIS (see address given above).

NCEER-87-0019   "Modal Analysis of Nonclassically Damped Structural Systems Using Canonical Transformation," by J.N. Yang, S. Sarkani and F.X. Long, 9/27/87, (PB88-187851, A04, MF-A01).

NCEER-87-0020   "A Nonstationary Solution in Random Vibration Theory," by J.R. Red-Horse and P.D. Spanos, 11/3/87, (PB88-163746, A03, MF-A01).

NCEER-87-0021   "Horizontal Impedances for Radially Inhomogeneous Viscoelastic Soil Layers," by A.S. Veletsos and K.W. Dotson, 10/15/87, (PB88-150859, A04, MF-A01).

NCEER-87-0022   "Seismic Damage Assessment of Reinforced Concrete Members," by Y.S. Chung, C. Meyer and M. Shinozuka, 10/9/87, (PB88-150867, A05, MF-A01). This report is available only through NTIS (see address given above).

NCEER-87-0023   "Active Structural Control in Civil Engineering," by T.T. Soong, 11/11/87, (PB88-187778, A03, MF-A01).

NCEER-87-0024   "Vertical and Torsional Impedances for Radially Inhomogeneous Viscoelastic Soil Layers," by K.W. Dotson and A.S. Veletsos, 12/87, (PB88-187786, A03, MF-A01).

NCEER-87-0025   "Proceedings from the Symposium on Seismic Hazards, Ground Motions, Soil-Liquefaction and Engineering Practice in Eastern North America," October 20-22, 1987, edited by K.H. Jacob, 12/87, (PB88-188115, A23, MF-A01). This report is available only through NTIS (see address given above).

NCEER-87-0026   "Report on the Whittier-Narrows, California, Earthquake of October 1, 1987," by J. Pantelic and A. Reinhorn, 11/87, (PB88-187752, A03, MF-A01). This report is available only through NTIS (see address given above).

NCEER-87-0027   "Design of a Modular Program for Transient Nonlinear Analysis of Large 3-D Building Structures," by S. Srivastav and J.F. Abel, 12/30/87, (PB88-187950, A05, MF-A01). This report is only available through NTIS (see address given above).

NCEER-87-0028   "Second-Year Program in Research, Education and Technology Transfer," 3/8/88, (PB88-219480, A04, MF-A01).

NCEER-88-0001   "Workshop on Seismic Computer Analysis and Design of Buildings With Interactive Graphics," by W. McGuire, J.F. Abel and C.H. Conley, 1/18/88, (PB88-187760, A03, MF-A01). This report is only available through NTIS (see address given above).

NCEER-88-0002   "Optimal Control of Nonlinear Flexible Structures," by J.N. Yang, F.X. Long and D. Wong, 1/22/88, (PB88-213772, A06, MF-A01).

NCEER-88-0003   "Substructuring Techniques in the Time Domain for Primary-Secondary Structural Systems," by G.D. Manolis and G. Juhn, 2/10/88, (PB88-213780, A04, MF-A01).

NCEER-88-0004   "Iterative Seismic Analysis of Primary-Secondary Systems," by A. Singhal, L.D. Lutes and P.D. Spanos, 2/23/88, (PB88-213798, A04, MF-A01).

NCEER-88-0005   "Stochastic Finite Element Expansion for Random Media," by P.D. Spanos and R. Ghanem, 3/14/88, (PB88-213806, A03, MF-A01).

NCEER-88-0006   "Combining Structural Optimization and Structural Control," by F.Y. Cheng and C.P. Pantelides, 1/10/88, (PB88-213814, A05, MF-A01).

NCEER-88-0007   "Seismic Performance Assessment of Code-Designed Structures," by H.H-M. Hwang, J-W. Jaw and H-J. Shau, 3/20/88, (PB88-219423, A04, MF-A01). This report is only available through NTIS (see address given above).

NCEER-88-0008   "Reliability Analysis of Code-Designed Structures Under Natural Hazards," by H.H-M. Hwang, H. Ushiba and M. Shinozuka, 2/29/88, (PB88-229471, A07, MF-A01). This report is only available through NTIS (see address given above).

NCEER-88-0009   "Seismic Fragility Analysis of Shear Wall Structures," by J-W Jaw and H.H-M. Hwang, 4/30/88, (PB89-102867, A04, MF-A01).

NCEER-88-0010   "Base Isolation of a Multi-Story Building Under a Harmonic Ground Motion - A Comparison of Performances of Various Systems," by F-G Fan, G. Ahmadi and I.G. Tadjbakhsh, 5/18/88, (PB89-122238, A06, MF-A01). This report is only available through NTIS (see address given above).

NCEER-88-0011   "Seismic Floor Response Spectra for a Combined System by Green's Functions," by F.M. Lavelle, L.A. Bergman and P.D. Spanos, 5/1/88, (PB89-102875, A03, MF-A01).

NCEER-88-0012   "A New Solution Technique for Randomly Excited Hysteretic Structures," by G.Q. Cai and Y.K. Lin, 5/16/88, (PB89-102883, A03, MF-A01).

NCEER-88-0013   "A Study of Radiation Damping and Soil-Structure Interaction Effects in the Centrifuge," by K. Weissman, supervised by J.H. Prevost, 5/24/88, (PB89-144703, A06, MF-A01).

NCEER-88-0014   "Parameter Identification and Implementation of a Kinematic Plasticity Model for Frictional Soils," by J.H. Prevost and D.V. Griffiths, to be published.

NCEER-88-0015   "Two- and Three- Dimensional Dynamic Finite Element Analyses of the Long Valley Dam," by D.V. Griffiths and J.H. Prevost, 6/17/88, (PB89-144711, A04, MF-A01).

NCEER-88-0016   "Damage Assessment of Reinforced Concrete Structures in Eastern United States," by A.M. Reinhorn, M.J. Seidel, S.K. Kunnath and Y.J. Park, 6/15/88, (PB89-122220, A04, MF-A01). This report is only available through NTIS (see address given above).

NCEER-88-0017   "Dynamic Compliance of Vertically Loaded Strip Foundations in Multilayered Viscoelastic Soils," by S. Ahmad and A.S.M. Israil, 6/17/88, (PB89-102891, A04, MF-A01).

NCEER-88-0018   "An Experimental Study of Seismic Structural Response With Added Viscoelastic Dampers," by R.C. Lin, Z. Liang, T.T. Soong and R.H. Zhang, 6/30/88, (PB89-122212, A05, MF-A01). This report is available only through NTIS (see address given above).

NCEER-88-0019   "Experimental Investigation of Primary - Secondary System Interaction," by G.D. Manolis, G. Juhn and A.M. Reinhorn, 5/27/88, (PB89-122204, A04, MF-A01).

NCEER-88-0020   "A Response Spectrum Approach For Analysis of Nonclassically Damped Structures," by J.N. Yang, S. Sarkani and F.X. Long, 4/22/88, (PB89-102909, A04, MF-A01).

NCEER-88-0021   "Seismic Interaction of Structures and Soils: Stochastic Approach," by A.S. Veletsos and A.M. Prasad, 7/21/88, (PB89-122196, A04, MF-A01). This report is only available through NTIS (see address given above).

NCEER-88-0022   "Identification of the Serviceability Limit State and Detection of Seismic Structural Damage," by E. DiPasquale and A.S. Cakmak, 6/15/88, (PB89-122188, A05, MF-A01). This report is available only through NTIS (see address given above).

NCEER-88-0023   "Multi-Hazard Risk Analysis: Case of a Simple Offshore Structure," by B.K. Bhartia and E.H. Vanmarcke, 7/21/88, (PB89-145213, A05, MF-A01).

NCEER-88-0024   "Automated Seismic Design of Reinforced Concrete Buildings," by Y.S. Chung, C. Meyer and M. Shinozuka, 7/5/88, (PB89-122170, A06, MF-A01). This report is available only through NTIS (see address given above).

NCEER-88-0025   "Experimental Study of Active Control of MDOF Structures Under Seismic Excitations," by L.L. Chung, R.C. Lin, T.T. Soong and A.M. Reinhorn, 7/10/88, (PB89-122600, A04, MF-A01).

NCEER-88-0026   "Earthquake Simulation Tests of a Low-Rise Metal Structure," by J.S. Hwang, K.C. Chang, G.C. Lee and R.L. Ketter, 8/1/88, (PB89-102917, A04, MF-A01).

NCEER-88-0027   "Systems Study of Urban Response and Reconstruction Due to Catastrophic Earthquakes," by F. Kozin and H.K. Zhou, 9/22/88, (PB90-162348, A04, MF-A01).

NCEER-88-0028   "Seismic Fragility Analysis of Plane Frame Structures," by H.H-M. Hwang and Y.K. Low, 7/31/88, (PB89-131445, A06, MF-A01).

NCEER-88-0029   "Response Analysis of Stochastic Structures," by A. Kardara, C. Bucher and M. Shinozuka, 9/22/88, (PB89-174429, A04, MF-A01).

NCEER-88-0030   "Nonnormal Accelerations Due to Yielding in a Primary Structure," by D.C.K. Chen and L.D. Lutes, 9/19/88, (PB89-131437, A04, MF-A01).

NCEER-88-0031   "Design Approaches for Soil-Structure Interaction," by A.S. Veletsos, A.M. Prasad and Y. Tang, 12/30/88, (PB89-174437, A03, MF-A01). This report is available only through NTIS (see address given above).

NCEER-88-0032   "A Re-evaluation of Design Spectra for Seismic Damage Control," by C.J. Turkstra and A.G. Tallin, 11/7/88, (PB89-145221, A05, MF-A01).

NCEER-88-0033   "The Behavior and Design of Noncontact Lap Splices Subjected to Repeated Inelastic Tensile Loading," by V.E. Sagan, P. Gergely and R.N. White, 12/8/88, (PB89-163737, A08, MF-A01).

NCEER-88-0034   "Seismic Response of Pile Foundations," by S.M. Mamoon, P.K. Banerjee and S. Ahmad, 11/1/88, (PB89-145239, A04, MF-A01).

NCEER-88-0035   "Modeling of R/C Building Structures With Flexible Floor Diaphragms (IDARC2)," by A.M. Reinhorn, S.K. Kunnath and N. Panahshahi, 9/7/88, (PB89-207153, A07, MF-A01).

NCEER-88-0036   "Solution of the Dam-Reservoir Interaction Problem Using a Combination of FEM, BEM with Particular Integrals, Modal Analysis, and Substructuring," by C-S. Tsai, G.C. Lee and R.L. Ketter, 12/31/88, (PB89-207146, A04, MF-A01).

NCEER-88-0037   "Optimal Placement of Actuators for Structural Control," by F.Y. Cheng and C.P. Pantelides, 8/15/88, (PB89-162846, A05, MF-A01).

NCEER-88-0038   "Teflon Bearings in Aseismic Base Isolation: Experimental Studies and Mathematical Modeling," by A. Mokha, M.C. Constantinou and A.M. Reinhorn, 12/5/88, (PB89-218457, A10, MF-A01). This report is available only through NTIS (see address given above).

NCEER-88-0039   "Seismic Behavior of Flat Slab High-Rise Buildings in the New York City Area," by P. Weidlinger and M. Ettouney, 10/15/88, (PB90-145681, A04, MF-A01).

NCEER-88-0040   "Evaluation of the Earthquake Resistance of Existing Buildings in New York City," by P. Weidlinger and M. Ettouney, 10/15/88, to be published.

NCEER-88-0041   "Small-Scale Modeling Techniques for Reinforced Concrete Structures Subjected to Seismic Loads," by W. Kim, A. El-Attar and R.N. White, 11/22/88, (PB89-189625, A05, MF-A01).

NCEER-88-0042   "Modeling Strong Ground Motion from Multiple Event Earthquakes," by G.W. Ellis and A.S. Cakmak, 10/15/88, (PB89-174445, A03, MF-A01).

NCEER-88-0043   "Nonstationary Models of Seismic Ground Acceleration," by M. Grigoriu, S.E. Ruiz and E. Rosenblueth, 7/15/88, (PB89-189617, A04, MF-A01).

NCEER-88-0044   "SARCF User's Guide: Seismic Analysis of Reinforced Concrete Frames," by Y.S. Chung, C. Meyer and M. Shinozuka, 11/9/88, (PB89-174452, A08, MF-A01).

NCEER-88-0045   "First Expert Panel Meeting on Disaster Research and Planning," edited by J. Pantelic and J. Stoyle, 9/15/88, (PB89-174460, A05, MF-A01).

NCEER-88-0046   "Preliminary Studies of the Effect of Degrading Infill Walls on the Nonlinear Seismic Response of Steel Frames," by C.Z. Chrysostomou, P. Gergely and J.F. Abel, 12/19/88, (PB89-208383, A05, MF-A01).

NCEER-88-0047   "Reinforced Concrete Frame Component Testing Facility - Design, Construction, Instrumentation and Operation," by S.P. Pessiki, C. Conley, T. Bond, P. Gergely and R.N. White, 12/16/88, (PB89-174478, A04, MF-A01).

NCEER-89-0001   "Effects of Protective Cushion and Soil Compliancy on the Response of Equipment Within a Seismically Excited Building," by J.A. HoLung, 2/16/89, (PB89-207179, A04, MF-A01).

NCEER-89-0002   "Statistical Evaluation of Response Modification Factors for Reinforced Concrete Structures," by H.H-M. Hwang and J-W. Jaw, 2/17/89, (PB89-207187, A05, MF-A01).

NCEER-89-0003   "Hysteretic Columns Under Random Excitation," by G-Q. Cai and Y.K. Lin, 1/9/89, (PB89-196513, A03, MF-A01).

NCEER-89-0004   "Experimental Study of `Elephant Foot Bulge' Instability of Thin-Walled Metal Tanks," by Z-H. Jia and R.L. Ketter, 2/22/89, (PB89-207195, A03, MF-A01).

NCEER-89-0005   "Experiment on Performance of Buried Pipelines Across San Andreas Fault," by J. Isenberg, E. Richardson and T.D. O'Rourke, 3/10/89, (PB89-218440, A04, MF-A01). This report is available only through NTIS (see address given above).

NCEER-89-0006   "A Knowledge-Based Approach to Structural Design of Earthquake-Resistant Buildings," by M. Subramani, P. Gergely, C.H. Conley, J.F. Abel and A.H. Zaghw, 1/15/89, (PB89-218465, A06, MF-A01).

NCEER-89-0007   "Liquefaction Hazards and Their Effects on Buried Pipelines," by T.D. O'Rourke and P.A. Lane, 2/1/89, (PB89-218481, A09, MF-A01).

NCEER-89-0008   "Fundamentals of System Identification in Structural Dynamics," by H. Imai, C-B. Yun, O. Maruyama and M. Shinozuka, 1/26/89, (PB89-207211, A04, MF-A01).

NCEER-89-0009   "Effects of the 1985 Michoacan Earthquake on Water Systems and Other Buried Lifelines in Mexico," by A.G. Ayala and M.J. O'Rourke, 3/8/89, (PB89-207229, A06, MF-A01).

NCEER-89-R010   "NCEER Bibliography of Earthquake Education Materials," by K.E.K. Ross, Second Revision, 9/1/89, (PB90-125352, A05, MF-A01). This report is replaced by NCEER-92-0018.

NCEER-89-0011   "Inelastic Three-Dimensional Response Analysis of Reinforced Concrete Building Structures (IDARC-3D), Part I - Modeling," by S.K. Kunnath and A.M. Reinhorn, 4/17/89, (PB90-114612, A07, MF-A01). This report is available only through NTIS (see address given above).

NCEER-89-0012   "Recommended Modifications to ATC-14," by C.D. Poland and J.O. Malley, 4/12/89, (PB90-108648, A15, MF-A01).

NCEER-89-0013   "Repair and Strengthening of Beam-to-Column Connections Subjected to Earthquake Loading," by M. Corazao and A.J. Durrani, 2/28/89, (PB90-109885, A06, MF-A01).

NCEER-89-0014   "Program EXKAL2 for Identification of Structural Dynamic Systems," by O. Maruyama, C-B. Yun, M. Hoshiya and M. Shinozuka, 5/19/89, (PB90-109877, A09, MF-A01).

NCEER-89-0015   "Response of Frames With Bolted Semi-Rigid Connections, Part I - Experimental Study and Analytical Predictions," by P.J. DiCorso, A.M. Reinhorn, J.R. Dickerson, J.B. Radziminski and W.L. Harper, 6/1/89, to be published.

NCEER-89-0016   "ARMA Monte Carlo Simulation in Probabilistic Structural Analysis," by P.D. Spanos and M.P. Mignolet, 7/10/89, (PB90-109893, A03, MF-A01).

NCEER-89-P017   "Preliminary Proceedings from the Conference on Disaster Preparedness - The Place of Earthquake Education in Our Schools," Edited by K.E.K. Ross, 6/23/89, (PB90-108606, A03, MF-A01).

NCEER-89-0017   "Proceedings from the Conference on Disaster Preparedness - The Place of Earthquake Education in Our Schools," Edited by K.E.K. Ross, 12/31/89, (PB90-207895, A012, MF-A02). This report is available only through NTIS (see address given above).

NCEER-89-0018   "Multidimensional Models of Hysteretic Material Behavior for Vibration Analysis of Shape Memory Energy Absorbing Devices, by E.J. Graesser and F.A. Cozzarelli, 6/7/89, (PB90-164146, A04, MF-A01).

NCEER-89-0019   "Nonlinear Dynamic Analysis of Three-Dimensional Base Isolated Structures (3D-BASIS)," by S. Nagarajaiah, A.M. Reinhorn and M.C. Constantinou, 8/3/89, (PB90-161936, A06, MF-A01). This report has been replaced by NCEER-93-0011.

NCEER-89-0020   "Structural Control Considering Time-Rate of Control Forces and Control Rate Constraints," by F.Y. Cheng and C.P. Pantelides, 8/3/89, (PB90-120445, A04, MF-A01).

NCEER-89-0021   "Subsurface Conditions of Memphis and Shelby County," by K.W. Ng, T-S. Chang and H-H.M. Hwang, 7/26/89, (PB90-120437, A03, MF-A01).

NCEER-89-0022   "Seismic Wave Propagation Effects on Straight Jointed Buried Pipelines," by K. Elhmadi and M.J. O'Rourke, 8/24/89, (PB90-162322, A10, MF-A02).

NCEER-89-0023   "Workshop on Serviceability Analysis of Water Delivery Systems," edited by M. Grigoriu, 3/6/89, (PB90-127424, A03, MF-A01).

NCEER-89-0024   "Shaking Table Study of a 1/5 Scale Steel Frame Composed of Tapered Members," by K.C. Chang, J.S. Hwang and G.C. Lee, 9/18/89, (PB90-160169, A04, MF-A01).

NCEER-89-0025   "DYNA1D: A Computer Program for Nonlinear Seismic Site Response Analysis - Technical Documentation," by Jean H. Prevost, 9/14/89, (PB90-161944, A07, MF-A01). This report is available only through NTIS (see address given above).

NCEER-89-0026   "1:4 Scale Model Studies of Active Tendon Systems and Active Mass Dampers for Aseismic Protection," by A.M. Reinhorn, T.T. Soong, R.C. Lin, Y.P. Yang, Y. Fukao, H. Abe and M. Nakai, 9/15/89, (PB90-173246, A10, MF-A02). This report is available only through NTIS (see address given above).

NCEER-89-0027   "Scattering of Waves by Inclusions in a Nonhomogeneous Elastic Half Space Solved by Boundary Element Methods," by P.K. Hadley, A. Askar and A.S. Cakmak, 6/15/89, (PB90-145699, A07, MF-A01).

NCEER-89-0028   "Statistical Evaluation of Deflection Amplification Factors for Reinforced Concrete Structures," by H.H.M. Hwang, J-W. Jaw and A.L. Ch'ng, 8/31/89, (PB90-164633, A05, MF-A01).

NCEER-89-0029   "Bedrock Accelerations in Memphis Area Due to Large New Madrid Earthquakes," by H.H.M. Hwang, C.H.S. Chen and G. Yu, 11/7/89, (PB90-162330, A04, MF-A01).

NCEER-89-0030   "Seismic Behavior and Response Sensitivity of Secondary Structural Systems," by Y.Q. Chen and T.T. Soong, 10/23/89, (PB90-164658, A08, MF-A01).

NCEER-89-0031   "Random Vibration and Reliability Analysis of Primary-Secondary Structural Systems," by Y. Ibrahim, M. Grigoriu and T.T. Soong, 11/10/89, (PB90-161951, A04, MF-A01).

NCEER-89-0032   "Proceedings from the Second U.S. - Japan Workshop on Liquefaction, Large Ground Deformation and Their Effects on Lifelines, September 26-29, 1989," Edited by T.D. O'Rourke and M. Hamada, 12/1/89, (PB90-209388, A22, MF-A03).

NCEER-89-0033   "Deterministic Model for Seismic Damage Evaluation of Reinforced Concrete Structures," by J.M. Bracci, A.M. Reinhorn, J.B. Mander and S.K. Kunnath, 9/27/89, (PB91-108803, A06, MF-A01).

NCEER-89-0034   "On the Relation Between Local and Global Damage Indices," by E. DiPasquale and A.S. Cakmak, 8/15/89, (PB90-173865, A05, MF-A01).

NCEER-89-0035   "Cyclic Undrained Behavior of Nonplastic and Low Plasticity Silts," by A.J. Walker and H.E. Stewart, 7/26/89, (PB90-183518, A10, MF-A01).

NCEER-89-0036   "Liquefaction Potential of Surficial Deposits in the City of Buffalo, New York," by M. Budhu, R. Giese and L. Baumgrass, 1/17/89, (PB90-208455, A04, MF-A01).

NCEER-89-0037   "A Deterministic Assessment of Effects of Ground Motion Incoherence," by A.S. Veletsos and Y. Tang, 7/15/89, (PB90-164294, A03, MF-A01).

NCEER-89-0038   "Workshop on Ground Motion Parameters for Seismic Hazard Mapping," July 17-18, 1989, edited by R.V. Whitman, 12/1/89, (PB90-173923, A04, MF-A01).

NCEER-89-0039   "Seismic Effects on Elevated Transit Lines of the New York City Transit Authority," by C.J. Costantino, C.A. Miller and E. Heymsfield, 12/26/89, (PB90-207887, A06, MF-A01).

NCEER-89-0040   "Centrifugal Modeling of Dynamic Soil-Structure Interaction," by K. Weissman, Supervised by J.H. Prevost, 5/10/89, (PB90-207879, A07, MF-A01).

NCEER-89-0041   "Linearized Identification of Buildings With Cores for Seismic Vulnerability Assessment," by I-K. Ho and A.E. Aktan, 11/1/89, (PB90-251943, A07, MF-A01).

NCEER-90-0001   "Geotechnical and Lifeline Aspects of the October 17, 1989 Loma Prieta Earthquake in San Francisco," by T.D. O'Rourke, H.E. Stewart, F.T. Blackburn and T.S. Dickerman, 1/90, (PB90-208596, A05, MF-A01).

NCEER-90-0002   "Nonnormal Secondary Response Due to Yielding in a Primary Structure," by D.C.K. Chen and L.D. Lutes, 2/28/90, (PB90-251976, A07, MF-A01).

NCEER-90-0003   "Earthquake Education Materials for Grades K-12," by K.E.K. Ross, 4/16/90, (PB91-251984, A05, MF-A05). This report has been replaced by NCEER-92-0018.

NCEER-90-0004   "Catalog of Strong Motion Stations in Eastern North America," by R.W. Busby, 4/3/90, (PB90-251984, A05, MF-A01).

NCEER-90-0005   "NCEER Strong-Motion Data Base: A User Manual for the GeoBase Release (Version 1.0 for the Sun3)," by P. Friberg and K. Jacob, 3/31/90 (PB90-258062, A04, MF-A01).

NCEER-90-0006   "Seismic Hazard Along a Crude Oil Pipeline in the Event of an 1811-1812 Type New Madrid Earthquake," by H.H.M. Hwang and C-H.S. Chen, 4/16/90, (PB90-258054, A04, MF-A01).

NCEER-90-0007   "Site-Specific Response Spectra for Memphis Sheahan Pumping Station," by H.H.M. Hwang and C.S. Lee, 5/15/90, (PB91-108811, A05, MF-A01).

NCEER-90-0008   "Pilot Study on Seismic Vulnerability of Crude Oil Transmission Systems," by T. Ariman, R. Dobry, M. Grigoriu, F. Kozin, M. O'Rourke, T. O'Rourke and M. Shinozuka, 5/25/90, (PB91-108837, A06, MF-A01).

NCEER-90-0009   "A Program to Generate Site Dependent Time Histories: EQGEN," by G.W. Ellis, M. Srinivasan and A.S. Cakmak, 1/30/90, (PB91-108829, A04, MF-A01).

NCEER-90-0010   "Active Isolation for Seismic Protection of Operating Rooms," by M.E. Talbott, Supervised by M. Shinozuka, 6/8/9, (PB91-110205, A05, MF-A01).

NCEER-90-0011   "Program LINEARID for Identification of Linear Structural Dynamic Systems," by C-B. Yun and M. Shinozuka, 6/25/90, (PB91-110312, A08, MF-A01).

NCEER-90-0012   "Two-Dimensional Two-Phase Elasto-Plastic Seismic Response of Earth Dams," by A.N. Yiagos, Supervised by J.H. Prevost, 6/20/90, (PB91-110197, A13, MF-A02).

NCEER-90-0013   "Secondary Systems in Base-Isolated Structures: Experimental Investigation, Stochastic Response and Stochastic Sensitivity," by G.D. Manolis, G. Juhn, M.C. Constantinou and A.M. Reinhorn, 7/1/90, (PB91-110320, A08, MF-A01).

NCEER-90-0014   "Seismic Behavior of Lightly-Reinforced Concrete Column and Beam-Column Joint Details," by S.P. Pessiki, C.H. Conley, P. Gergely and R.N. White, 8/22/90, (PB91-108795, A11, MF-A02).

NCEER-90-0015   "Two Hybrid Control Systems for Building Structures Under Strong Earthquakes," by J.N. Yang and A. Danielians, 6/29/90, (PB91-125393, A04, MF-A01).

NCEER-90-0016   "Instantaneous Optimal Control with Acceleration and Velocity Feedback," by J.N. Yang and Z. Li, 6/29/90, (PB91-125401, A03, MF-A01).

NCEER-90-0017   "Reconnaissance Report on the Northern Iran Earthquake of June 21, 1990," by M. Mehrain, 10/4/90, (PB91-125377, A03, MF-A01).

NCEER-90-0018   "Evaluation of Liquefaction Potential in Memphis and Shelby County," by T.S. Chang, P.S. Tang, C.S. Lee and H. Hwang, 8/10/90, (PB91-125427, A09, MF-A01).

NCEER-90-0019   "Experimental and Analytical Study of a Combined Sliding Disc Bearing and Helical Steel Spring Isolation System," by M.C. Constantinou, A.S. Mokha and A.M. Reinhorn, 10/4/90, (PB91-125385, A06, MF-A01). This report is available only through NTIS (see address given above).

NCEER-90-0020   "Experimental Study and Analytical Prediction of Earthquake Response of a Sliding Isolation System with a Spherical Surface," by A.S. Mokha, M.C. Constantinou and A.M. Reinhorn, 10/11/90, (PB91-125419, A05, MF-A01).

NCEER-90-0021   "Dynamic Interaction Factors for Floating Pile Groups," by G. Gazetas, K. Fan, A. Kaynia and E. Kausel, 9/10/90, (PB91-170381, A05, MF-A01).

NCEER-90-0022   "Evaluation of Seismic Damage Indices for Reinforced Concrete Structures," by S. Rodriguez-Gomez and A.S. Cakmak, 9/30/90, PB91-171322, A06, MF-A01).

NCEER-90-0023   "Study of Site Response at a Selected Memphis Site," by H. Desai, S. Ahmad, E.S. Gazetas and M.R. Oh, 10/11/90, (PB91-196857, A03, MF-A01).

NCEER-90-0024   "A User's Guide to Strongmo: Version 1.0 of NCEER's Strong-Motion Data Access Tool for PCs and Terminals," by P.A. Friberg and C.A.T. Susch, 11/15/90, (PB91-171272, A03, MF-A01).

NCEER-90-0025   "A Three-Dimensional Analytical Study of Spatial Variability of Seismic Ground Motions," by L-L. Hong and A.H.-S. Ang, 10/30/90, (PB91-170399, A09, MF-A01).

NCEER-90-0026   "MUMOID User's Guide - A Program for the Identification of Modal Parameters," by S. Rodriguez-Gomez and E. DiPasquale, 9/30/90, (PB91-171298, A04, MF-A01).

NCEER-90-0027   "SARCF-II User's Guide - Seismic Analysis of Reinforced Concrete Frames," by S. Rodriguez-Gomez, Y.S. Chung and C. Meyer, 9/30/90, (PB91-171280, A05, MF-A01).

NCEER-90-0028   "Viscous Dampers: Testing, Modeling and Application in Vibration and Seismic Isolation," by N. Makris and M.C. Constantinou, 12/20/90 (PB91-190561, A06, MF-A01).

NCEER-90-0029   "Soil Effects on Earthquake Ground Motions in the Memphis Area," by H. Hwang, C.S. Lee, K.W. Ng and T.S. Chang, 8/2/90, (PB91-190751, A05, MF-A01).

NCEER-91-0001   "Proceedings from the Third Japan-U.S. Workshop on Earthquake Resistant Design of Lifeline Facilities and Countermeasures for Soil Liquefaction, December 17-19, 1990," edited by T.D. O'Rourke and M. Hamada, 2/1/91, (PB91-179259, A99, MF-A04).

NCEER-91-0002   "Physical Space Solutions of Non-Proportionally Damped Systems," by M. Tong, Z. Liang and G.C. Lee, 1/15/91, (PB91-179242, A04, MF-A01).

NCEER-91-0003   "Seismic Response of Single Piles and Pile Groups," by K. Fan and G. Gazetas, 1/10/91, (PB92-174994, A04, MF-A01).

NCEER-91-0004   "Damping of Structures: Part 1 - Theory of Complex Damping," by Z. Liang and G. Lee, 10/10/91, (PB92-197235, A12, MF-A03).

NCEER-91-0005   "3D-BASIS - Nonlinear Dynamic Analysis of Three Dimensional Base Isolated Structures: Part II," by S. Nagarajaiah, A.M. Reinhorn and M.C. Constantinou, 2/28/91, (PB91-190553, A07, MF-A01). This report has been replaced by NCEER-93-0011.

NCEER-91-0006   "A Multidimensional Hysteretic Model for Plasticity Deforming Metals in Energy Absorbing Devices," by E.J. Graesser and F.A. Cozzarelli, 4/9/91, (PB92-108364, A04, MF-A01).

NCEER-91-0007   "A Framework for Customizable Knowledge-Based Expert Systems with an Application to a KBES for Evaluating the Seismic Resistance of Existing Buildings," by E.G. Ibarra-Anaya and S.J. Fenves, 4/9/91, (PB91-210930, A08, MF-A01).

NCEER-91-0008   "Nonlinear Analysis of Steel Frames with Semi-Rigid Connections Using the Capacity Spectrum Method," by G.G. Deierlein, S-H. Hsieh, Y-J. Shen and J.F. Abel, 7/2/91, (PB92-113828, A05, MF-A01).

NCEER-91-0009   "Earthquake Education Materials for Grades K-12," by K.E.K. Ross, 4/30/91, (PB91-212142, A06, MF-A01). This report has been replaced by NCEER-92-0018.

NCEER-91-0010   "Phase Wave Velocities and Displacement Phase Differences in a Harmonically Oscillating Pile," by N. Makris and G. Gazetas, 7/8/91, (PB92-108356, A04, MF-A01).

NCEER-91-0011   "Dynamic Characteristics of a Full-Size Five-Story Steel Structure and a 2/5 Scale Model," by K.C. Chang, G.C. Yao, G.C. Lee, D.S. Hao and Y.C. Yeh," 7/2/91, (PB93-116648, A06, MF-A02).

NCEER-91-0012   "Seismic Response of a 2/5 Scale Steel Structure with Added Viscoelastic Dampers," by K.C. Chang, T.T. Soong, S-T. Oh and M.L. Lai, 5/17/91, (PB92-110816, A05, MF-A01).

NCEER-91-0013   "Earthquake Response of Retaining Walls; Full-Scale Testing and Computational Modeling," by S. Alampalli and A-W.M. Elgamal, 6/20/91, to be published.

NCEER-91-0014   "3D-BASIS-M: Nonlinear Dynamic Analysis of Multiple Building Base Isolated Structures," by P.C. Tsopelas, S. Nagarajaiah, M.C. Constantinou and A.M. Reinhorn, 5/28/91, (PB92-113885, A09, MF-A02).

NCEER-91-0015   "Evaluation of SEAOC Design Requirements for Sliding Isolated Structures," by D. Theodossiou and M.C. Constantinou, 6/10/91, (PB92-114602, A11, MF-A03).

NCEER-91-0016   "Closed-Loop Modal Testing of a 27-Story Reinforced Concrete Flat Plate-Core Building," by H.R. Somaprasad, T. Toksoy, H. Yoshiyuki and A.E. Aktan, 7/15/91, (PB92-129980, A07, MF-A02).

NCEER-91-0017   "Shake Table Test of a 1/6 Scale Two-Story Lightly Reinforced Concrete Building," by A.G. El-Attar, R.N. White and P. Gergely, 2/28/91, (PB92-222447, A06, MF-A02).

NCEER-91-0018   "Shake Table Test of a 1/8 Scale Three-Story Lightly Reinforced Concrete Building," by A.G. El-Attar, R.N. White and P. Gergely, 2/28/91, (PB93-116630, A08, MF-A02).

NCEER-91-0019   "Transfer Functions for Rigid Rectangular Foundations," by A.S. Veletsos, A.M. Prasad and W.H. Wu, 7/31/91, to be published.

NCEER-91-0020   "Hybrid Control of Seismic-Excited Nonlinear and Inelastic Structural Systems," by J.N. Yang, Z. Li and A. Danielians, 8/1/91, (PB92-143171, A06, MF-A02).

NCEER-91-0021   "The NCEER-91 Earthquake Catalog: Improved Intensity-Based Magnitudes and Recurrence Relations for U.S. Earthquakes East of New Madrid," by L. Seeber and J.G. Armbruster, 8/28/91, (PB92-176742, A06, MF-A02).

NCEER-91-0022   "Proceedings from the Implementation of Earthquake Planning and Education in Schools: The Need for Change - The Roles of the Changemakers," by K.E.K. Ross and F. Winslow, 7/23/91, (PB92-129998, A12, MF-A03).

NCEER-91-0023   "A Study of Reliability-Based Criteria for Seismic Design of Reinforced Concrete Frame Buildings," by H.H.M. Hwang and H-M. Hsu, 8/10/91, (PB92-140235, A09, MF-A02).

NCEER-91-0024   "Experimental Verification of a Number of Structural System Identification Algorithms," by R.G. Ghanem, H. Gavin and M. Shinozuka, 9/18/91, (PB92-176577, A18, MF-A04).

NCEER-91-0025   "Probabilistic Evaluation of Liquefaction Potential," by H.H.M. Hwang and C.S. Lee," 11/25/91, (PB92-143429, A05, MF-A01).

NCEER-91-0026   "Instantaneous Optimal Control for Linear, Nonlinear and Hysteretic Structures - Stable Controllers," by J.N. Yang and Z. Li, 11/15/91, (PB92-163807, A04, MF-A01).

NCEER-91-0027   "Experimental and Theoretical Study of a Sliding Isolation System for Bridges," by M.C. Constantinou, A. Kartoum, A.M. Reinhorn and P. Bradford, 11/15/91, (PB92-176973, A10, MF-A03).

NCEER-92-0001   "Case Studies of Liquefaction and Lifeline Performance During Past Earthquakes, Volume 1: Japanese Case Studies," Edited by M. Hamada and T. O'Rourke, 2/17/92, (PB92-197243, A18, MF-A04).

NCEER-92-0002   "Case Studies of Liquefaction and Lifeline Performance During Past Earthquakes, Volume 2: United States Case Studies," Edited by T. O'Rourke and M. Hamada, 2/17/92, (PB92-197250, A20, MF-A04).

NCEER-92-0003   "Issues in Earthquake Education," Edited by K. Ross, 2/3/92, (PB92-222389, A07, MF-A02).

NCEER-92-0004   "Proceedings from the First U.S. - Japan Workshop on Earthquake Protective Systems for Bridges," Edited by I.G. Buckle, 2/4/92, (PB94-142239, A99, MF-A06).

NCEER-92-0005   "Seismic Ground Motion from a Haskell-Type Source in a Multiple-Layered Half-Space," A.P. Theoharis, G. Deodatis and M. Shinozuka, 1/2/92, to be published.

NCEER-92-0006   "Proceedings from the Site Effects Workshop," Edited by R. Whitman, 2/29/92, (PB92-197201, A04, MF-A01).

NCEER-92-0007   "Engineering Evaluation of Permanent Ground Deformations Due to Seismically-Induced Liquefaction," by M.H. Baziar, R. Dobry and A-W.M. Elgamal, 3/24/92, (PB92-222421, A13, MF-A03).

NCEER-92-0008   "A Procedure for the Seismic Evaluation of Buildings in the Central and Eastern United States," by C.D. Poland and J.O. Malley, 4/2/92, (PB92-222439, A20, MF-A04).

NCEER-92-0009   "Experimental and Analytical Study of a Hybrid Isolation System Using Friction Controllable Sliding Bearings," by M.Q. Feng, S. Fujii and M. Shinozuka, 5/15/92, (PB93-150282, A06, MF-A02).

NCEER-92-0010   "Seismic Resistance of Slab-Column Connections in Existing Non-Ductile Flat-Plate Buildings," by A.J. Durrani and Y. Du, 5/18/92, (PB93-116812, A06, MF-A02).

NCEER-92-0011   "The Hysteretic and Dynamic Behavior of Brick Masonry Walls Upgraded by Ferrocement Coatings Under Cyclic Loading and Strong Simulated Ground Motion," by H. Lee and S.P. Prawel, 5/11/92, to be published.

NCEER-92-0012   "Study of Wire Rope Systems for Seismic Protection of Equipment in Buildings," by G.F. Demetriades, M.C. Constantinou and A.M. Reinhorn, 5/20/92, (PB93-116655, A08, MF-A02).

NCEER-92-0013   "Shape Memory Structural Dampers: Material Properties, Design and Seismic Testing," by P.R. Witting and F.A. Cozzarelli, 5/26/92, (PB93-116663, A05, MF-A01).

NCEER-92-0014   "Longitudinal Permanent Ground Deformation Effects on Buried Continuous Pipelines," by M.J. O'Rourke, and C. Nordberg, 6/15/92, (PB93-116671, A08, MF-A02).

NCEER-92-0015   "A Simulation Method for Stationary Gaussian Random Functions Based on the Sampling Theorem," by M. Grigoriu and S. Balopoulou, 6/11/92, (PB93-127496, A05, MF-A01).

NCEER-92-0016   "Gravity-Load-Designed Reinforced Concrete Buildings: Seismic Evaluation of Existing Construction and Detailing Strategies for Improved Seismic Resistance," by G.W. Hoffmann, S.K. Kunnath, A.M. Reinhorn and J.B. Mander, 7/15/92, (PB94-142007, A08, MF-A02).

NCEER-92-0017   "Observations on Water System and Pipeline Performance in the Limón Area of Costa Rica Due to the April 22, 1991 Earthquake," by M. O'Rourke and D. Ballantyne, 6/30/92, (PB93-126811, A06, MF-A02).

NCEER-92-0018   "Fourth Edition of Earthquake Education Materials for Grades K-12," Edited by K.E.K. Ross, 8/10/92, (PB93-114023, A07, MF-A02).

NCEER-92-0019   "Proceedings from the Fourth Japan-U.S. Workshop on Earthquake Resistant Design of Lifeline Facilities and Countermeasures for Soil Liquefaction," Edited by M. Hamada and T.D. O'Rourke, 8/12/92, (PB93-163939, A99, MF-E11).

NCEER-92-0020   "Active Bracing System: A Full Scale Implementation of Active Control," by A.M. Reinhorn, T.T. Soong, R.C. Lin, M.A. Riley, Y.P. Wang, S. Aizawa and M. Higashino, 8/14/92, (PB93-127512, A06, MF-A02).

NCEER-92-0021   "Empirical Analysis of Horizontal Ground Displacement Generated by Liquefaction-Induced Lateral Spreads," by S.F. Bartlett and T.L. Youd, 8/17/92, (PB93-188241, A06, MF-A02).

NCEER-92-0022   "IDARC Version 3.0: Inelastic Damage Analysis of Reinforced Concrete Structures," by S.K. Kunnath, A.M. Reinhorn and R.F. Lobo, 8/31/92, (PB93-227502, A07, MF-A02).

NCEER-92-0023   "A Semi-Empirical Analysis of Strong-Motion Peaks in Terms of Seismic Source, Propagation Path and Local Site Conditions, by M. Kamiyama, M.J. O'Rourke and R. Flores-Berrones, 9/9/92, (PB93-150266, A08, MF-A02).

NCEER-92-0024   "Seismic Behavior of Reinforced Concrete Frame Structures with Nonductile Details, Part I: Summary of Experimental Findings of Full Scale Beam-Column Joint Tests," by A. Beres, R.N. White and P. Gergely, 9/30/92, (PB93-227783, A05, MF-A01).

NCEER-92-0025   "Experimental Results of Repaired and Retrofitted Beam-Column Joint Tests in Lightly Reinforced Concrete Frame Buildings," by A. Beres, S. El-Borgi, R.N. White and P. Gergely, 10/29/92, (PB93-227791, A05, MF-A01).

NCEER-92-0026   "A Generalization of Optimal Control Theory: Linear and Nonlinear Structures," by J.N. Yang, Z. Li and S. Vongchavalitkul, 11/2/92, (PB93-188621, A05, MF-A01).

NCEER-92-0027   "Seismic Resistance of Reinforced Concrete Frame Structures Designed Only for Gravity Loads: Part I - Design and Properties of a One-Third Scale Model Structure," by J.M. Bracci, A.M. Reinhorn and J.B. Mander, 12/1/92, (PB94-104502, A08, MF-A02).

NCEER-92-0028   "Seismic Resistance of Reinforced Concrete Frame Structures Designed Only for Gravity Loads: Part II - Experimental Performance of Subassemblages," by L.E. Aycardi, J.B. Mander and A.M. Reinhorn, 12/1/92, (PB94-104510, A08, MF-A02).

NCEER-92-0029   "Seismic Resistance of Reinforced Concrete Frame Structures Designed Only for Gravity Loads: Part III - Experimental Performance and Analytical Study of a Structural Model," by J.M. Bracci, A.M. Reinhorn and J.B. Mander, 12/1/92, (PB93-227528, A09, MF-A01).

NCEER-92-0030   "Evaluation of Seismic Retrofit of Reinforced Concrete Frame Structures: Part I - Experimental Performance of Retrofitted Subassemblages," by D. Choudhuri, J.B. Mander and A.M. Reinhorn, 12/8/92, (PB93-198307, A07, MF-A02).

NCEER-92-0031   "Evaluation of Seismic Retrofit of Reinforced Concrete Frame Structures: Part II - Experimental Performance and Analytical Study of a Retrofitted Structural Model," by J.M. Bracci, A.M. Reinhorn and J.B. Mander, 12/8/92, (PB93-198315, A09, MF-A03).

NCEER-92-0032   "Experimental and Analytical Investigation of Seismic Response of Structures with Supplemental Fluid Viscous Dampers," by M.C. Constantinou and M.D. Symans, 12/21/92, (PB93-191435, A10, MF-A03). This report is available only through NTIS (see address given above).

NCEER-92-0033   "Reconnaissance Report on the Cairo, Egypt Earthquake of October 12, 1992," by M. Khater, 12/23/92, (PB93-188621, A03, MF-A01).

NCEER-92-0034   "Low-Level Dynamic Characteristics of Four Tall Flat-Plate Buildings in New York City," by H. Gavin, S. Yuan, J. Grossman, E. Pekelis and K. Jacob, 12/28/92, (PB93-188217, A07, MF-A02).

NCEER-93-0001   "An Experimental Study on the Seismic Performance of Brick-Infilled Steel Frames With and Without Retrofit," by J.B. Mander, B. Nair, K. Wojtkowski and J. Ma, 1/29/93, (PB93-227510, A07, MF-A02).

NCEER-93-0002   "Social Accounting for Disaster Preparedness and Recovery Planning," by S. Cole, E. Pantoja and V. Razak, 2/22/93, (PB94-142114, A12, MF-A03).

NCEER-93-0003   "Assessment of 1991 NEHRP Provisions for Nonstructural Components and Recommended Revisions," by T.T. Soong, G. Chen, Z. Wu, R-H. Zhang and M. Grigoriu, 3/1/93, (PB93-188639, A06, MF-A02).

NCEER-93-0004   "Evaluation of Static and Response Spectrum Analysis Procedures of SEAOC/UBC for Seismic Isolated Structures," by C.W. Winters and M.C. Constantinou, 3/23/93, (PB93-198299, A10, MF-A03).

NCEER-93-0005   "Earthquakes in the Northeast - Are We Ignoring the Hazard? A Workshop on Earthquake Science and Safety for Educators," edited by K.E.K. Ross, 4/2/93, (PB94-103066, A09, MF-A02).

NCEER-93-0006   "Inelastic Response of Reinforced Concrete Structures with Viscoelastic Braces," by R.F. Lobo, J.M. Bracci, K.L. Shen, A.M. Reinhorn and T.T. Soong, 4/5/93, (PB93-227486, A05, MF-A02).

NCEER-93-0007   "Seismic Testing of Installation Methods for Computers and Data Processing Equipment," by K. Kosar, T.T. Soong, K.L. Shen, J.A. HoLung and Y.K. Lin, 4/12/93, (PB93-198299, A07, MF-A02).

NCEER-93-0008   "Retrofit of Reinforced Concrete Frames Using Added Dampers," by A. Reinhorn, M. Constantinou and C. Li, to be published.

NCEER-93-0009   "Seismic Behavior and Design Guidelines for Steel Frame Structures with Added Viscoelastic Dampers," by K.C. Chang, M.L. Lai, T.T. Soong, D.S. Hao and Y.C. Yeh, 5/1/93, (PB94-141959, A07, MF-A02).

NCEER-93-0010   "Seismic Performance of Shear-Critical Reinforced Concrete Bridge Piers," by J.B. Mander, S.M. Waheed, M.T.A. Chaudhary and S.S. Chen, 5/12/93, (PB93-227494, A08, MF-A02).

NCEER-93-0011   "3D-BASIS-TABS: Computer Program for Nonlinear Dynamic Analysis of Three Dimensional Base Isolated Structures," by S. Nagarajaiah, C. Li, A.M. Reinhorn and M.C. Constantinou, 8/2/93, (PB94-141819, A09, MF-A02).

NCEER-93-0012   "Effects of Hydrocarbon Spills from an Oil Pipeline Break on Ground Water," by O.J. Helweg and H.H.M. Hwang, 8/3/93, (PB94-141942, A06, MF-A02).

NCEER-93-0013   "Simplified Procedures for Seismic Design of Nonstructural Components and Assessment of Current Code Provisions," by M.P. Singh, L.E. Suarez, E.E. Matheu and G.O. Maldonado, 8/4/93, (PB94-141827, A09, MF-A02).

NCEER-93-0014   "An Energy Approach to Seismic Analysis and Design of Secondary Systems," by G. Chen and T.T. Soong, 8/6/93, (PB94-142767, A11, MF-A03).

NCEER-93-0015   "Proceedings from School Sites: Becoming Prepared for Earthquakes - Commemorating the Third Anniversary of the Loma Prieta Earthquake," Edited by F.E. Winslow and K.E.K. Ross, 8/16/93, (PB94-154275, A16, MF-A02).

NCEER-93-0016   "Reconnaissance Report of Damage to Historic Monuments in Cairo, Egypt Following the October 12, 1992 Dahshur Earthquake," by D. Sykora, D. Look, G. Croci, E. Karaesmen and E. Karaesmen, 8/19/93, (PB94-142221, A08, MF-A02).

NCEER-93-0017   "The Island of Guam Earthquake of August 8, 1993," by S.W. Swan and S.K. Harris, 9/30/93, (PB94-141843, A04, MF-A01).

NCEER-93-0018   "Engineering Aspects of the October 12, 1992 Egyptian Earthquake," by A.W. Elgamal, M. Amer, K. Adalier and A. Abul-Fadl, 10/7/93, (PB94-141983, A05, MF-A01).

NCEER-93-0019   "Development of an Earthquake Motion Simulator and its Application in Dynamic Centrifuge Testing," by I. Krstelj, Supervised by J.H. Prevost, 10/23/93, (PB94-181773, A-10, MF-A03).

NCEER-93-0020   "NCEER-Taisei Corporation Research Program on Sliding Seismic Isolation Systems for Bridges: Experimental and Analytical Study of a Friction Pendulum System (FPS)," by M.C. Constantinou, P. Tsopelas, Y-S. Kim and S. Okamoto, 11/1/93, (PB94-142775, A08, MF-A02).

NCEER-93-0021   "Finite Element Modeling of Elastomeric Seismic Isolation Bearings," by L.J. Billings, Supervised by R. Shepherd, 11/8/93, to be published.

NCEER-93-0022   "Seismic Vulnerability of Equipment in Critical Facilities: Life-Safety and Operational Consequences," by K. Porter, G.S. Johnson, M.M. Zadeh, C. Scawthorn and S. Eder, 11/24/93, (PB94-181765, A16, MF-A03).

NCEER-93-0023   "Hokkaido Nansei-oki, Japan Earthquake of July 12, 1993, by P.I. Yanev and C.R. Scawthorn, 12/23/93, (PB94-181500, A07, MF-A01).

NCEER-94-0001   "An Evaluation of Seismic Serviceability of Water Supply Networks with Application to the San Francisco Auxiliary Water Supply System," by I. Markov, Supervised by M. Grigoriu and T. O'Rourke, 1/21/94, (PB94-204013, A07, MF-A02).

NCEER-94-0002   "NCEER-Taisei Corporation Research Program on Sliding Seismic Isolation Systems for Bridges: Experimental and Analytical Study of Systems Consisting of Sliding Bearings, Rubber Restoring Force Devices and Fluid Dampers," Volumes I and II, by P. Tsopelas, S. Okamoto, M.C. Constantinou, D. Ozaki and S. Fujii, 2/4/94, (PB94-181740, A09, MF-A02 and PB94-181757, A12, MF-A03).

NCEER-94-0003   "A Markov Model for Local and Global Damage Indices in Seismic Analysis," by S. Rahman and M. Grigoriu, 2/18/94, (PB94-206000, A12, MF-A03).

NCEER-94-0004   "Proceedings from the NCEER Workshop on Seismic Response of Masonry Infills," edited by D.P. Abrams, 3/1/94, (PB94-180783, A07, MF-A02).

NCEER-94-0005   "The Northridge, California Earthquake of January 17, 1994: General Reconnaissance Report," edited by J.D. Goltz, 3/11/94, (PB94-193943, A10, MF-A03).

NCEER-94-0006   "Seismic Energy Based Fatigue Damage Analysis of Bridge Columns: Part I - Evaluation of Seismic Capacity," by G.A. Chang and J.B. Mander, 3/14/94, (PB94-219185, A11, MF-A03).

NCEER-94-0007   "Seismic Isolation of Multi-Story Frame Structures Using Spherical Sliding Isolation Systems," by T.M. Al-Hussaini, V.A. Zayas and M.C. Constantinou, 3/17/94, (PB94-193745, A09, MF-A02).

NCEER-94-0008   "The Northridge, California Earthquake of January 17, 1994: Performance of Highway Bridges," edited by I.G. Buckle, 3/24/94, (PB94-193851, A06, MF-A02).

NCEER-94-0009   "Proceedings of the Third U.S.-Japan Workshop on Earthquake Protective Systems for Bridges," edited by I.G. Buckle and I. Friedland, 3/31/94, (PB94-195815, A99, MF-A06).

NCEER-94-0010   "3D-BASIS-ME: Computer Program for Nonlinear Dynamic Analysis of Seismically Isolated Single and Multiple Structures and Liquid Storage Tanks," by P.C. Tsopelas, M.C. Constantinou and A.M. Reinhorn, 4/12/94, (PB94-204922, A09, MF-A02).

NCEER-94-0011   "The Northridge, California Earthquake of January 17, 1994: Performance of Gas Transmission Pipelines," by T.D. O'Rourke and M.C. Palmer, 5/16/94, (PB94-204989, A05, MF-A01).

NCEER-94-0012   "Feasibility Study of Replacement Procedures and Earthquake Performance Related to Gas Transmission Pipelines," by T.D. O'Rourke and M.C. Palmer, 5/25/94, (PB94-206638, A09, MF-A02).

NCEER-94-0013   "Seismic Energy Based Fatigue Damage Analysis of Bridge Columns: Part II - Evaluation of Seismic Demand," by G.A. Chang and J.B. Mander, 6/1/94, (PB95-18106, A08, MF-A02).

NCEER-94-0014   "NCEER-Taisei Corporation Research Program on Sliding Seismic Isolation Systems for Bridges: Experimental and Analytical Study of a System Consisting of Sliding Bearings and Fluid Restoring Force/Damping Devices," by P. Tsopelas and M.C. Constantinou, 6/13/94, (PB94-219144, A10, MF-A03).

NCEER-94-0015   "Generation of Hazard-Consistent Fragility Curves for Seismic Loss Estimation Studies," by H. Hwang and J-R. Huo, 6/14/94, (PB95-181996, A09, MF-A02).

NCEER-94-0016   "Seismic Study of Building Frames with Added Energy-Absorbing Devices," by W.S. Pong, C.S. Tsai and G.C. Lee, 6/20/94, (PB94-219136, A10, A03).

NCEER-94-0017   "Sliding Mode Control for Seismic-Excited Linear and Nonlinear Civil Engineering Structures," by J. Yang, J. Wu, A. Agrawal and Z. Li, 6/21/94, (PB95-138483, A06, MF-A02).

NCEER-94-0018   "3D-BASIS-TABS Version 2.0: Computer Program for Nonlinear Dynamic Analysis of Three Dimensional Base Isolated Structures," by A.M. Reinhorn, S. Nagarajaiah, M.C. Constantinou, P. Tsopelas and R. Li, 6/22/94, (PB95-182176, A08, MF-A02).

NCEER-94-0019   "Proceedings of the International Workshop on Civil Infrastructure Systems: Application of Intelligent Systems and Advanced Materials on Bridge Systems," Edited by G.C. Lee and K.C. Chang, 7/18/94, (PB95-252474, A20, MF-A04).

NCEER-94-0020   "Study of Seismic Isolation Systems for Computer Floors," by V. Lambrou and M.C. Constantinou, 7/19/94, (PB95-138533, A10, MF-A03).

NCEER-94-0021   "Proceedings of the U.S.-Italian Workshop on Guidelines for Seismic Evaluation and Rehabilitation of Unreinforced Masonry Buildings," Edited by D.P. Abrams and G.M. Calvi, 7/20/94, (PB95-138749, A13, MF-A03).

NCEER-94-0022   "NCEER-Taisei Corporation Research Program on Sliding Seismic Isolation Systems for Bridges: Experimental and Analytical Study of a System Consisting of Lubricated PTFE Sliding Bearings and Mild Steel Dampers," by P. Tsopelas and M.C. Constantinou, 7/22/94, (PB95-182184, A08, MF-A02).

NCEER-94-0023   "Development of Reliability-Based Design Criteria for Buildings Under Seismic Load," by Y.K. Wen, H. Hwang and M. Shinozuka, 8/1/94, (PB95-211934, A08, MF-A02).

NCEER-94-0024   "Experimental Verification of Acceleration Feedback Control Strategies for an Active Tendon System," by S.J. Dyke, B.F. Spencer, Jr., P. Quast, M.K. Sain, D.C. Kaspari, Jr. and T.T. Soong, 8/29/94, (PB95-212320, A05, MF-A01).

NCEER-94-0025   "Seismic Retrofitting Manual for Highway Bridges," Edited by I.G. Buckle and I.F. Friedland, published by the Federal Highway Administration (PB95-212676, A15, MF-A03).

NCEER-94-0026   "Proceedings from the Fifth U.S.-Japan Workshop on Earthquake Resistant Design of Lifeline Facilities and Countermeasures Against Soil Liquefaction," Edited by T.D. O'Rourke and M. Hamada, 11/7/94, (PB95-220802, A99, MF-E08).

NCEER-95-0001 "Experimental and Analytical Investigation of Seismic Retrofit of Structures with Supplemental Damping: Part 1 - Fluid Viscous Damping Devices," by A.M. Reinhorn, C. Li and M.C. Constantinou, 1/3/95, (PB95-266599, A09, MF-A02).

NCEER-95-0002 "Experimental and Analytical Study of Low-Cycle Fatigue Behavior of Semi-Rigid Top-And-Seat Angle Connections," by G. Pekcan, J.B. Mander and S.S. Chen, 1/5/95, (PB95-220042, A07, MF-A02).

NCEER-95-0003 "NCEER-ATC Joint Study on Fragility of Buildings," by T. Anagnos, C. Rojahn and A.S. Kiremidjian, 1/20/95, (PB95-220026, A06, MF-A02).

NCEER-95-0004 "Nonlinear Control Algorithms for Peak Response Reduction," by Z. Wu, T.T. Soong, V. Gattulli and R.C. Lin, 2/16/95, (PB95-220349, A05, MF-A01).

NCEER-95-0005 "Pipeline Replacement Feasibility Study: A Methodology for Minimizing Seismic and Corrosion Risks to Underground Natural Gas Pipelines," by R.T. Eguchi, H.A. Seligson and D.G. Honegger, 3/2/95, (PB95-252326, A06, MF-A02).

NCEER-95-0006 "Evaluation of Seismic Performance of an 11-Story Frame Building During the 1994 Northridge Earthquake," by F. Naeim, R. DiSulio, K. Benuska, A. Reinhorn and C. Li, to be published.

NCEER-95-0007 "Prioritization of Bridges for Seismic Retrofitting," by N. Basöz and A.S. Kiremidjian, 4/24/95, (PB95-252300, A08, MF-A02).

NCEER-95-0008 "Method for Developing Motion Damage Relationships for Reinforced Concrete Frames," by A. Singhal and A.S. Kiremidjian, 5/11/95, (PB95-266607, A06, MF-A02).

NCEER-95-0009 "Experimental and Analytical Investigation of Seismic Retrofit of Structures with Supplemental Damping: Part II - Friction Devices," by C. Li and A.M. Reinhorn, 7/6/95, (PB96-128087, A11, MF-A03).

NCEER-95-0010 "Experimental Performance and Analytical Study of a Non-Ductile Reinforced Concrete Frame Structure Retrofitted with Elastomeric Spring Dampers," by G. Pekcan, J.B. Mander and S.S. Chen, 7/14/95, (PB96-137161, A08, MF-A02).

NCEER-95-0011 "Development and Experimental Study of Semi-Active Fluid Damping Devices for Seismic Protection of Structures," by M.D. Symans and M.C. Constantinou, 8/3/95, (PB96-136940, A23, MF-A04).

NCEER-95-0012 "Real-Time Structural Parameter Modification (RSPM): Development of Innervated Structures," by Z. Liang, M. Tong and G.C. Lee, 4/11/95, (PB96-137153, A06, MF-A01).

NCEER-95-0013 "Experimental and Analytical Investigation of Seismic Retrofit of Structures with Supplemental Damping: Part III - Viscous Damping Walls," by A.M. Reinhorn and C. Li, 10/1/95, (PB96-176409, A11, MF-A03).

NCEER-95-0014 "Seismic Fragility Analysis of Equipment and Structures in a Memphis Electric Substation," by J-R. Huo and H.H.M. Hwang, 8/10/95, (PB96-128087, A09, MF-A02).

NCEER-95-0015 "The Hanshin-Awaji Earthquake of January 17, 1995: Performance of Lifelines," Edited by M. Shinozuka, 11/3/95, (PB96-176383, A15, MF-A03).

NCEER-95-0016 "Highway Culvert Performance During Earthquakes," by T.L. Youd and C.J. Beckman, available as NCEER-96-0015.

NCEER-95-0017 "The Hanshin-Awaji Earthquake of January 17, 1995: Performance of Highway Bridges," Edited by I.G. Buckle, 12/1/95, to be published.

NCEER-95-0018 "Modeling of Masonry Infill Panels for Structural Analysis," by A.M. Reinhorn, A. Madan, R.E. Valles, Y. Reichmann and J.B. Mander, 12/8/95, (PB97-110886, MF-A01, A06).

NCEER-95-0019 "Optimal Polynomial Control for Linear and Nonlinear Structures," by A.K. Agrawal and J.N. Yang, 12/11/95, (PB96-168737, A07, MF-A02).

NCEER-95-0020   "Retrofit of Non-Ductile Reinforced Concrete Frames Using Friction Dampers," by R.S. Rao, P. Gergely and R.N. White, 12/22/95, (PB97-133508, A10, MF-A02).

NCEER-95-0021   "Parametric Results for Seismic Response of Pile-Supported Bridge Bents," by G. Mylonakis, A. Nikolaou and G. Gazetas, 12/22/95, (PB97-100242, A12, MF-A03).

NCEER-95-0022   "Kinematic Bending Moments in Seismically Stressed Piles," by A. Nikolaou, G. Mylonakis and G. Gazetas, 12/23/95, (PB97-113914, MF-A03, A13).

NCEER-96-0001   "Dynamic Response of Unreinforced Masonry Buildings with Flexible Diaphragms," by A.C. Costley and D.P. Abrams," 10/10/96, (PB97-133573, MF-A03, A15).

NCEER-96-0002   "State of the Art Review: Foundations and Retaining Structures," by I. Po Lam, to be published.

NCEER-96-0003   "Ductility of Rectangular Reinforced Concrete Bridge Columns with Moderate Confinement," by N. Wehbe, M. Saiidi, D. Sanders and B. Douglas, 11/7/96, (PB97-133557, A06, MF-A02).

NCEER-96-0004   "Proceedings of the Long-Span Bridge Seismic Research Workshop," edited by I.G. Buckle and I.M. Friedland, to be published.

NCEER-96-0005   "Establish Representative Pier Types for Comprehensive Study: Eastern United States," by J. Kulicki and Z. Prucz, 5/28/96, (PB98-119217, A07, MF-A02).

NCEER-96-0006   "Establish Representative Pier Types for Comprehensive Study: Western United States," by R. Imbsen, R.A. Schamber and T.A. Osterkamp, 5/28/96, (PB98-118607, A07, MF-A02).

NCEER-96-0007   "Nonlinear Control Techniques for Dynamical Systems with Uncertain Parameters," by R.G. Ghanem and M.I. Bujakov, 5/27/96, (PB97-100259, A17, MF-A03).

NCEER-96-0008   "Seismic Evaluation of a 30-Year Old Non-Ductile Highway Bridge Pier and Its Retrofit," by J.B. Mander, B. Mahmoodzadegan, S. Bhadra and S.S. Chen, 5/31/96, (PB97-110902, MF-A03, A10).

NCEER-96-0009   "Seismic Performance of a Model Reinforced Concrete Bridge Pier Before and After Retrofit," by J.B. Mander, J.H. Kim and C.A. Ligozio, 5/31/96, (PB97-110910, MF-A02, A10).

NCEER-96-0010   "IDARC2D Version 4.0: A Computer Program for the Inelastic Damage Analysis of Buildings," by R.E. Valles, A.M. Reinhorn, S.K. Kunnath, C. Li and A. Madan, 6/3/96, (PB97-100234, A17, MF-A03).

NCEER-96-0011   "Estimation of the Economic Impact of Multiple Lifeline Disruption: Memphis Light, Gas and Water Division Case Study," by S.E. Chang, H.A. Seligson and R.T. Eguchi, 8/16/96, (PB97-133490, A11, MF-A03).

NCEER-96-0012   "Proceedings from the Sixth Japan-U.S. Workshop on Earthquake Resistant Design of Lifeline Facilities and Countermeasures Against Soil Liquefaction, Edited by M. Hamada and T. O'Rourke, 9/11/96, (PB97-133581, A99, MF-A06).

NCEER-96-0013   "Chemical Hazards, Mitigation and Preparedness in Areas of High Seismic Risk: A Methodology for Estimating the Risk of Post-Earthquake Hazardous Materials Release," by H.A. Seligson, R.T. Eguchi, K.J. Tierney and K. Richmond, 11/7/96, (PB97-133565, MF-A02, A08).

NCEER-96-0014   "Response of Steel Bridge Bearings to Reversed Cyclic Loading," by J.B. Mander, D-K. Kim, S.S. Chen and G.J. Premus, 11/13/96, (PB97-140735, A12, MF-A03).

NCEER-96-0015   "Highway Culvert Performance During Past Earthquakes," by T.L. Youd and C.J. Beckman, 11/25/96, (PB97-133532, A06, MF-A01).

NCEER-97-0001   "Evaluation, Prevention and Mitigation of Pounding Effects in Building Structures," by R.E. Valles and A.M. Reinhorn, 2/20/97, (PB97-159552, A14, MF-A03).

NCEER-97-0002   "Seismic Design Criteria for Bridges and Other Highway Structures," by C. Rojahn, R. Mayes, D.G. Anderson, J. Clark, J.H. Hom, R.V. Nutt and M.J. O'Rourke, 4/30/97, (PB97-194658, A06, MF-A03).

NCEER-97-0003   "Proceedings of the U.S.-Italian Workshop on Seismic Evaluation and Retrofit," Edited by D.P. Abrams and G.M. Calvi, 3/19/97, (PB97-194666, A13, MF-A03).

NCEER-97-0004   "Investigation of Seismic Response of Buildings with Linear and Nonlinear Fluid Viscous Dampers," by A.A. Seleemah and M.C. Constantinou, 5/21/97, (PB98-109002, A15, MF-A03).

NCEER-97-0005   "Proceedings of the Workshop on Earthquake Engineering Frontiers in Transportation Facilities," edited by G.C. Lee and I.M. Friedland, 8/29/97, (PB98-128911, A25, MR-A04).

NCEER-97-0006   "Cumulative Seismic Damage of Reinforced Concrete Bridge Piers," by S.K. Kunnath, A. El-Bahy, A. Taylor and W. Stone, 9/2/97, (PB98-108814, A11, MF-A03).

NCEER-97-0007   "Structural Details to Accommodate Seismic Movements of Highway Bridges and Retaining Walls," by R.A. Imbsen, R.A. Schamber, E. Thorkildsen, A. Kartoum, B.T. Martin, T.N. Rosser and J.M. Kulicki, 9/3/97, (PB98-108996, A09, MF-A02).

NCEER-97-0008   "A Method for Earthquake Motion-Damage Relationships with Application to Reinforced Concrete Frames," by A. Singhal and A.S. Kiremidjian, 9/10/97, (PB98-108988, A13, MF-A03).

NCEER-97-0009   "Seismic Analysis and Design of Bridge Abutments Considering Sliding and Rotation," by K. Fishman and R. Richards, Jr., 9/15/97, (PB98-108897, A06, MF-A02).

NCEER-97-0010   "Proceedings of the FHWA/NCEER Workshop on the National Representation of Seismic Ground Motion for New and Existing Highway Facilities," edited by I.M. Friedland, M.S. Power and R.L. Mayes, 9/22/97, (PB98-128903, A21, MF-A04).

NCEER-97-0011   "Seismic Analysis for Design or Retrofit of Gravity Bridge Abutments," by K.L. Fishman, R. Richards, Jr. and R.C. Divito, 10/2/97, (PB98-128937, A08, MF-A02).

NCEER-97-0012   "Evaluation of Simplified Methods of Analysis for Yielding Structures," by P. Tsopelas, M.C. Constantinou, C.A. Kircher and A.S. Whittaker, 10/31/97, (PB98-128929, A10, MF-A03).

NCEER-97-0013   "Seismic Design of Bridge Columns Based on Control and Repairability of Damage," by C-T. Cheng and J.B. Mander, 12/8/97, (PB98-144249, A11, MF-A03).

NCEER-97-0014   "Seismic Resistance of Bridge Piers Based on Damage Avoidance Design," by J.B. Mander and C-T. Cheng, 12/10/97, (PB98-144223, A09, MF-A02).

NCEER-97-0015   "Seismic Response of Nominally Symmetric Systems with Strength Uncertainty," by S. Balopoulou and M. Grigoriu, 12/23/97, (PB98-153422, A11, MF-A03).

NCEER-97-0016   "Evaluation of Seismic Retrofit Methods for Reinforced Concrete Bridge Columns," by T.J. Wipf, F.W. Klaiber and F.M. Russo, 12/28/97, (PB98-144215, A12, MF-A03).

NCEER-97-0017   "Seismic Fragility of Existing Conventional Reinforced Concrete Highway Bridges," by C.L. Mullen and A.S. Cakmak, 12/30/97, (PB98-153406, A08, MF-A02).

NCEER-97-0018   "Loss Asssessment of Memphis Buildings," edited by D.P. Abrams and M. Shinozuka, 12/31/97, (PB98-144231, A13, MF-A03).

NCEER-97-0019   "Seismic Evaluation of Frames with Infill Walls Using Quasi-static Experiments," by K.M. Mosalam, R.N. White and P. Gergely, 12/31/97, (PB98-153455, A07, MF-A02).

NCEER-97-0020   "Seismic Evaluation of Frames with Infill Walls Using Pseudo-dynamic Experiments," by K.M. Mosalam, R.N. White and P. Gergely, 12/31/97, (PB98-153430, A07, MF-A02).

NCEER-97-0021   "Computational Strategies for Frames with Infill Walls: Discrete and Smeared Crack Analyses and Seismic Fragility," by K.M. Mosalam, R.N. White and P. Gergely, 12/31/97, (PB98-153414, A10, MF-A02).

NCEER-97-0022   "Proceedings of the NCEER Workshop on Evaluation of Liquefaction Resistance of Soils," edited by T.L. Youd and I.M. Idriss, 12/31/97, (PB98-155617, A15, MF-A03).

MCEER-98-0001   "Extraction of Nonlinear Hysteretic Properties of Seismically Isolated Bridges from Quick-Release Field Tests," by Q. Chen, B.M. Douglas, E.M. Maragakis and I.G. Buckle, 5/26/98, (PB99-118838, A06, MF-A01).

MCEER-98-0002   "Methodologies for Evaluating the Importance of Highway Bridges," by A. Thomas, S. Eshenaur and J. Kulicki, 5/29/98, (PB99-118846, A10, MF-A02).

MCEER-98-0003   "Capacity Design of Bridge Piers and the Analysis of Overstrength," by J.B. Mander, A. Dutta and P. Goel, 6/1/98, (PB99-118853, A09, MF-A02).

MCEER-98-0004   "Evaluation of Bridge Damage Data from the Loma Prieta and Northridge, California Earthquakes," by N. Basoz and A. Kiremidjian, 6/2/98, (PB99-118861, A15, MF-A03).

MCEER-98-0005   "Screening Guide for Rapid Assessment of Liquefaction Hazard at Highway Bridge Sites," by T. L. Youd, 6/16/98, (PB99-118879, A06, not available on microfiche).

MCEER-98-0006   "Structural Steel and Steel/Concrete Interface Details for Bridges," by P. Ritchie, N. Kauhl and J. Kulicki, 7/13/98, (PB99-118945, A06, MF-A01).

MCEER-98-0007   "Capacity Design and Fatigue Analysis of Confined Concrete Columns," by A. Dutta and J.B. Mander, 7/14/98, (PB99-118960, A14, MF-A03).

MCEER-98-0008   "Proceedings of the Workshop on Performance Criteria for Telecommunication Services Under Earthquake Conditions," edited by A.J. Schiff, 7/15/98, (PB99-118952, A08, MF-A02).

MCEER-98-0009   "Fatigue Analysis of Unconfined Concrete Columns," by J.B. Mander, A. Dutta and J.H. Kim, 9/12/98, (PB99-123655, A10, MF-A02).

MCEER-98-0010   "Centrifuge Modeling of Cyclic Lateral Response of Pile-Cap Systems and Seat-Type Abutments in Dry Sands," by A.D. Gadre and R. Dobry, 10/2/98, (PB99-123606, A13, MF-A03).

MCEER-98-0011   "IDARC-BRIDGE: A Computational Platform for Seismic Damage Assessment of Bridge Structures," by A.M. Reinhorn, V. Simeonov, G. Mylonakis and Y. Reichman, 10/2/98, (PB99-162919, A15, MF-A03).

MCEER-98-0012   "Experimental Investigation of the Dynamic Response of Two Bridges Before and After Retrofitting with Elastomeric Bearings," by D.A. Wendichansky, S.S. Chen and J.B. Mander, 10/2/98, (PB99-162927, A15, MF-A03).

MCEER-98-0013   "Design Procedures for Hinge Restrainers and Hinge Sear Width for Multiple-Frame Bridges," by R. Des Roches and G.L. Fenves, 11/3/98, (PB99-140477, A13, MF-A03).

MCEER-98-0014   "Response Modification Factors for Seismically Isolated Bridges," by M.C. Constantinou and J.K. Quarshie, 11/3/98, (PB99-140485, A14, MF-A03).

MCEER-98-0015   "Proceedings of the U.S.-Italy Workshop on Seismic Protective Systems for Bridges," edited by I.M. Friedland and M.C. Constantinou, 11/3/98, (PB2000-101711, A22, MF-A04).

MCEER-98-0016   "Appropriate Seismic Reliability for Critical Equipment Systems: Recommendations Based on Regional Analysis of Financial and Life Loss," by K. Porter, C. Scawthorn, C. Taylor and N. Blais, 11/10/98, (PB99-157265, A08, MF-A02).

MCEER-98-0017   "Proceedings of the U.S. Japan Joint Seminar on Civil Infrastructure Systems Research," edited by M. Shinozuka and A. Rose, 11/12/98, (PB99-156713, A16, MF-A03).

MCEER-98-0018   "Modeling of Pile Footings and Drilled Shafts for Seismic Design," by I. PoLam, M. Kapuskar and D. Chaudhuri, 12/21/98, (PB99-157257, A09, MF-A02).

MCEER-99-0001 "Seismic Evaluation of a Masonry Infilled Reinforced Concrete Frame by Pseudodynamic Testing," by S.G. Buonopane and R.N. White, 2/16/99, (PB99-162851, A09, MF-A02).

MCEER-99-0002 "Response History Analysis of Structures with Seismic Isolation and Energy Dissipation Systems: Verification Examples for Program SAP2000," by J. Scheller and M.C. Constantinou, 2/22/99, (PB99-162869, A08, MF-A02).

MCEER-99-0003 "Experimental Study on the Seismic Design and Retrofit of Bridge Columns Including Axial Load Effects," by A. Dutta, T. Kokorina and J.B. Mander, 2/22/99, (PB99-162877, A09, MF-A02).

MCEER-99-0004 "Experimental Study of Bridge Elastomeric and Other Isolation and Energy Dissipation Systems with Emphasis on Uplift Prevention and High Velocity Near-source Seismic Excitation," by A. Kasalanati and M. C. Constantinou, 2/26/99, (PB99-162885, A12, MF-A03).

MCEER-99-0005 "Truss Modeling of Reinforced Concrete Shear-flexure Behavior," by J.H. Kim and J.B. Mander, 3/8/99, (PB99-163693, A12, MF-A03).

MCEER-99-0006 "Experimental Investigation and Computational Modeling of Seismic Response of a 1:4 Scale Model Steel Structure with a Load Balancing Supplemental Damping System," by G. Pekcan, J.B. Mander and S.S. Chen, 4/2/99, (PB99-162893, A11, MF-A03).

MCEER-99-0007 "Effect of Vertical Ground Motions on the Structural Response of Highway Bridges," by M.R. Button, C.J. Cronin and R.L. Mayes, 4/10/99, (PB2000-101411, A10, MF-A03).

MCEER-99-0008 "Seismic Reliability Assessment of Critical Facilities: A Handbook, Supporting Documentation, and Model Code Provisions," by G.S. Johnson, R.E. Sheppard, M.D. Quilici, S.J. Eder and C.R. Scawthorn, 4/12/99, (PB2000-101701, A18, MF-A04).

MCEER-99-0009 "Impact Assessment of Selected MCEER Highway Project Research on the Seismic Design of Highway Structures," by C. Rojahn, R. Mayes, D.G. Anderson, J.H. Clark, D'Appolonia Engineering, S. Gloyd and R.V. Nutt, 4/14/99, (PB99-162901, A10, MF-A02).

MCEER-99-0010 "Site Factors and Site Categories in Seismic Codes," by R. Dobry, R. Ramos and M.S. Power, 7/19/99, (PB2000-101705, A08, MF-A02).

MCEER-99-0011 "Restrainer Design Procedures for Multi-Span Simply-Supported Bridges," by M.J. Randall, M. Saiidi, E. Maragakis and T. Isakovic, 7/20/99, (PB2000-101702, A10, MF-A02).

MCEER-99-0012 "Property Modification Factors for Seismic Isolation Bearings," by M.C. Constantinou, P. Tsopelas, A. Kasalanati and E. Wolff, 7/20/99, (PB2000-103387, A11, MF-A03).

MCEER-99-0013 "Critical Seismic Issues for Existing Steel Bridges," by P. Ritchie, N. Kauhl and J. Kulicki, 7/20/99, (PB2000-101697, A09, MF-A02).

MCEER-99-0014 "Nonstructural Damage Database," by A. Kao, T.T. Soong and A. Vender, 7/24/99, (PB2000-101407, A06, MF-A01).

MCEER-99-0015 "Guide to Remedial Measures for Liquefaction Mitigation at Existing Highway Bridge Sites," by H.G. Cooke and J. K. Mitchell, 7/26/99, (PB2000-101703, A11, MF-A03).

MCEER-99-0016 "Proceedings of the MCEER Workshop on Ground Motion Methodologies for the Eastern United States," edited by N. Abrahamson and A. Becker, 8/11/99, (PB2000-103385, A07, MF-A02).

MCEER-99-0017 "Quindío, Colombia Earthquake of January 25, 1999: Reconnaissance Report," by A.P. Asfura and P.J. Flores, 10/4/99, (PB2000-106893, A06, MF-A01).

MCEER-99-0018 "Hysteretic Models for Cyclic Behavior of Deteriorating Inelastic Structures," by M.V. Sivaselvan and A.M. Reinhorn, 11/5/99, (PB2000-103386, A08, MF-A02).

MCEER-99-0019   "Proceedings of the 7th U.S.- Japan Workshop on Earthquake Resistant Design of Lifeline Facilities and Countermeasures Against Soil Liquefaction," edited by T.D. O'Rourke, J.P. Bardet and M. Hamada, 11/19/99, (PB2000-103354, A99, MF-A06).

MCEER-99-0020   "Development of Measurement Capability for Micro-Vibration Evaluations with Application to Chip Fabrication Facilities," by G.C. Lee, Z. Liang, J.W. Song, J.D. Shen and W.C. Liu, 12/1/99, (PB2000-105993, A08, MF-A02).

MCEER-99-0021   "Design and Retrofit Methodology for Building Structures with Supplemental Energy Dissipating Systems," by G. Pekcan, J.B. Mander and S.S. Chen, 12/31/99, (PB2000-105994, A11, MF-A03).

MCEER-00-0001   "The Marmara, Turkey Earthquake of August 17, 1999: Reconnaissance Report," edited by C. Scawthorn; with major contributions by M. Bruneau, R. Eguchi, T. Holzer, G. Johnson, J. Mander, J. Mitchell, W. Mitchell, A. Papageorgiou, C. Scaethorn, and G. Webb, 3/23/00, (PB2000-106200, A11, MF-A03).

MCEER-00-0002   "Proceedings of the MCEER Workshop for Seismic Hazard Mitigation of Health Care Facilities," edited by G.C. Lee, M. Ettouney, M. Grigoriu, J. Hauer and J. Nigg, 3/29/00, (PB2000-106892, A08, MF-A02).

MCEER-00-0003   "The Chi-Chi, Taiwan Earthquake of September 21, 1999: Reconnaissance Report," edited by G.C. Lee and C.H. Loh, with major contributions by G.C. Lee, M. Bruneau, I.G. Buckle, S.E. Chang, P.J. Flores, T.D. O'Rourke, M. Shinozuka, T.T. Soong, C-H. Loh, K-C. Chang, Z-J. Chen, J-S. Hwang, M-L. Lin, G-Y. Liu, K-C. Tsai, G.C. Yao and C-L. Yen, 4/30/00, (PB2001-100980, A10, MF-A02).

MCEER-00-0004   "Seismic Retrofit of End-Sway Frames of Steel Deck-Truss Bridges with a Supplemental Tendon System: Experimental and Analytical Investigation," by G. Pekcan, J.B. Mander and S.S. Chen, 7/1/00, (PB2001-100982, A10, MF-A02).

MCEER-00-0005   "Sliding Fragility of Unrestrained Equipment in Critical Facilities," by W.H. Chong and T.T. Soong, 7/5/00, (PB2001-100983, A08, MF-A02).

MCEER-00-0006   "Seismic Response of Reinforced Concrete Bridge Pier Walls in the Weak Direction," by N. Abo-Shadi, M. Saiidi and D. Sanders, 7/17/00, (PB2001-100981, A17, MF-A03).

MCEER-00-0007   "Low-Cycle Fatigue Behavior of Longitudinal Reinforcement in Reinforced Concrete Bridge Columns," by J. Brown and S.K. Kunnath, 7/23/00, (PB2001-104392, A08, MF-A02).

MCEER-00-0008   "Soil Structure Interaction of Bridges for Seismic Analysis," I. PoLam and H. Law, 9/25/00, (PB2001-105397, A08, MF-A02).

MCEER-00-0009   "Proceedings of the First MCEER Workshop on Mitigation of Earthquake Disaster by Advanced Technologies (MEDAT-1), edited by M. Shinozuka, D.J. Inman and T.D. O'Rourke, 11/10/00, (PB2001-105399, A14, MF-A03).

MCEER-00-0010   "Development and Evaluation of Simplified Procedures for Analysis and Design of Buildings with Passive Energy Dissipation Systems, Revision 01," by O.M. Ramirez, M.C. Constantinou, C.A. Kircher, A.S. Whittaker, M.W. Johnson, J.D. Gomez and C. Chrysostomou, 11/16/01, (PB2001-105523, A23, MF-A04).

MCEER-00-0011   "Dynamic Soil-Foundation-Structure Interaction Analyses of Large Caissons," by C-Y. Chang, C-M. Mok, Z-L. Wang, R. Settgast, F. Waggoner, M.A. Ketchum, H.M. Gonnermann and C-C. Chin, 12/30/00, (PB2001-104373, A07, MF-A02).

MCEER-00-0012   "Experimental Evaluation of Seismic Performance of Bridge Restrainers," by A.G. Vlassis, E.M. Maragakis and M. Saiid Saiidi, 12/30/00, (PB2001-104354, A09, MF-A02).

MCEER-00-0013   "Effect of Spatial Variation of Ground Motion on Highway Structures," by M. Shinozuka, V. Saxena and G. Deodatis, 12/31/00, (PB2001-108755, A13, MF-A03).

MCEER-00-0014   "A Risk-Based Methodology for Assessing the Seismic Performance of Highway Systems," by S.D. Werner, C.E. Taylor, J.E. Moore, II, J.S. Walton and S. Cho, 12/31/00, (PB2001-108756, A14, MF-A03).

MCEER-01-0001 "Experimental Investigation of P-Delta Effects to Collapse During Earthquakes," by D. Vian and M. Bruneau, 6/25/01, (PB2002-100534, A17, MF-A03).

MCEER-01-0002 "Proceedings of the Second MCEER Workshop on Mitigation of Earthquake Disaster by Advanced Technologies (MEDAT-2)," edited by M. Bruneau and D.J. Inman, 7/23/01, (PB2002-100434, A16, MF-A03).

MCEER-01-0003 "Sensitivity Analysis of Dynamic Systems Subjected to Seismic Loads," by C. Roth and M. Grigoriu, 9/18/01, (PB2003-100884, A12, MF-A03).

MCEER-01-0004 "Overcoming Obstacles to Implementing Earthquake Hazard Mitigation Policies: Stage 1 Report," by D.J. Alesch and W.J. Petak, 12/17/01, (PB2002-107949, A07, MF-A02).

MCEER-01-0005 "Updating Real-Time Earthquake Loss Estimates: Methods, Problems and Insights," by C.E. Taylor, S.E. Chang and R.T. Eguchi, 12/17/01, (PB2002-107948, A05, MF-A01).

MCEER-01-0006 "Experimental Investigation and Retrofit of Steel Pile Foundations and Pile Bents Under Cyclic Lateral Loadings," by A. Shama, J. Mander, B. Blabac and S. Chen, 12/31/01, (PB2002-107950, A13, MF-A03).

MCEER-02-0001 "Assessment of Performance of Bolu Viaduct in the 1999 Duzce Earthquake in Turkey" by P.C. Roussis, M.C. Constantinou, M. Erdik, E. Durukal and M. Dicleli, 5/8/02, (PB2003-100883, A08, MF-A02).

MCEER-02-0002 "Seismic Behavior of Rail Counterweight Systems of Elevators in Buildings," by M.P. Singh, Rildova and L.E. Suarez, 5/27/02. (PB2003-100882, A11, MF-A03).

MCEER-02-0003 "Development of Analysis and Design Procedures for Spread Footings," by G. Mylonakis, G. Gazetas, S. Nikolaou and A. Chauncey, 10/02/02, (PB2004-101636, A13, MF-A03, CD-A13).

MCEER-02-0004 "Bare-Earth Algorithms for Use with SAR and LIDAR Digital Elevation Models," by C.K. Huyck, R.T. Eguchi and B. Houshmand, 10/16/02, (PB2004-101637, A07, CD-A07).

MCEER-02-0005 "Review of Energy Dissipation of Compression Members in Concentrically Braced Frames," by K.Lee and M. Bruneau, 10/18/02, (PB2004-101638, A10, CD-A10).

MCEER-03-0001 "Experimental Investigation of Light-Gauge Steel Plate Shear Walls for the Seismic Retrofit of Buildings" by J. Berman and M. Bruneau, 5/2/03, (PB2004-101622, A10, MF-A03, CD-A10).

MCEER-03-0002 "Statistical Analysis of Fragility Curves," by M. Shinozuka, M.Q. Feng, H. Kim, T. Uzawa and T. Ueda, 6/16/03, (PB2004-101849, A09, CD-A09).

MCEER-03-0003 "Proceedings of the Eighth U.S.-Japan Workshop on Earthquake Resistant Design f Lifeline Facilities and Countermeasures Against Liquefaction," edited by M. Hamada, J.P. Bardet and T.D. O'Rourke, 6/30/03, (PB2004-104386, A99, CD-A99).

MCEER-03-0004 "Proceedings of the PRC-US Workshop on Seismic Analysis and Design of Special Bridges," edited by L.C. Fan and G.C. Lee, 7/15/03, (PB2004-104387, A14, CD-A14).

MCEER-03-0005 "Urban Disaster Recovery: A Framework and Simulation Model," by S.B. Miles and S.E. Chang, 7/25/03, (PB2004-104388, A07, CD-A07).

MCEER-03-0006 "Behavior of Underground Piping Joints Due to Static and Dynamic Loading," by R.D. Meis, M. Maragakis and R. Siddharthan, 11/17/03, (PB2005-102194, A13, MF-A03, CD-A00).

MCEER-04-0001 "Experimental Study of Seismic Isolation Systems with Emphasis on Secondary System Response and Verification of Accuracy of Dynamic Response History Analysis Methods," by E. Wolff and M. Constantinou, 1/16/04 (PB2005-102195, A99, MF-E08, CD-A00).

MCEER-04-0002 "Tension, Compression and Cyclic Testing of Engineered Cementitious Composite Materials," by K. Kesner and S.L. Billington, 3/1/04, (PB2005-102196, A08, CD-A08).

MCEER-04-0003   "Cyclic Testing of Braces Laterally Restrained by Steel Studs to Enhance Performance During Earthquakes," by O.C. Celik, J.W. Berman and M. Bruneau, 3/16/04, (PB2005-102197, A13, MF-A03, CD-A00).

MCEER-04-0004   "Methodologies for Post Earthquake Building Damage Detection Using SAR and Optical Remote Sensing: Application to the August 17, 1999 Marmara, Turkey Earthquake," by C.K. Huyck, B.J. Adams, S. Cho, R.T. Eguchi, B. Mansouri and B. Houshmand, 6/15/04, (PB2005-104888, A10, CD-A00).

MCEER-04-0005   "Nonlinear Structural Analysis Towards Collapse Simulation: A Dynamical Systems Approach," by M.V. Sivaselvan and A.M. Reinhorn, 6/16/04, (PB2005-104889, A11, MF-A03, CD-A00).

MCEER-04-0006   "Proceedings of the Second PRC-US Workshop on Seismic Analysis and Design of Special Bridges," edited by G.C. Lee and L.C. Fan, 6/25/04, (PB2005-104890, A16, CD-A00).

MCEER-04-0007   "Seismic Vulnerability Evaluation of Axially Loaded Steel Built-up Laced Members," by K. Lee and M. Bruneau, 6/30/04, (PB2005-104891, A16, CD-A00).

MCEER-04-0008   "Evaluation of Accuracy of Simplified Methods of Analysis and Design of Buildings with Damping Systems for Near-Fault and for Soft-Soil Seismic Motions," by E.A. Pavlou and M.C. Constantinou, 8/16/04, (PB2005-104892, A08, MF-A02, CD-A00).

MCEER-04-0009   "Assessment of Geotechnical Issues in Acute Care Facilities in California," by M. Lew, T.D. O'Rourke, R. Dobry and M. Koch, 9/15/04, (PB2005-104893, A08, CD-A00).

MCEER-04-0010   "Scissor-Jack-Damper Energy Dissipation System," by A.N. Sigaher-Boyle and M.C. Constantinou, 12/1/04 (PB2005-108221).

MCEER-04-0011   "Seismic Retrofit of Bridge Steel Truss Piers Using a Controlled Rocking Approach," by M. Pollino and M. Bruneau, 12/20/04 (PB2006-105795).

MCEER-05-0001   "Experimental and Analytical Studies of Structures Seismically Isolated with an Uplift-Restraint Isolation System," by P.C. Roussis and M.C. Constantinou, 1/10/05 (PB2005-108222).

MCEER-05-0002   "A Versatile Experimentation Model for Study of Structures Near Collapse Applied to Seismic Evaluation of Irregular Structures," by D. Kusumastuti, A.M. Reinhorn and A. Rutenberg, 3/31/05 (PB2006-101523).

MCEER-05-0003   "Proceedings of the Third PRC-US Workshop on Seismic Analysis and Design of Special Bridges," edited by L.C. Fan and G.C. Lee, 4/20/05, (PB2006-105796).

MCEER-05-0004   "Approaches for the Seismic Retrofit of Braced Steel Bridge Piers and Proof-of-Concept Testing of an Eccentrically Braced Frame with Tubular Link," by J.W. Berman and M. Bruneau, 4/21/05 (PB2006-101524).

MCEER-05-0005   "Simulation of Strong Ground Motions for Seismic Fragility Evaluation of Nonstructural Components in Hospitals," by A. Wanitkorkul and A. Filiatrault, 5/26/05 (PB2006-500027).

MCEER-05-0006   "Seismic Safety in California Hospitals: Assessing an Attempt to Accelerate the Replacement or Seismic Retrofit of Older Hospital Facilities," by D.J. Alesch, L.A. Arendt and W.J. Petak, 6/6/05 (PB2006-105794).

MCEER-05-0007   "Development of Seismic Strengthening and Retrofit Strategies for Critical Facilities Using Engineered Cementitious Composite Materials," by K. Kesner and S.L. Billington, 8/29/05 (PB2006-111701).

MCEER-05-0008   "Experimental and Analytical Studies of Base Isolation Systems for Seismic Protection of Power Transformers," by N. Murota, M.Q. Feng and G-Y. Liu, 9/30/05 (PB2006-111702).

MCEER-05-0009   "3D-BASIS-ME-MB: Computer Program for Nonlinear Dynamic Analysis of Seismically Isolated Structures," by P.C. Tsopelas, P.C. Roussis, M.C. Constantinou, R. Buchanan and A.M. Reinhorn, 10/3/05 (PB2006-111703).

MCEER-05-0010   "Steel Plate Shear Walls for Seismic Design and Retrofit of Building Structures," by D. Vian and M. Bruneau, 12/15/05 (PB2006-111704).

MCEER-05-0011 "The Performance-Based Design Paradigm," by M.J. Astrella and A. Whittaker, 12/15/05 (PB2006-111705).

MCEER-06-0001 "Seismic Fragility of Suspended Ceiling Systems," H. Badillo-Almaraz, A.S. Whittaker, A.M. Reinhorn and G.P. Cimellaro, 2/4/06 (PB2006-111706).

MCEER-06-0002 "Multi-Dimensional Fragility of Structures," by G.P. Cimellaro, A.M. Reinhorn and M. Bruneau, 3/1/06 (PB2007-106974, A09, MF-A02, CD A00).

MCEER-06-0003 "Built-Up Shear Links as Energy Dissipators for Seismic Protection of Bridges," by P. Dusicka, A.M. Itani and I.G. Buckle, 3/15/06 (PB2006-111708).

MCEER-06-0004 "Analytical Investigation of the Structural Fuse Concept," by R.E. Vargas and M. Bruneau, 3/16/06 (PB2006-111709).

MCEER-06-0005 "Experimental Investigation of the Structural Fuse Concept," by R.E. Vargas and M. Bruneau, 3/17/06 (PB2006-111710).

MCEER-06-0006 "Further Development of Tubular Eccentrically Braced Frame Links for the Seismic Retrofit of Braced Steel Truss Bridge Piers," by J.W. Berman and M. Bruneau, 3/27/06 (PB2007-105147).

MCEER-06-0007 "REDARS Validation Report," by S. Cho, C.K. Huyck, S. Ghosh and R.T. Eguchi, 8/8/06 (PB2007-106983).

MCEER-06-0008 "Review of Current NDE Technologies for Post-Earthquake Assessment of Retrofitted Bridge Columns," by J.W. Song, Z. Liang and G.C. Lee, 8/21/06 (PB2007-106984).

MCEER-06-0009 "Liquefaction Remediation in Silty Soils Using Dynamic Compaction and Stone Columns," by S. Thevanayagam, G.R. Martin, R. Nashed, T. Shenthan, T. Kanagalingam and N. Ecemis, 8/28/06 (PB2007-106985).

MCEER-06-0010 "Conceptual Design and Experimental Investigation of Polymer Matrix Composite Infill Panels for Seismic Retrofitting," by W. Jung, M. Chiewanichakorn and A.J. Aref, 9/21/06 (PB2007-106986).

MCEER-06-0011 "A Study of the Coupled Horizontal-Vertical Behavior of Elastomeric and Lead-Rubber Seismic Isolation Bearings," by G.P. Warn and A.S. Whittaker, 9/22/06 (PB2007-108679).

MCEER-06-0012 "Proceedings of the Fourth PRC-US Workshop on Seismic Analysis and Design of Special Bridges: Advancing Bridge Technologies in Research, Design, Construction and Preservation," Edited by L.C. Fan, G.C. Lee and L. Ziang, 10/12/06 (PB2007-109042).

MCEER-06-0013 "Cyclic Response and Low Cycle Fatigue Characteristics of Plate Steels," by P. Dusicka, A.M. Itani and I.G. Buckle, 11/1/06 06 (PB2007-106987).

MCEER-06-0014 "Proceedings of the Second US-Taiwan Bridge Engineering Workshop," edited by W.P. Yen, J. Shen, J-Y. Chen and M. Wang, 11/15/06 (PB2008-500041).

MCEER-06-0015 "User Manual and Technical Documentation for the REDARS™ Import Wizard," by S. Cho, S. Ghosh, C.K. Huyck and S.D. Werner, 11/30/06 (PB2007-114766).

MCEER-06-0016 "Hazard Mitigation Strategy and Monitoring Technologies for Urban and Infrastructure Public Buildings: Proceedings of the China-US Workshops," edited by X.Y. Zhou, A.L. Zhang, G.C. Lee and M. Tong, 12/12/06 (PB2008-500018).

MCEER-07-0001 "Static and Kinetic Coefficients of Friction for Rigid Blocks," by C. Kafali, S. Fathali, M. Grigoriu and A.S. Whittaker, 3/20/07 (PB2007-114767).

MCEER-07-0002 "Hazard Mitigation Investment Decision Making: Organizational Response to Legislative Mandate," by L.A. Arendt, D.J. Alesch and W.J. Petak, 4/9/07 (PB2007-114768).

MCEER-07-0003 "Seismic Behavior of Bidirectional-Resistant Ductile End Diaphragms with Unbonded Braces in Straight or Skewed Steel Bridges," by O. Celik and M. Bruneau, 4/11/07 (PB2008-105141).

MCEER-07-0004   "Modeling Pile Behavior in Large Pile Groups Under Lateral Loading," by A.M. Dodds and G.R. Martin, 4/16/07(PB2008-105142).

MCEER-07-0005   "Experimental Investigation of Blast Performance of Seismically Resistant Concrete-Filled Steel Tube Bridge Piers," by S. Fujikura, M. Bruneau and D. Lopez-Garcia, 4/20/07 (PB2008-105143).

MCEER-07-0006   "Seismic Analysis of Conventional and Isolated Liquefied Natural Gas Tanks Using Mechanical Analogs," by I.P. Christovasilis and A.S. Whittaker, 5/1/07.

MCEER-07-0007   "Experimental Seismic Performance Evaluation of Isolation/Restraint Systems for Mechanical Equipment – Part 1: Heavy Equipment Study," by S. Fathali and A. Filiatrault, 6/6/07 (PB2008-105144).

MCEER-07-0008   "Seismic Vulnerability of Timber Bridges and Timber Substructures," by A.A. Sharma, J.B. Mander, I.M. Friedland and D.R. Allicock, 6/7/07 (PB2008-105145).

MCEER-07-0009   "Experimental and Analytical Study of the XY-Friction Pendulum (XY-FP) Bearing for Bridge Applications," by C.C. Marin-Artieda, A.S. Whittaker and M.C. Constantinou, 6/7/07 (PB2008-105191).

MCEER-07-0010   "Proceedings of the PRC-US Earthquake Engineering Forum for Young Researchers," Edited by G.C. Lee and X.Z. Qi, 6/8/07 (PB2008-500058).

MCEER-07-0011   "Design Recommendations for Perforated Steel Plate Shear Walls," by R. Purba and M. Bruneau, 6/18/07, (PB2008-105192).

MCEER-07-0012   "Performance of Seismic Isolation Hardware Under Service and Seismic Loading," by M.C. Constantinou, A.S. Whittaker, Y. Kalpakidis, D.M. Fenz and G.P. Warn, 8/27/07, (PB2008-105193).

MCEER-07-0013   "Experimental Evaluation of the Seismic Performance of Hospital Piping Subassemblies," by E.R. Goodwin, E. Maragakis and A.M. Itani, 9/4/07, (PB2008-105194).

MCEER-07-0014   "A Simulation Model of Urban Disaster Recovery and Resilience: Implementation for the 1994 Northridge Earthquake," by S. Miles and S.E. Chang, 9/7/07, (PB2008-106426).

MCEER-07-0015   "Statistical and Mechanistic Fragility Analysis of Concrete Bridges," by M. Shinozuka, S. Banerjee and S-H. Kim, 9/10/07, (PB2008-106427).

MCEER-07-0016   "Three-Dimensional Modeling of Inelastic Buckling in Frame Structures," by M. Schachter and AM. Reinhorn, 9/13/07, (PB2008-108125).

MCEER-07-0017   "Modeling of Seismic Wave Scattering on Pile Groups and Caissons," by I. Po Lam, H. Law and C.T. Yang, 9/17/07 (PB2008-108150).

MCEER-07-0018   "Bridge Foundations: Modeling Large Pile Groups and Caissons for Seismic Design," by I. Po Lam, H. Law and G.R. Martin (Coordinating Author), 12/1/07 (PB2008-111190).

MCEER-07-0019   "Principles and Performance of Roller Seismic Isolation Bearings for Highway Bridges," by G.C. Lee, Y.C. Ou, Z. Liang, T.C. Niu and J. Song, 12/10/07 (PB2009-110466).

MCEER-07-0020   "Centrifuge Modeling of Permeability and Pinning Reinforcement Effects on Pile Response to Lateral Spreading," by L.L Gonzalez-Lagos, T. Abdoun and R. Dobry, 12/10/07 (PB2008-111191).

MCEER-07-0021   "Damage to the Highway System from the Pisco, Perú Earthquake of August 15, 2007," by J.S. O'Connor, L. Mesa and M. Nykamp, 12/10/07, (PB2008-108126).

MCEER-07-0022   "Experimental Seismic Performance Evaluation of Isolation/Restraint Systems for Mechanical Equipment – Part 2: Light Equipment Study," by S. Fathali and A. Filiatrault, 12/13/07 (PB2008-111192).

MCEER-07-0023   "Fragility Considerations in Highway Bridge Design," by M. Shinozuka, S. Banerjee and S.H. Kim, 12/14/07 (PB2008-111193).

MCEER-07-0024 "Performance Estimates for Seismically Isolated Bridges," by G.P. Warn and A.S. Whittaker, 12/30/07 (PB2008-112230).

MCEER-08-0001 "Seismic Performance of Steel Girder Bridge Superstructures with Conventional Cross Frames," by L.P. Carden, A.M. Itani and I.G. Buckle, 1/7/08, (PB2008-112231).

MCEER-08-0002 "Seismic Performance of Steel Girder Bridge Superstructures with Ductile End Cross Frames with Seismic Isolators," by L.P. Carden, A.M. Itani and I.G. Buckle, 1/7/08 (PB2008-112232).

MCEER-08-0003 "Analytical and Experimental Investigation of a Controlled Rocking Approach for Seismic Protection of Bridge Steel Truss Piers," by M. Pollino and M. Bruneau, 1/21/08 (PB2008-112233).

MCEER-08-0004 "Linking Lifeline Infrastructure Performance and Community Disaster Resilience: Models and Multi-Stakeholder Processes," by S.E. Chang, C. Pasion, K. Tatebe and R. Ahmad, 3/3/08 (PB2008-112234).

MCEER-08-0005 "Modal Analysis of Generally Damped Linear Structures Subjected to Seismic Excitations," by J. Song, Y-L. Chu, Z. Liang and G.C. Lee, 3/4/08 (PB2009-102311).

MCEER-08-0006 "System Performance Under Multi-Hazard Environments," by C. Kafali and M. Grigoriu, 3/4/08 (PB2008-112235).

MCEER-08-0007 "Mechanical Behavior of Multi-Spherical Sliding Bearings," by D.M. Fenz and M.C. Constantinou, 3/6/08 (PB2008-112236).

MCEER-08-0008 "Post-Earthquake Restoration of the Los Angeles Water Supply System," by T.H.P. Tabucchi and R.A. Davidson, 3/7/08 (PB2008-112237).

MCEER-08-0009 "Fragility Analysis of Water Supply Systems," by A. Jacobson and M. Grigoriu, 3/10/08 (PB2009-105545).

MCEER-08-0010 "Experimental Investigation of Full-Scale Two-Story Steel Plate Shear Walls with Reduced Beam Section Connections," by B. Qu, M. Bruneau, C-H. Lin and K-C. Tsai, 3/17/08 (PB2009-106368).

MCEER-08-0011 "Seismic Evaluation and Rehabilitation of Critical Components of Electrical Power Systems," S. Ersoy, B. Feizi, A. Ashrafi and M. Ala Saadeghvaziri, 3/17/08 (PB2009-105546).

MCEER-08-0012 "Seismic Behavior and Design of Boundary Frame Members of Steel Plate Shear Walls," by B. Qu and M. Bruneau, 4/26/08 . (PB2009-106744).

MCEER-08-0013 "Development and Appraisal of a Numerical Cyclic Loading Protocol for Quantifying Building System Performance," by A. Filiatrault, A. Wanitkorkul and M. Constantinou, 4/27/08 (PB2009-107906).

MCEER-08-0014 "Structural and Nonstructural Earthquake Design: The Challenge of Integrating Specialty Areas in Designing Complex, Critical Facilities," by W.J. Petak and D.J. Alesch, 4/30/08 (PB2009-107907).

MCEER-08-0015 "Seismic Performance Evaluation of Water Systems," by Y. Wang and T.D. O'Rourke, 5/5/08 (PB2009-107908).

MCEER-08-0016 "Seismic Response Modeling of Water Supply Systems," by P. Shi and T.D. O'Rourke, 5/5/08 (PB2009-107910).

MCEER-08-0017 "Numerical and Experimental Studies of Self-Centering Post-Tensioned Steel Frames," by D. Wang and A. Filiatrault, 5/12/08 (PB2009-110479).

MCEER-08-0018 "Development, Implementation and Verification of Dynamic Analysis Models for Multi-Spherical Sliding Bearings," by D.M. Fenz and M.C. Constantinou, 8/15/08 (PB2009-107911).

MCEER-08-0019 "Performance Assessment of Conventional and Base Isolated Nuclear Power Plants for Earthquake Blast Loadings," by Y.N. Huang, A.S. Whittaker and N. Luco, 10/28/08 (PB2009-107912).

MCEER-08-0020 "Remote Sensing for Resilient Multi-Hazard Disaster Response – Volume I: Introduction to Damage Assessment Methodologies," by B.J. Adams and R.T. Eguchi, 11/17/08.

MCEER-08-0021   "Remote Sensing for Resilient Multi-Hazard Disaster Response – Volume II: Counting the Number of Collapsed Buildings Using an Object-Oriented Analysis: Case Study of the 2003 Bam Earthquake," by L. Gusella, C.K. Huyck and B.J. Adams, 11/17/08.

MCEER-08-0022   "Remote Sensing for Resilient Multi-Hazard Disaster Response – Volume III: Multi-Sensor Image Fusion Techniques for Robust Neighborhood-Scale Urban Damage Assessment," by B.J. Adams and A. McMillan, 11/17/08.

MCEER-08-0023   "Remote Sensing for Resilient Multi-Hazard Disaster Response – Volume IV: A Study of Multi-Temporal and Multi-Resolution SAR Imagery for Post-Katrina Flood Monitoring in New Orleans," by A. McMillan, J.G. Morley, B.J. Adams and S. Chesworth, 11/17/08.

MCEER-08-0024   "Remote Sensing for Resilient Multi-Hazard Disaster Response – Volume V: Integration of Remote Sensing Imagery and VIEWS^{TM} Field Data for Post-Hurricane Charley Building Damage Assessment," by J.A. Womble, K. Mehta and B.J. Adams, 11/17/08.

MCEER-08-0025   "Building Inventory Compilation for Disaster Management: Application of Remote Sensing and Statistical Modeling," by P. Sarabandi, A.S. Kiremidjian, R.T. Eguchi and B. J. Adams, 11/20/08 (PB2009-110484).

MCEER-08-0026   "New Experimental Capabilities and Loading Protocols for Seismic Qualification and Fragility Assessment of Nonstructural Systems," by R. Retamales, G. Mosqueda, A. Filiatrault and A. Reinhorn, 11/24/08 (PB2009-110485).

MCEER-08-0027   "Effects of Heating and Load History on the Behavior of Lead-Rubber Bearings," by I.V. Kalpakidis and M.C. Constantinou, 12/1/08.

MCEER-08-0028   "Experimental and Analytical Investigation of Blast Performance of Seismically Resistant Bridge Piers," by S.Fujikura and M. Bruneau, 12/8/08.

MCEER-08-0029   "Evolutionary Methodology for Aseismic Decision Support," by Y. Hu and G. Dargush, 12/15/08.

MCEER-08-0030   "Development of a Steel Plate Shear Wall Bridge Pier System Conceived from a Multi-Hazard Perspective," by D. Keller and M. Bruneau, 12/19/08.

MCEER-09-0001   "Modal Analysis of Arbitrarily Damped Three-Dimensional Linear Structures Subjected to Seismic Excitations," by Y.L. Chu, J. Song and G.C. Lee, 1/31/09.

MCEER-09-0002   "Air-Blast Effects on Structural Shapes," by G. Ballantyne, A.S. Whittaker, A.J. Aref and G.F. Dargush, 2/2/09.